Delft University of Technology

Early observability of EOR process effectiveness

Fatemi, S.A.

DOI
10.4233/uuid:c4e6a875-4117-4552-88f6-ce0abeb80c54

Publication date
2021

Document Version
Final published version

Citation (APA)
Fatemi, S. A. (2021). *Early observability of EOR process effectiveness*. [Dissertation (TU Delft), Delft University of Technology]. https://doi.org/10.4233/uuid:c4e6a875-4117-4552-88f6-ce0abeb80c54

Important note
To cite this publication, please use the final published version (if applicable).
Please check the document version above.

Copyright
Other than for strictly personal use, it is not permitted to download, forward or distribute the text or part of it, without the consent of the author(s) and/or copyright holder(s), unless the work is under an open content license such as Creative Commons.

Takedown policy
Please contact us and provide details if you believe this document breaches copyrights.
We will remove access to the work immediately and investigate your claim.

This work is downloaded from Delft University of Technology.
For technical reasons the number of authors shown on this cover page is limited to a maximum of 10.

EARLY OBSERVABILITY OF EOR PROCESS EFFECTIVENESS

EARLY OBSERVABILITY OF EOR PROCESS EFFECTIVENESS

Proefschrift

Ter verkrijging van de graad van doctor
aan de Technische Universiteit Delft,
op gezag van de Rector Magnificus Prof.dr.ir. T.H.J.J. van der Hagen,
voorzitter van het College voor Promoties,
in het openbaar te verdedigen op 7 september 2021 om 15:00 uur

door

Amin FATEMI

Master of Science in Chemical Engineering - Hydrocarbon Reservoirs, Iran
Geboren te Kerman, Iran.

Dit proefschrift is goedgekeurd door de:

Promoter: Prof. dr. W. R. Rossen

Samenstelling promotiecommissie:

Rector Magnificus,	voorzitter
Prof. dr. W. R. Rossen	Technische Universiteit Delft, promotor

Onafhankelijke leden:

Prof. A. Hiorth,	University of Stavanger Norway,
Prof.dr. A.W. Martinius,	Technische Universiteit Delft,
Dr.ir. O. Leeuwenburgh,	TNO,
Prof.dr.ir. P.L.J. Zitha,	Technische Universiteit Delft,
Prof.dr.ir. A.W. Heemink,	Technische Universiteit Delft,
Prof.dr.ir. J.D. Jansen,	Technische Universiteit Delft.

This research was carried out within the context of the Recovery Factory program, a joint project of Shell Global Solutions International and Delft University of Technology.

Copyright © 2021 by Amin Fatemi

Cover Design: Matin Yasseri and Amin Fatemi

Printed by ProefschriftMaken

All Rights reserved.

An Electronic version of this dissertation will be available at
http://repository.tudelft.nl/.

To

My dear parents

Matin, the love of my life

Shabnam and Shohre, my beloved sisters

تقدیم به

پدر و مادرم عزیزم

همسر نازنینم

و خواهرهای دوست داشتنیم

CONTENTS

LIST OF FIGURES **xi**

LIST OF TABLES **xv**

1 INTRODUCTION 1

1.1 POLYMER FLOODING 1

1.2 UNCERTAINTY IN RESERVOIR MODELING 2

1.3 EOR PROCESS UNCERTAINTY 3

1.4 SCOPE OF THE DISSERTATION 4

1.5 THESIS OUTLINE 5

1.5.1 CHAPTER 2: DISCERNING IN-SITU PERFORMANCE OF AN EOR AGENT IN THE MIDST OF GEOLOGICAL UNCERTAINTY I: LAYER CAKE RESERVOIR MODEL 5

1.5.2 CHAPTER 3: DISCERNING IN-SITU PERFORMANCE OF AN EOR AGENT IN THE MIDST OF GEOLOGICAL UNCERTAINTY II: FLUIVIAL-DEPOSIT RESERVOIR 6

1.5.3 CHAPTER 4: DISCERNING IN-SITU PERFORMANCE OF AN EOR AGENT IN THE MIDST OF GEOLOGICAL UNCERTAINTY III: NORNE FIELD 8

1.5.4 CHAPTER 5: CONCLUSIONS AND RECOMMENDATIONS 9

2 DISCERNING IN-SITU PERFORMANCE OF AN EOR AGENT IN THE MIDST OF GEOLOGICAL UNCERTAINTY I: LAYER CAKE RESERVOIR MODEL 11

2.1 INTRODUCTION 12

2.2 PROPOSED WORKFLOW 13

2.3 CASE STUDY 15

2.3.1 REPRESENTATION OF UNCERTAINTY IN POLYMER-FLOOD PERFORMANCE 17

2.3.2 REPRESENTATION OF GEOLOGICAL UNCERTAINTY 18

2.4 DEVELOPMENT SCENARIO AND PROCEDURE 20

2.5 RESULTS 21

2.6 CONCLUSIONS AND DISCUSSION 23

APPENDIX 2.A: FRACTIONAL-FLOW THEORY IN POLYMER FLOODING 25

APPENDIX 2.B: EFFECT OF GRAVITY 27

APPENDIX 2.C: CONFIDENCE INTERVALS BASED ON THE T-DISTRIBUTION 28

APPENDIX 2.D: DIFFERENT SCENARIOS OF POLYMER IN-SITU VISCOSITY LOSS 29

3 DISCERNING IN-SITU PERFORMANCE OF AN EOR AGENT IN THE MIDST OF GEOLOGICAL UNCERTAINTY: II. FLUVIAL-DEPOSIT RESERVOIR 32

3.1 INTRODUCTION 33

3.2 CASE STUDY DESCRIPTION 35

3.2.1 REPRESENTATION OF UNCERTAINTY IN POLYMER PERFORMANCE 37

3.2.1.1 FRACTIONAL-FLOW THEORY IN POLYMER FLOODING 37

3.2.2 REPRESENTATION OF GEOLOGICAL UNCERTAINTY 38

3.3 DEVELOPMENT SCENARIO AND PROCEDURE 40

3.4 VERTICAL SWEEP 42

3.5 SUMMARY AND DISCUSSION 47

APPENDIX 3.A 48

APPENDIX 3.B 49

4 DISCERNING IN-SITU PERFORMANCE OF AN EOR AGENT IN THE MIDST OF GEOLOGICAL UNCERTAINTY III: NORNE FIELD 54

4.1 INTRODUCTION 55

4.2 NORNE FIELD 57

4.3 CASE-STUDY DESCRIPTION 57

4.4 REPRESENTING GEOLOGICAL UNCERTAINTY USING ENSEMBLE KALMAN FILTER (ENKF) 61

4.4.1 HISTORY-MATCH RESULTS 63

4.5 DEVELOPMENT SCENARIO AND PROCEDURE 65

4.6 RESULTS 66

4.7 SUMMARY AND CONCLUSIONS 70

5 CONCLUSIONS AND RECOMMENDATIONS 72

5.1 CONCLUSIONS 72

5.1.1 LAYER-CAKE MODEL 73

5.1.2 FLUVIAL RESERVOIR (EGG MODEL) 74

5.1.3 NORNE FIELD MODEL 74

5.2 RECOMMENDATIONS 75

REFERENCES 76

LIST OF PUBLICATIONS 85

SUMMARY 87

SAMENVATTING 91

ACKNOWLEDGEMENTS 95

ABOUT THE AUTHOR 97

LIST OF FIGURES

Figure 1.1: Schematic of the polymer waterflooding process. Mobility ratio is improved and flow through more-permeable channels is reduced, resulting in increased volumetric sweep (Lake et al., 2014). 2

Figure 1.2: A five-layer rectangular reservoir with one producer and one injector. Schematic of spatial ordering of layer permeabilities in the three cases examined. 6

Figure 1.3: Permeability field and well locations in one realization of the 'Egg Model' (Jansen et al., 2014; after Van Essen et al., 2009). 7

Figure 1.4: Horizontal permeability field (in md) of realization number 1 after Norne Field case study and the top view of the well locations. Black circles show the injectors and red triangles show the producers. 8

Figure 2.1: Workflow to determine criteria to distinguish EOR process performance in-situ in the midst of geological uncertainties. 15

Figure 2.2: The case study: a five-layer rectangular reservoir with one producer and one injector. 16

Figure 2.3: Schematic of spatial ordering of layer permeabilities. 19

Figure 2.4: Production/injection profile for the geological description corresponding to V_{dp} = 0.9 and layer ordering of schematic A. 20

Figure 2.5: Comparing signals of the process with 60 cp polymer viscosity (design) with the 12 cp polymer viscosity (failure) 21

Figure 2.A.1: Graphical construction of water and polymer fractional flow in secondary mode for the design polymer in-situ viscosity of 60 cp. 26

Figure 2.A.2: Graphical construction of water and polymer fractional flow in secondary mode for the reduced polymer in-situ viscosity of 12 cp. 26

Figure 2.B.1: Effect of gravity on Cumulative Oil Production (after 10 years of waterflood) in different permeability arrangements. 27

Figure 3.1: Permeability field and well locations (Jansen et al., 2014; after Van Essen et al., 2009). 36
Figure 3.2: Permeability field of six randomly chosen realizations out of a set of 100, showing alternative fluvial structures (Jansen et al., 2014; after Van Essen et al., 2009). 36
Figure 3.3: Water production in four producers in one realization. Water breakthrough happens early in the simulation. 39
Figure 3.4: Injection BHP of eight injectors. 41
Figure 3.5: Polymer slug production rate in four producers and total polymer production rate. 41
Figure 3.6: Oil production rate in the four producers and total oil production rate. 42
Figure 3.7: Slice of the permeability map of layer 4 of realization no.1. 43
Figure 3.8: Oil saturation in realization no. 1 at (A): water breakthrough time, (B): end of waterflood period, (C): end of polymer flood for 20 cp case and (D): end of polymer flood for 6 cp case. 43

Figure 4.1: The location and structure of the Norne Field (Adlam, 1995). 57
Figure 4.2: Horizontal permeability field (in md) of realization number 1 and the top view of the well locations. Black circles show the injectors and red triangles show the producers. 59
Figure 4.3: Horizontal permeability field (in md) for layers 1, 5, 12 and 22 of realization 1. 59
Figure 4.4: Decay factor map in layer 22 of realization number 50: (a) τ = 10 year, (b) τ = 2 year. Deep red corresponds to initial viscosity, and light blue to complete loss of viscosity. 61
Figure 4.5: Water cut for the producers; grey is the prior ensemble waterflood, blue is the posterior ensemble mean and red is the synthetic truth. 63
Figure 4. 6: Injection bottom-hole pressure for the injectors; grey is the prior ensemble waterflood, blue is the posterior ensemble mean and red is the synthetic truth. 63
Figure 4.7: Permeability maps of the prior and posterior estimates for several layers of realization 10. 64

Figure 4.8: Signal analysis of scenario #1: values of five signals for the design and failure cases. Blue squares are the design signal values and red triangles are the failure signal values. 66

Figure 4.9: Signal analysis of scenario #2: values of five signals for the design and failure cases. Blue squares are the design signal values and red triangles are the failure signal values. 67

Figure 4.10: Signal analysis of scenario #3: values of five signals for the design and failure cases. Blue squares are the design signal values and red triangles are the failure signal values. 68

Figure 4.11: Signal analysis of scenario #4: values of five signals for the design and failure cases. Blue squares are the design signal values and red triangles are the failure signal values. 69

LIST OF TABLES

Table 2.1: Reservoir dimensions 16

Table 2.2: Case-study reservoir and injection fluid properties. 16

Table 2.3: Suggested ranges of values for a reservoir candidate for a polymer flooding (Dickson et al., 2010 and Saleh et al., 2014). 17

Table 2.4: Layer permeability values for V_{dp} = 0.6, 0.75 and 0.9; k_{avg} = 1000 md in all cases. 19

Table 2.5: Signal values calculated for the nine geological cases with 60 cp polymer viscosity, with upper and lower bounds of the 95% confidence interval (CI+, CI-) for each signal. 22

Table 2.6: Discerning the process with 12 cp polymer viscosity from the case with 60 cp polymer viscosity. 23

Table 2.A.1: Recoveries after polymer breakthrough for the design viscosity case versus reduced viscosity. 25

Table 2.D.1: Discerning the process with 54 cp polymer viscosity from the case with 60 cp polymer viscosity. 29

Table 2.D.2: Discerning the process with 48 cp polymer viscosity from the case with 60 cp polymer viscosity. 29

Table 2.D.3: Discerning the process with 30 cp polymer viscosity from the case with 60 cp polymer viscosity. 29

Table 2.D.4: Discerning the process with 24 cp polymer viscosity from the case with 60 cp polymer viscosity. 30

Table 2.D.5: Discerning the process with 18 cp polymer viscosity from the case with 60 cp polymer viscosity. 30

Table 2.D.6: Discerning the process with 9 cp polymer viscosity from the case with 60 cp polymer viscosity. 30

Table 2.D.7: Discerning the process with 6 cp polymer viscosity from the case with 60 cp polymer viscosity. 31

Table 3.1: Reservoir and fluid properties of the modified Egg Model. 36

Table 3.2: Suggested values for a reservoir candidate to go through a polymer flood process Saleh et al., 2014. 37

Table 3.3: Recoveries after polymer breakthrough for the design viscosity case versus reduced viscosity in 1D secondary polymer flood. 37

Table 3.4: Water breakthrough time of four producers in two different realizations (1, 2) and their typical distance value. 39

Table 3.5: Summary of the results of discerning the process with 6 cp polymer viscosity from the case with 20 cp polymer viscosity for the first 10-member set of geological realizations. 45

Table 3.6: Summary of the results of discerning the process with 6 cp polymer viscosity from the case with 20 cp polymer viscosity for the second 10-member set of geological realizations. 46

Table 3.A.1: Water breakthrough time of the four producers in members of the three sets. 48

Table 3.B.1: Signal values of the first 10-member set of geological cases calculated for the case with 20 cp polymer viscosity, with upper and lower bounds of the 95% confidence interval (CI+, CI-) for each signal. 49

Table 4.1: Reservoir and fluid properties of the modified Norne Field 58

Table 4.2: Results of signal analysis of scenario #1. 67

Table 4.3: Result of signal analysis of scenario #2. 68

Table 4.4: Result of signal analysis of scenario #3. 69

Table 4.5: Result of signal analysis of scenario #4. 70

1

INTRODUCTION

1.1 POLYMER FLOODING

While the exploration and development of new oil reserves continues, the implementation of enhanced oil recovery (EOR) techniques has become more and more popular. The implementation of the EOR provides an opportunity to extract more of the original oil reserves that could not be extracted through conventional methods. Typical EOR mechanisms include chemical flooding, gas injection and thermal recovery. The displacement methods include the addition of the displacing substance into the reservoir through the injection well to displace the remaining oil. Chemical flooding includes the addition of water with some chemicals (polymers) to enhance the oil displacement ability. Polymer flooding has been used in the last decades to effectively recover the remaining oil from the reservoir, up to 30% of the original oil in place (Green and Willhite, 2018). Due to decreased water production and enhanced oil production, the total cost of using the polymer flooding technique is less than that of water flooding (Wang et al., 2003). During a polymer waterflood, a high-molecular-weight and viscosity-enhancing polymer is added to the water of the waterflood to decrease the mobility of the flood water and, as a consequence, improve the sweep efficiency of the waterflood. The primary purpose of adding polymer to most polymer waterfloods is to increase the viscosity of the flood water; however, polymer addition to the water in many instances also imparts a secondary permeability-reduction component. Polymer waterflooding is normally applied when the waterflood mobility ratio is high or the heterogeneity of the reservoir is great. Fig. 1.1 is a schematic of the polymer waterflooding process (Lake et al., 2014).

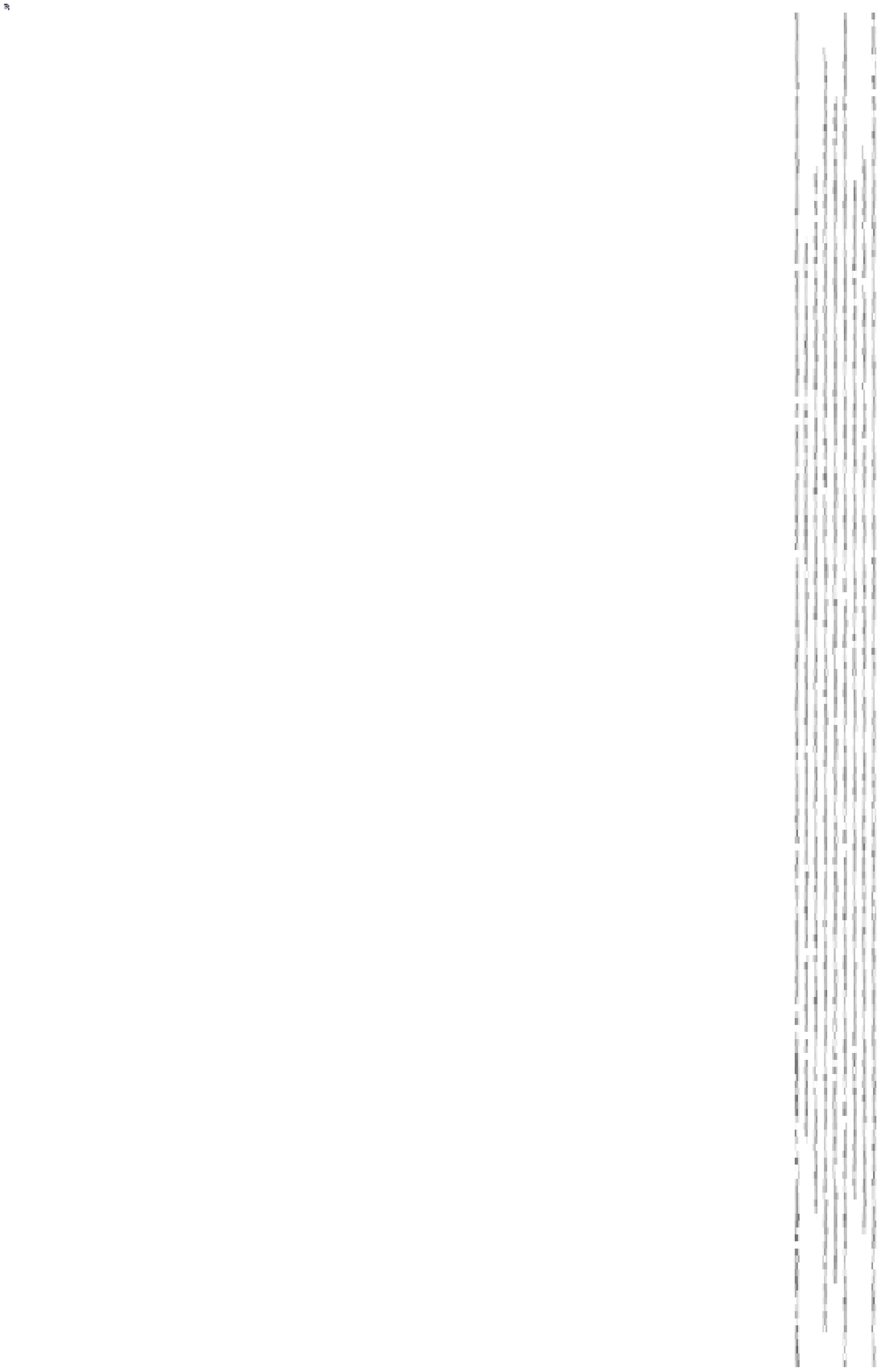

1.2 UNCERTAINTY IN RESERVOIR MODELING

Uncertainty is present in many aspects of scientific work and engineering as well as everyday life. Each field of study uses different terminologies and ways to describe, quantify and assess uncertainty. Uncertainty in reservoir modeling is in large part due to incomplete and imprecise knowledge of the underground, as a result of limited sampling of the subsurface heterogeneities (Ma, 2019). Well data and seismic data have incomplete coverage and finite resolution and thus the interpretations are uncertain. Geo-modeling is the process of populating a reservoir model with properties such as permeabilities, porosities etc., which is a highly uncertain procedure. The uncertainty arises from a lack of knowledge about the reservoir and more importantly from interpretations of uncertain data sources such as seismic, well logs, core data, etc. Interpretation of any data source is always subject to uncertainty. Building a model of uncertainty that includes all possible aspects of what is uncertain is too difficult and often not needed in the first place (Scheidt et al., 2018).

Reservoirs are heterogeneous and difficult to predict away from wells. Ignoring uncertainty and locking-in important model parameters and choices amounts to an assumption of perfect knowledge and is generally an unacceptable approach. Uncertainty must be explicitly modeled. Understanding the (1) sources of uncertainty, (2) methods to represent uncertainty, (3) the formalisms of uncertainty, and (4) uncertainty modeling methods and workflows are essential steps for the integration of all reservoir information sources and providing good models for decision making in the presence of uncertainty (Pyrcz and Deutsch, 2014). Reservoir simulation is routinely employed in the prediction of reservoir performance under different depletion and operating scenarios. Usually, a single history-matched model, conditioned to production data, is obtained. The model is then used to forecast future production profiles. Because the history-match is non-unique, the forecast production profiles are therefore uncertain (Subbey et al., 2004).

1.3 EOR PROCESS UNCERTAINTY

Any enhanced-oil-recovery (EOR) field trial can produce unexpected results arising from a misunderstanding of either the geology of the reservoir or of the EOR process. Separate evaluation of the impacts of geological and process uncertainties on the performance of an EOR is important because a process that did not achieve the desired objectives in one formation might be successful in another field if it demonstrates that it achieved its technical objectives.

Researchers have studied uncertainty in EOR process performance and uncertainty in the geological description, but not the two together. Previous research has examined uncertainty in chemical flooding, CO_2-EOR and thermal-EOR process-performance parameters (Brown and Smith, 1984; Nasr-El-Din et al., 1992; Flaaten et al., 2009; Denney, 2011; Elraies, 2012; Stanley, 2014; Alkhatib and King, 2015; Aguiar and Mansur, 2016; Levitt and Bourrel, 2016; Adepoju et al., 2017; Esposito et al., 2017; Lyon and Popov, 2017; Hocine et al., 2018; Khan and Khan, 2018; Phukan et al., 2019; Hazarika and Gogoi, 2019; Wang et al., 2020). Reservoir heterogeneity also plays an important role on the success of chemical enhanced oil recovery. Experimental data from Craig (1993) and Gharbi et al. (1997), field data from Sorbie and Clifford (1988) and Khataniar and Peters (1992) and simulation studies from Al-Honi et al. (2002), Akkutlu and Yorisos (2005) and Jia (2018) are examples of studies that have demonstrated the detrimental effects of reservoir heterogeneity on the performance of oil-displacement processes. Heterogeneity and geological factors have different impacts on the various EOR processes, including polymer and alkaline-surfactant-polymer, thermal and gas-injection (miscible and immiscible) EOR. There are a lot of examples of research that study the effects of geological heterogeneity and uncertainty on EOR performance (Ballin et al., 1992; Damsleth and Omre, 1997; Chen et al., 2008; Odell and Lindsey, 2010; Popov et al., 2010; Rashid et al., 2010; Soleimani et al., 2011; Fedutenko et al., 2012; Al-Mudhafar and Rao, 2016; Nguyen et al., 2016; Chiotoroiu et al., 2017; Kumar et al., 2017; Koneshloo et al., 2018; Pollack and Mukerji, 2019; Torrealba et al., 2019; Sacconi and Mahgerefteh, 2020). In this dissertation we investigate the impact of both sources of uncertainty together.

1.4 SCOPE OF THE DISSERTATION

This dissertation focuses on polymer flooding, as an example of an EOR process. Chemical floods such as polymer floods are EOR techniques intended to increase sweep and/or displacement efficiency. Even though the compatibility and the efficiency of the injected chemicals are thoroughly tested and validated in the laboratory, uncertainty still remains regarding their actual performance in the reservoir. These uncertainties can result from the differences in the scale of investigation (core scale to field scale), lack of adequate understanding of geological, mineralogical and petrophysical properties of the formation, and the long-term performance of the chemical slug in the reservoir. Therefore, in addition to thorough laboratory tests, practitioners should compare the uncertainty surrounding the performance of the EOR agent in-situ to that arising from geological uncertainty, because, as noted, a process that did succeed in one formation might succeed in another field if achieves its technical objectives. In this dissertation, the effects of polymer rheology, mixing with different brines in-situ, temperature, pressure, adsorption, permeability reduction, inaccessible pore volume and non-Newtonian behavior on chemical-flood effectiveness is represented here indirectly as a simple loss of polymer viscosity in situ from that projected for the process. To discern the performance of the EOR agent in-situ in the midst of geological uncertainty, we propose a general workflow and present three case studies for this challenge. This workflow could be extended to another EOR process by including mechanisms or manifestations of technical failure corresponding to that process.

1.5 THESIS OUTLINE

This dissertation contains several articles which are either published or have been submitted for publication in peer-reviewed journals. Below is an executive summary of the chapters included in this dissertation.

1.5.1 CHAPTER 2: DISCERNING IN-SITU PERFORMANCE OF AN EOR AGENT IN THE MIDST OF GEOLOGICAL UNCERTAINTY I: LAYER CAKE RESERVOIR MODEL

In the first case study, we propose a polymer EOR process in a 2D layer-cake reservoir where the polymer is designed to have a viscosity of 60 cp in-situ. Then, we allow that the polymer process might fail in-situ and viscosity could be only 20% of that intended. This failure could be the result of mechanical degradation in surface facilities or on entering the perforations, faulty translation from laboratory-measured properties to properties in-situ, or faulty characterization of resident reservoir brine. Several of these adverse events would give different polymer properties in different regions of the reservoir. For simplicity, in this initial study, we assume that throughout the reservoir polymer viscosity is everywhere a fixed fraction of that intended. We test whether the signals of this failure at the injection and production wells would be statistically significant in the midst of the geological uncertainty in the reservoir description. The five-layer 2D rectangular reservoir and the layer-permeability ordering is illustrated in Fig. 1.2. We assume three spatial distributions of permeability: specifically, from top to bottom, high-permeability to low-permeability, low-permeability to high-permeability, and a distribution with the lowest permeability in the middle.

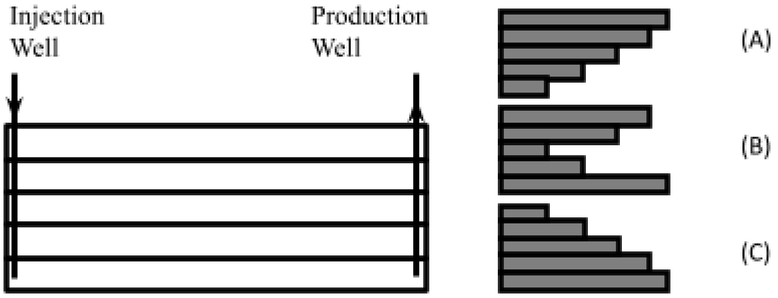

Figure 1.2: A five-layer rectangular reservoir with one producer and one injector. Schematic of spatial ordering of layer permeabilities in the three cases examined.

For a population of 9 reservoirs representing geological uncertainty, we compare the deviation caused by loss of polymer viscosity to the scatter caused by the geological uncertainty using the 95%-confidence-interval statistical approach. Various signals are monitored to see which are the most reliable indications of whether a polymer viscosity was maintained in-situ. We further investigate the statistical significance of each signal.

In addition to the application in this cases study, this chapter describes a workflow for such an evaluation that could be extended to any EOR process.

1.5.2 CHAPTER 3: DISCERNING IN-SITU PERFORMANCE OF AN EOR AGENT IN THE MIDST OF GEOLOGICAL UNCERTAINTY II: FLUIVIAL-DEPOSIT RESERVOIR

For the second case study, we apply the workflow to a case with a more-sophisticated geological model. This chapter presents a case study based on the “modified Egg Model” (Jansen et al., 2014): a polymer EOR process designed for a 3D fluvial-deposit water-oil reservoir. The polymer is designed to have a viscosity of

20 cp in situ. We start with 100 realizations of this 3D reservoir to reflect the range of possible geological structures honoring the statistics of the initial geological uncertainties. The well locations and absolute-permeability field of one realization of the set are depicted in Fig. 1.3.

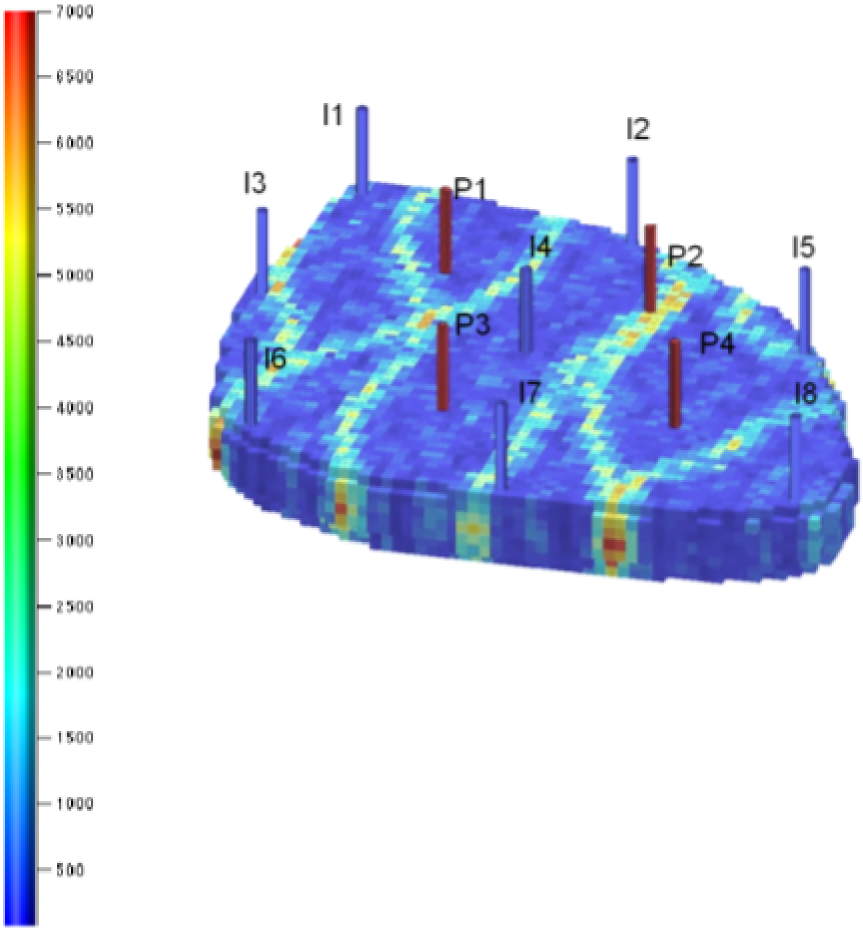

Figure 1.3: Permeability field and well locations in one realization of the ‘Egg Model’ (Jansen et al., 2014; after Van Essen et al., 2009).

Next we group the realizations on the basis of a measure of similarity that reflects the interaction between heterogeneity and the reservoir flow mechanisms (Mantilla and Srinivasan, 2011). After five years of waterflooding, we rank the reservoir models into different groups of 10 realizations, out of the initial 100 equi-probable realizations, with similar water breakthrough dates at the four production wells. Each group of realizations thus represents reservoirs with roughly similar waterflood histories. As a group they represent the reduced geological uncertainty remaining after this period of waterflooding. To represent EOR process failure, we allow that the polymer process might fail in situ and viscosity could be 30% of that intended. We then simulate five years of polymer injection. We assume that throughout the reservoir polymer viscosity is less than the design value. We test whether the signals of this difference at injection and production wells would be statistically significant in the midst of the geological uncertainty: in other words, whether the process failure would be clearly visible in the midst of reservoir uncertainty.

1.5.3 CHAPTER 4: DISCERNING IN-SITU PERFORMANCE OF AN EOR AGENT IN THE MIDST OF GEOLOGICAL UNCERTAINTY III: NORNE FIELD

For the third case study, we apply the workflow to a case with a more-realistic geological model, based on a real reservoir, and a level of uncertainty more representative of a field after a period of waterflood: the “Norne Field” case study (Møyner and Lie, 2016). Fig. 1.4 shows the permeability field and top view of the Norne field model.

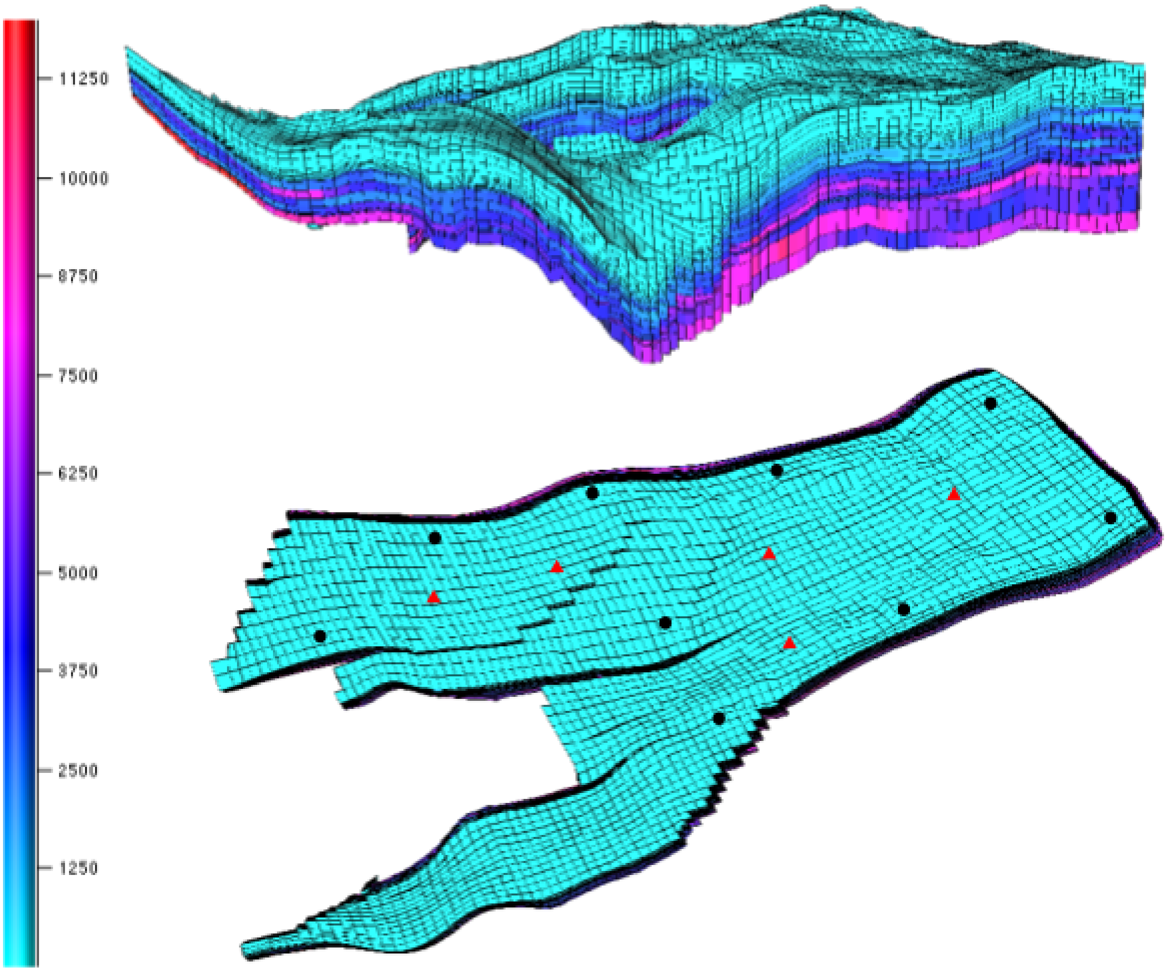

Figure 1.4: Horizontal permeability field (in md) of realization number 1 after Norne Field case study and the top view of the well locations. Black circles show the injectors and red triangles show the producers.

In addition, we test the ability to distinguish between two different modes of process failure. We start with 50 realizations of this reservoir model to show the variety of possible fluvial-deposit scenarios for the geological description. We then use the Ensemble Kalman Filter (EnKF) to update the initial reservoir ensemble, integrating 30 years of waterflood production data. We use the updated reservoir models to simulate a polymer EOR process with an in-situ viscosity of 18 cp. To represent EOR process failure, we allow that the polymer process might fail in situ through either or both of two different mechanisms. The first is a global viscosity loss, where we stipulate that viscosity could be half of that intended, everywhere in the reservoir. The second is a progressive viscosity loss upon injection, where polymer decays and loses its viscosifying power over time (and therefore distance from the injection well). This second mechanism represents process where polymer viscosity is maintained near the injection well but not far away. These processes would reflect chemical degradation of polymer in situ or, more broadly, polymer absorption. We test whether the signals of these differences at injection and production wells would be statistically significant in the midst of the updated geological uncertainty, and whether the signals can distinguish which mechanism of failure has occurred.

The workflow presented here could be applied to other EOR processes by defining possible mechanism of failure for those processes. For example, the technical criteria for success for an EOR agent in-situ could be ultralow interfacial tension (IFT) or low residual oil saturation for a surfactant process, a given mobility or injectivity for a foam process, minimum miscibility pressure, degree of swelling, or absence of asphaltene deposition for a CO_2-EOR process, etc.

1.5.4 CHAPTER 5: CONCLUSIONS AND RECOMMENDATIONS

The dissertation concludes with a brief summary of results of the all three chapters, conclusions and recommendations for future work.

Note from the author: This text includes published papers in reviewed journals and scientific conferences. Consequently, the reader may find similar texts and sentences in some parts of the thesis.

2

DISCERNING IN-SITU PERFORMANCE OF AN EOR AGENT IN THE MIDST OF GEOLOGICAL UNCERTAINTY I: LAYER CAKE RESERVOIR MODEL

An enhanced-oil-recovery (EOR) pilot test has multiple goals, among them to demonstrate oil recovery, verify the properties of the EOR agent in-situ, and provide the information needed for scale-up to an economic process. Given the complexity of EOR processes and the inherent uncertainty in the reservoir description, it is a challenge to discern the properties of the EOR agent in-situ in the midst of geological uncertainty. We propose a general workflow and present a case study to illustrate this challenge: a polymer EOR process in a 2D layer-cake reservoir. The polymer is designed to have a viscosity of 60 cp in-situ. There is uncertainty in the reservoir description, represented here by a range of values of Dykstra Parsons coefficient and different spatial arrangements of layers. We allow that the polymer process might fail in-situ and viscosity could be 20% of that intended. We test whether the signals of this difference at injection and production wells would be statistically significant in the midst of the geological uncertainty. Specifically, we compare the deviation caused by loss of

---

This chapter is from the published article: S.A. Fatemi, J.D. Jansen, W.R. Rossen, 2017. Discerning in-situ performance of an EOR agent in the midst of geological uncertainty I: Layer cake reservoir model. *Journal of Petroleum Science and Engineering* (158): 56-65.

polymer viscosity to the scatter caused by the geological uncertainty using the statistical 95% confidence interval. Among the signals considered, the 'rate of rise in injection pressure with polymer injection' and 'maximum injection pressure in the injector' give the most reliable indications of whether a polymer viscosity was maintained in-situ. If unintended and uncontrolled fracturing of the injection well is considered likely during polymer injection, however, injection pressure may be an unreliable indicator of in-situ polymer viscosity. In that case a diagnostic fracture-injection / falloff test could produce the needed indication of polymer viscosity in-situ. 'Polymer breakthrough time' and 'cumulative oil production at the end of process' give indications of polymer in-situ loss in some of the cases. With a more severe viscosity loss, e.g. 90% or worse, these signals give a statistically significant indication of loss of polymer viscosity in all of the cases.

2.1 INTRODUCTION

An EOR pilot test has multiple goals: to demonstrate oil recovery, verify the properties of the EOR agent in-situ, and provide the information needed for scale-up to an economic process. The first goal concerns whether the process achieves its overall objectives (oil recovery) in the given formation. Whether or not the first goal is reached, it is important to assess the process by the second criterion. This is important because a process that did not achieve the desired objectives in the given formation might be successful in another field if it demonstrates that it achieves its technical objectives. For example, the technical criteria for success for an EOR agent in-situ could be low interfacial tension (IFT) or low residual oil saturation for a surfactant process, a given mobility for a polymer process, etc. In a field pilot, one must determine the technical success of an EOR agent in the midst of geological uncertainty in the reservoir description while the EOR process is in progress.

Previous research has examined uncertainty in EOR process performance or uncertainty in the geological description, but not the two together. Studies on uncertainty in EOR process performance include Alkhatib and King (2015), Brown and Smith (1984), and Adepoju et al. (2017), examining surfactant-flood and polymer-flood processes. There have also been studies on the effect of geological heterogeneities and their uncertainty on how an EOR process performs. Heterogeneity and geological factors have different impacts on the various

EOR processes, including polymer and alkaline-surfactant-polymer, thermal and gas-injection (miscible and immiscible) EOR. Studies of the effects of geological heterogeneity and uncertainty on EOR performance include Kumar et al. (2006), Chen et al. (2008), Popov et al. (2010), Rashid et al. (2010), Soleimani et al. (2011), Chiotoroiu et al. (2017), and Kumar et al. (2017).

In this paper, we propose a workflow to discern the performance of the EOR agent in-situ in the midst of geological uncertainty. We further show how to implement the workflow in a case study to investigate the impact of both sources of uncertainty together in a statistical approach. We present a simple model to illustrate the issues involved: a polymer EOR process implemented in a 2D layer-cake reservoir. The polymer is intended to have a viscosity of 60 cp in-situ. Then, we allow that the polymer process might fail in-situ and viscosity could be 20% of that intended. This failure could be the result of mechanical degradation in surface facilities or on entering the perforations, faulty translation from laboratory-measured properties to properties in-situ, or faulty characterization of resident reservoir brine. Several of these adverse events would give different polymer properties in different regions of the reservoir. For simplicity, in this initial study we assume that throughout the reservoir polymer viscosity is less than that intended. We test whether the signals of this failure at the injection and production wells would be statistically significant in the midst of the geological uncertainty in the reservoir description. For a population of reservoirs representing geological uncertainty, we compare the deviation caused by loss of polymer viscosity to the scatter caused by the geological uncertainty using the 95% confidence interval statistical approach. Various signals are monitored to see which are the most reliable indications of whether a polymer viscosity was maintained in-situ. We further investigate the statistical significance of each signal. For this initial case study, the separate effects of adsorption, mixing with different brines in-situ, residual resistance factor, polymer degradation, shear-rate dependence (non-Newtonian behavior), permeability reduction and temperature have been ignored, except as they are represented indirectly in the loss of polymer viscosity.

2.2 PROPOSED WORKFLOW

Fig. 2.1 displays the key steps in discerning in-situ performance of an EOR process in the midst of geological uncertainty in a more organized structure. The left of the workflow shows two sources of uncertainty:

-uncertainty in the performance of the EOR process itself, where we identify a key EOR performance parameter and its value for a successful EOR process and in a failure: for example, the intended, or design, value of polymer viscosity in-situ and its value if the process fails.

-uncertainty in our knowledge of the subsurface, with the range of geological uncertainties represented by an ensemble of reservoir realizations.

The next step is to define and simulate the base case. A design EOR process is defined and simulated in the ensemble of geological representations. This design EOR process represents the successful intended EOR process. While an EOR process is in progress, there are a number of injection- or production-well data (signals) that reflect its performance in-situ. From the simulation results of the base case, we calculate the well signals of the design process. For each signal in the design process, based on the ensemble of reservoirs, we determine the 95% confidence interval (criteria for identifying an outlier). We then simulate what could represent a failed EOR process in the same ensemble of reservoirs (in this case study by dropping the design viscosity value to 20% of that intended). For each computed signal, we compare its value for the failed process to the confidence interval from the design process. When a given signal falls in the rejection-zone we label it as an outlier. If a signal reflects the process failure by being an outlier for all the reservoirs in the ensemble, it is a reliable indicator of process failure in the midst of geological uncertainty.

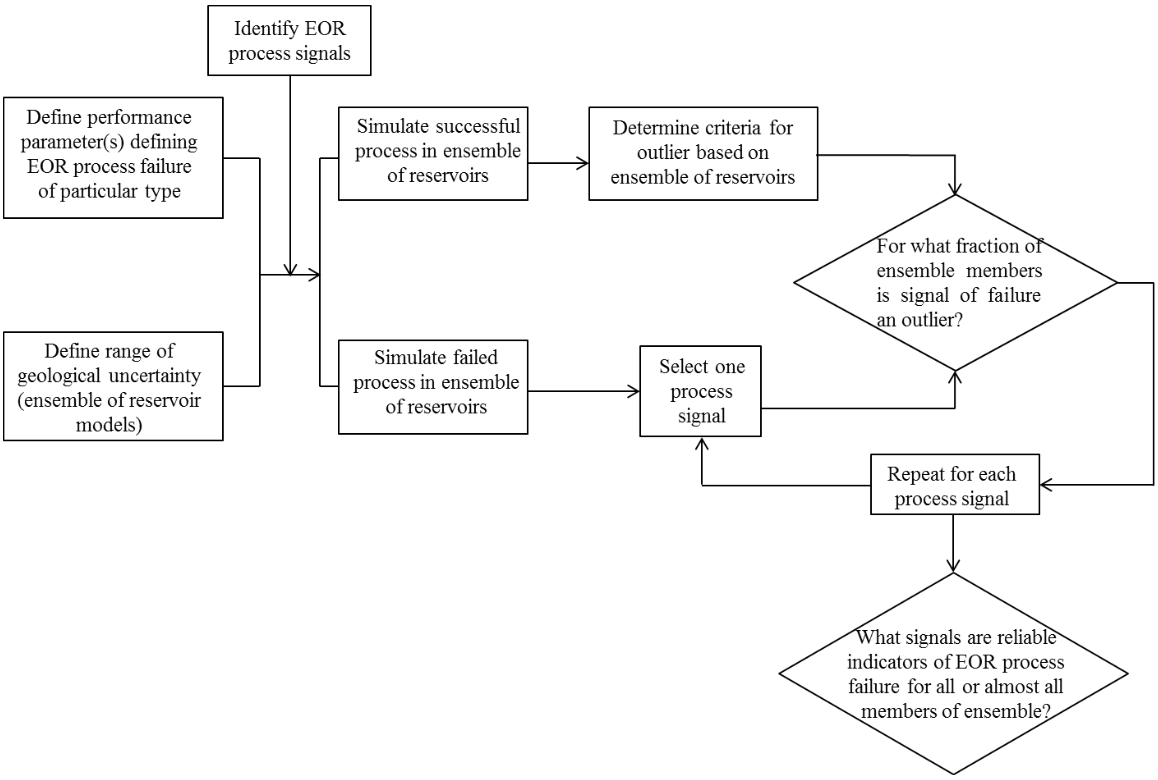
Identify EOR process signals
Define performance parameter(s) defining EOR process failure of particular type
Define range of geological uncertainty (ensemble of reservoir models)
Simulate successful process in ensemble of reservoirs
Simulate failed process in ensemble of reservoirs
Determine criteria for outlier based on ensemble of reservoirs
For what fraction of ensemble members is signal of failure an outlier?
Select one process signal
Repeat for each process signal
What signals are reliable indicators of EOR process failure for all or almost all members of ensemble?

Figure 2.1: Workflow to determine criteria to distinguish EOR process performance in-situ in the midst of geological uncertainties.

2.3 CASE STUDY

Table 2.1 presents the model dimensions and properties of the case study. The five-layer rectangular reservoir is shown in Fig. 2.2. Polymer-flood simulations were run with one injector and one producer, each penetrating the center of the first or last grid block in each layer. The producer bottom-hole pressure (BHP) is kept at 70 bars while the injector's BHP can go as high as 170 bars. The OOIP of the reservoir is 1382 m3. A polymer solution of 1200 ppm, which gives the viscosity of 60 cp in-situ at 150°F (based on the polymer-rheology algorithm in the simulator), is injected at a rate of 0.5 m3/day. Polymer viscosity reduces injectivity, but unintended fracturing near the wellbore during polymer injection can increase injectivity. The extent of this unintended fracturing may not be known (Seright et al., 2009). Therefore, for simplicity, we account for an uncertain extent of injectivity improvement due to fracturing by allowing the injector BHP in the simulation to be greater than what one would expect to be applied in a polymer EOR process.

Table 2.1: Reservoir dimensions

Description	Quantities	Units
Number of Grid Blocks (N_X, N_Y, N_Z)	25 × 1 × 5	-
Grid Block Size (Δx, Δy, Δz)	6.4 × 1 × 6.4	m
Total Dimensions	160 × 1 × 32	m
Porosity (φ)	0.3	

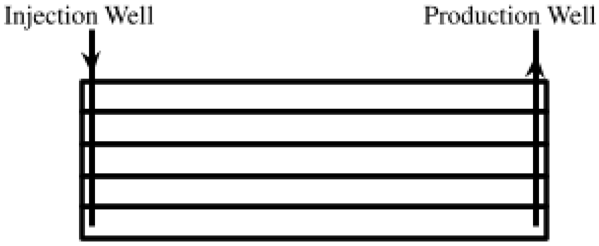

Figure 2.2: The case study: a five-layer rectangular reservoir with one producer and one injector.

Table 2.2 presents the reservoir and injected fluid properties. Water, oil and polymer-slug viscosity are constants in the simulations. Our case study fits the criteria for a polymer EOR candidate based on the screening benchmarks suggested in the literature (Alvarado and Manrique, 2010; Dickson et al., 2010; Saleh et al., 2014) as shown in Table 2.3.

Table 2.2: Case-study reservoir and injection fluid properties.

Description	Quantities	Units
Water density	1000	kg/m^3
Oil density	900	kg/m^3
Water viscosity	1.00×10^{-3}	Pa.s
Oil viscosity	60.00×10^{-3}	Pa.s
Water compressibility	1.00×10^{-10}	bar^{-1}
Oil compressibility	1.00×10^{-10}	bar^{-1}
Initial Reservoir Pressure	85	bar

Table 2.3: Suggested ranges of values for a reservoir candidate for a polymer flooding (Dickson et al., 2010 and Saleh et al., 2014).

	Suggested in Literature	**Case Study**
In-situ oil viscosity (cp)	10-1000	60
Average permeability, mD	>100 if (10<μ<100cp) >1000 if (100<μ<1000cp)	1000
Oil Saturation (%)	> 30%	90%

2.3.1 REPRESENTATION OF UNCERTAINTY IN POLYMER-FLOOD PERFORMANCE

We represent uncertainty in process performance using two different values of polymer viscosity in-situ: 12 cp and 60 cp. As mentioned above, for simplicity in this initial study, various detailed influential mechanisms on the polymer viscosity in-situ are excluded. In our simulations, we represent the failure to attain the design viscosity in-situ by injecting the polymer concentration corresponding to 12 cp (400 ppm) instead of that corresponding to 60 cp (1200 ppm). Since we exclude adsorption from our study, this change in polymer concentration in the simulation does not retard the advance of the polymer bank.

Appendix 2.A applies fractional-flow theory (Lake et al., 2014) to this polymer EOR process. It shows the incremental oil expected from a successful EOR process in 1D after 2 PV injection and loss in performance for the failed process. Fingering is not represented in this model, but the increase in mobility ratio at the shock suggests that the effects of heterogeneity would be worse in the failed process.

2.3.2 REPRESENTATION OF GEOLOGICAL UNCERTAINTY

Petroleum engineers usually consider permeability heterogeneity the most important source of uncertainty in reservoir performance (Craig, 1993). Modeling of permeability heterogeneities is usually based on a stochastic description, and realizations of such models are input parameters to reservoir simulators (Langtangen, 1991). We therefore represent geological uncertainty with a number of realizations reflecting a range of reservoir properties.

In this layer-cake model, each layer has a different permeability. The distribution of permeability values follows a log-normal distribution. The log-normal distribution has often been used to describe the permeability distribution of heterogeneous reservoirs (Dykstra and Parsons, 1956; Jensen et al., 2000; Lake et al., 2014). The degree of heterogeneity of a reservoir is often characterized by the dimensionless Dykstra-Parsons coefficient of permeability variation (Vdp). A homogeneous reservoir has a Vdp approaching zero, while an extremely heterogeneous reservoir would have a Vdp approaching one. A log-normal permeability distribution can be characterized by this coefficient and an average permeability (Craig, 1993; Hirasaki, 1984). To generate the permeability values for the five layers we use the inverse cumulative distribution function (CDF) of the log-normal distribution. Specifically, the permeability values are drawn from the 10%, 30%, 50%, 70% and 90% percentiles of the CDF. We adjust the magnitudes of the values so that all three distributions have the same arithmetic average permeability (Kavg). Therefore, in single-phase flow, injectivity would be the same for all the nine cases. Table 2.4 shows the permeability values generated for Vdp = 0.6, 0.75 and 0.9.

Table 2.4: Layer permeability values for V_{dp} = 0.6, 0.75 and 0.9; k_{avg} = 1000 md in all cases.

	Permeability Values (md)		
Percentile	$V_{dp} = 0.6$	$V_{dp} = 0.75$	$V_{dp} = 0.9$
0.1	218	84	9
0.3	444	244	53
0.5	726	511	189
0.7	1189	1067	664
0.9	2423	3093	4086

We assume three spatial distributions of permeability: specifically, from top to bottom, high-permeability to low-permeability, low-permeability to high-permeability, and a distribution with the lowest permeability in the middle. Fig. 2.3 shows schematically how layer permeabilities are ordered. Three Dykstra Parsons coefficients and three spatial arrangements of layers give nine different geological representations, to be used in simulations with two different polymer-flood in-situ viscosities.

This initial study illustrates the interplay between geological and process uncertainty using an extreme extent of geological uncertainty at the wellbore. A single successful well log could resolve much of this uncertainty. In the context of a layer-cake model, the range of layer permeabilities in our model represents the much larger uncertainty in reservoir properties between wells.

Appendix 2.B compares the competing effects of heterogeneity, gravity and arrangement of layers for the waterflood. Gravity reduces sweep efficiency in this case if the high-permeability layers are on the bottom, but is not as important as heterogeneity.

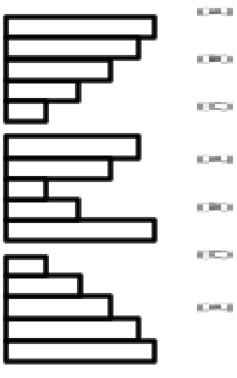

Figure 2.3: Schematic of spatial ordering of layer permeabilities.

2.4 DEVELOPMENT SCENARIO AND PROCEDURE

We run the polymer-flood simulations using Shell's in-house simulator MoReS (Van Doren et al., 2011). In each simulation, ten years of water injection is followed by twenty years of polymer-slug injection. A production/injection profile for one case is shown in Fig. 2.4.

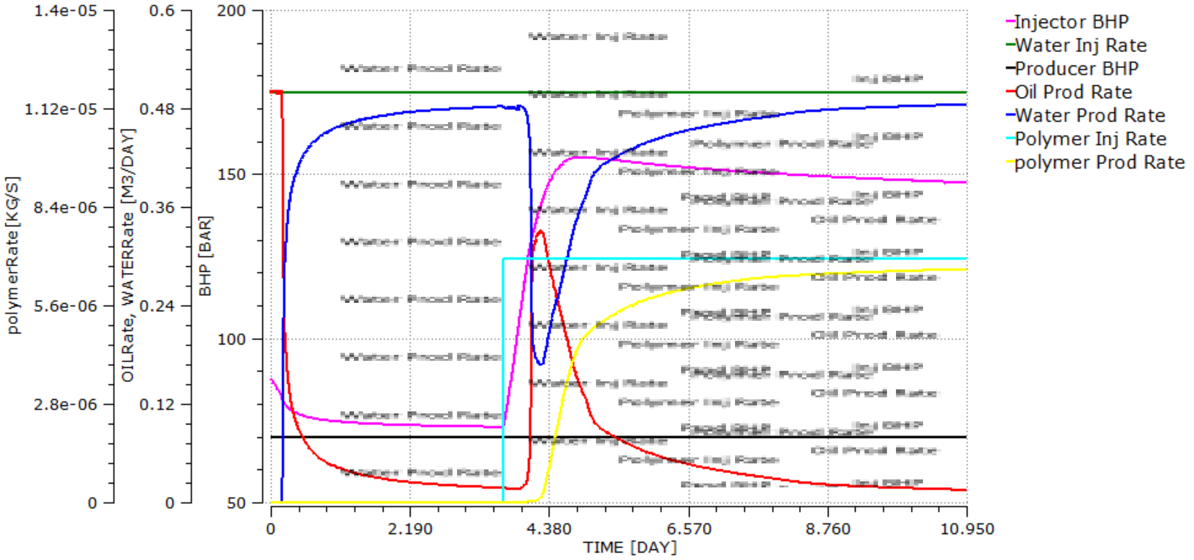

Figure 2.4: Production/injection profile for the geological description corresponding to $V_{dp} = 0.9$ and layer ordering of schematic A.

As shown in Fig. 2.4, water is injected for 10 years, and it breaks through early in the waterflood. A polymer slug is then injected and causes a rise in injection pressure and, later, incremental oil recovery, reflected in the rise in oil production shown in the red line. There are a number of signals that reflect the effectiveness of polymer:

- Polymer breakthrough time, years (Polymer BT)

- Rate of rise in P_{inj} upon polymer injection in six months, bars (Rise in P_{inj})

- Minimum oil cut (Min. oil cut)

- Time of initial increase in oil production rate, years (Oil Bank Arrival Time)

- Max injection pressure, bars (Max P_{inj})

- Cumulative oil production at end of process, m^3 (End Cumoil)

2.5 RESULTS

We allow that the polymer process might fail in-situ and viscosity could be 20% that intended. Fig. 2.5 shows a plot of the signal values of nine reservoir descriptions for a polymer viscosity in-situ of 60 cp and those for a viscosity of 12 cp. Fig. 2.5 shows that it is hardest to distinguish EOR process failure if the reservoir is relatively homogeneous (case 3, 6 and 9) and easiest if it lies toward the heterogeneous end of the spectrum of possibilities (cases 1, 4 and 7). Increasing reservoir heterogeneity produces results similar to EOR process failure in-situ: earlier polymer breakthrough and reduced cumulative oil recovery.

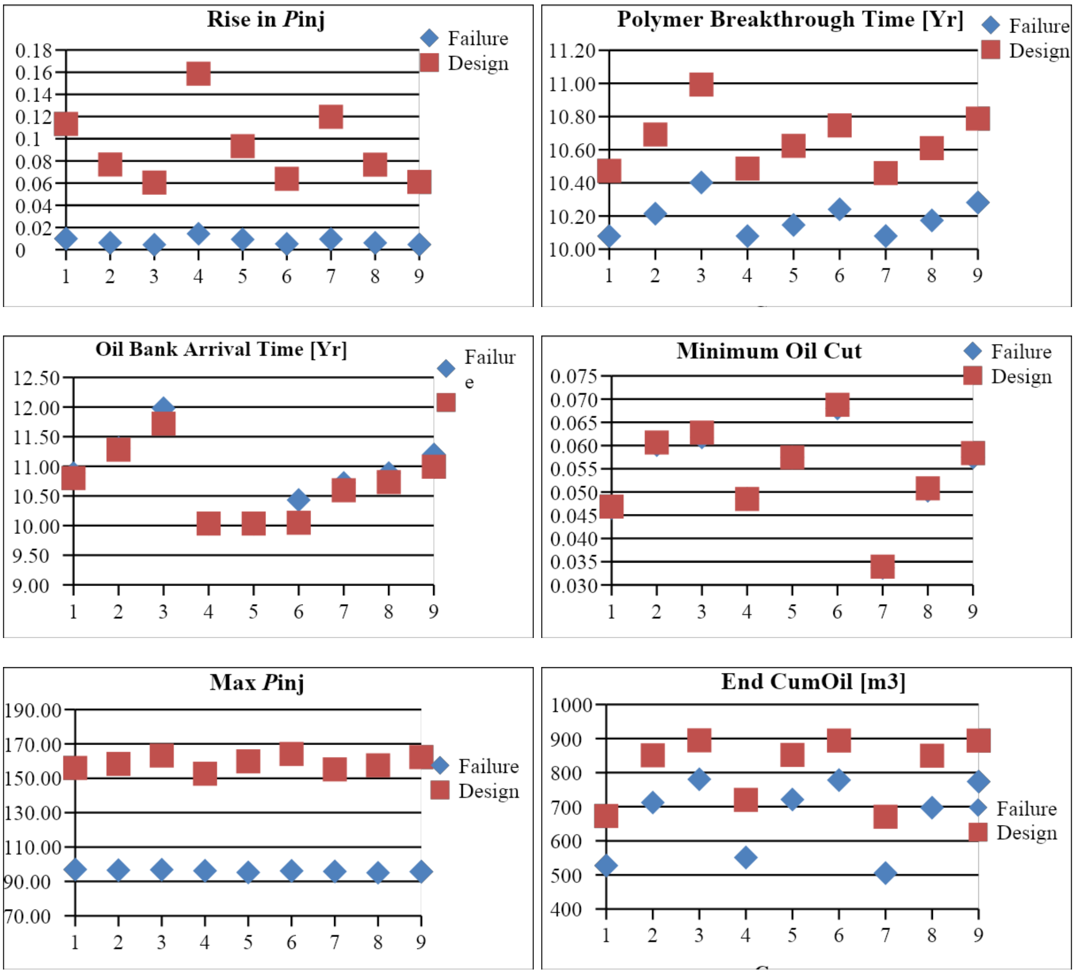
Rise in *Pinj*

Polymer Breakthrough Time [Yr]

Oil Bank Arrival Time [Yr]

Minimum Oil Cut

Max *Pinj*

End CumOil [m3]

Figure 2.5: Comparing signals of the process with 60 cp polymer viscosity (design) with the 12 cp polymer viscosity (failure)

Comparing the signals listed above we test whether the signals of this viscosity difference would be statistically significant (using the 95% confidence interval) in the midst of the geological uncertainty, represented by the nine reservoir descriptions. Specifically, we calculate the 95% confidence interval for each signal for the nine geological cases with 60 cp polymer viscosity. Refer to Appendix 2.C for more details on how to calculate the t-distribution 95% confidence interval. The results are shown in Table 2.5.

Table 2.5: Signal values calculated for the nine geological cases with 60 cp polymer viscosity, with upper and lower bounds of the 95% confidence interval (CI+, CI-) for each signal.

Case no.	Perm. Distribution	*Vdp*	Rise in P_{inj}	Polymer BT [Yr]	Oil Bank Arrival Time [Yr]	Min. oil cut	Max Pinj [Bar]	Cumoil at End [m^3]
1	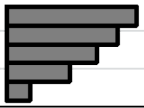	**0.9**	0.113	10.47	10.80	0.047	156.00	672.87
2		**0.75**	0.077	10.69	11.28	0.061	158.34	850.90
3		**0.6**	0.060	10.99	11.72	0.063	163.21	894.80
4	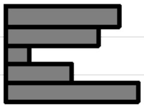	**0.9**	0.159	10.49	10.03	0.049	152.64	720.13
5		**0.75**	0.093	10.62	10.03	0.057	159.84	852.03
6		**0.6**	0.064	10.75	10.05	0.069	164.15	894.17
7	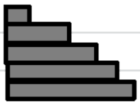	**0.9**	0.120	10.46	10.60	0.034	155.17	670.63
8		**0.75**	0.077	10.61	10.73	0.051	157.53	849.76
9		**0.6**	0.061	10.79	10.99	0.058	162.31	894.04
	Mean		0.09	10.65	10.69	0.05	158.80	811.04
	STD		0.03	0.17	0.59	0.01	3.91	95.30
	t*@95%	2.308						
	CI +		0.17	11.06	12.06	0.08	167.82	1030.99
	CI -		0.01	10.25	9.33	0.03	149.78	591.09

For each reservoir description we then ask if the given signal with 12 cp polymer viscosity lies in the rejection zone of the 95% confidence interval. If the answer is yes, then the signal is an outlier and failure of polymer in-situ is discernible in the midst of geological uncertainty. Table 2.6 shows the signal values for the cases with an in-situ viscosity of 12 cp. Next to each column with this signal value, a second column checks if the individual value falls in the rejection zone of results with 60 cp viscosity from Table 2.5. If the signal value falls in the rejection, it is labelled as an “Outlier” in the adjacent column (meaning the signal can be distinguished in the midst of geological uncertainty). Otherwise the entry is left as blank in the adjacent column, meaning the signal cannot be distinguished from geological uncertainty.

Table 2.6: Discerning the process with 12 cp polymer viscosity from the case with 60 cp polymer viscosity.

Case no.	Perm. Distribution	*Vdp*	Rise in P_{inj}		Polymer BT [Yr]		Oil Bank Arrival Time [Yr]		Min. Oil Cut		Max P_{inj} [Bar]		End Cumoil [m^3]	
1	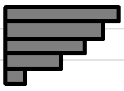	**0.9**	0.010	Outlier	10.08	Outlier	10.88	-	0.047	-	96.91	Outlier	527.5	Outlier
2		**0.75**	0.006	Outlier	10.21	Outlier	11.31	-	0.060	-	96.48	Outlier	712.3	-
3		**0.6**	0.004	Outlier	10.40	-	11.98	-	0.062	-	96.80	Outlier	780.6	-
4	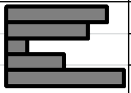	**0.9**	0.014	Outlier	10.08	Outlier	10.03	-	0.049	-	96.19	Outlier	550.9	Outlier
5		**0.75**	0.009	Outlier	10.15	Outlier	10.03	-	0.057	-	95.24	Outlier	721.1	-
6		**0.6**	0.005	Outlier	10.24	Outlier	10.43	-	0.068	-	96.12	Outlier	778	-
7	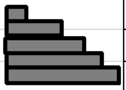	**0.9**	0.009	Outlier	10.08	Outlier	10.72	-	0.034	-	95.82	Outlier	505.4	Outlier
8		**0.75**	0.006	Outlier	10.17	Outlier	10.88	-	0.050	-	95.02	Outlier	697.3	-
9		**0.6**	0.005	Outlier	10.28	-	11.20	-	0.057	-	95.64	Outlier	773.7	-

Of the signals considered, there are two columns labelled entirely as outliers. One could discern the effect of viscosity with confidence in every case based on the 'rate of rise in Pinj in six months' and 'max injection pressure'. These two signals could discern the failure of the polymer in-situ in the midst of geological uncertainty. In both cases, the rise in pressure is less than with the greater polymer viscosity, as expected. 'Polymer breakthrough time' could discern the effect of viscosity in majority of the cases excluding the next homogeneous case. For 'cumulative oil production at end of simulation', failure can be discerned only in the most heterogeneous cases.

In this case study, we deal with an extreme reservoir heterogeneity description. Only when there is a severe in-situ viscosity loss is the difference in signals between the two populations statistically significant. Refer to Appendix 2.D for more results for different extent of in-situ viscosity loss. When there is a 10% viscosity loss, only the 'max Pinj' signal can discern the more heterogeneous cases. As the extent of viscosity loss increases, this effect is more statistically significant among the signals. In the very extreme in-situ viscosity loss of 90%, 'rate of rise in Pinj in six months', 'polymer breakthrough time' and 'max injection pressure' could discern the failure of the polymer in-situ in the midst of geological uncertainty in all of the cases and 'cumulative oil production at end of simulation' discerns the effect in the more heterogeneous cases.

2.6 CONCLUSIONS AND DISCUSSION

- We offer a workflow and a simple initial study of a polymer flood to illustrate the issues involved in attempting to distinguish EOR process performance from well data in the midst of geological uncertainty.

- Among the signals considered here, the rate of rise in injection pressure upon polymer injection and maximum pressure in the injection well give the most reliable indications of whether polymer viscosity was maintained in-situ. Given the chances of fracturing of the injection well (Seright et al., 2009), especially if the extent of this fracturing is unknown, injection pressure could be an unreliable indicator of in-situ polymer viscosity injection. In that case a diagnostic fracture-injection / falloff test could substitute for the well pressure data (Craig and Jackson, 2017).
- Among the other signals considered, it was hardest to distinguish failure of the EOR process in reservoirs that, among the ensemble of equi-probable reservoirs, were relatively homogeneous. For these cases waterflood by itself performed relatively well; the failure of the EOR process was hard to distinguish from the possibility of greater reservoir heterogeneity. Failure was easiest to identify if the actual reservoir was among the more heterogeneous cases considered possible. In that case the additional loss in performance from failure of the EOR process produced a result outside the confidence interval.
- Previous studies that considered the effect of geological uncertainty on EOR process performance, establish the range of outcomes for a process that performs in-situ as designed. In effect, they establish the confidence interval beyond which a failed EOR process could be identified.
- The range of geological uncertainty in this initial case study could be viewed as extreme. We assume that injectivity is known but that very little is known about the extent of reservoir heterogeneity, even at the wells. On the other hand, the extent of failure of the polymer in-situ, i.e. a loss of viscosity by a factor of 5, could be considered extreme as well. Moreover, we consider a two-well situation whereas in a multi-well setting the effect of viscosity changes may result in different signals in the various wells. Further study should include more realistic geological descriptions and polymer mechanisms and the effect of including more wells.

APPENDIX 2.A: FRACTIONAL-FLOW THEORY IN POLYMER FLOODING

It is useful to perform a 1D fractional-flow analysis of a reservoir to identify whether is suitable for a particular recovery process before undertaking a detailed reservoir simulation study. One of the simplest and most widely used methods of estimating the displacement efficiency in an immiscible displacement process is the Buckley-Leverett method (Fanchi, 2005; Craft et al., 1991; Dake, 2001; Lake et al., 2014). Our purpose here is to compare the displacement efficiency in 1D for the design polymer flood versus the reduced-viscosity polymer flood. The polymer-oil fractional flow curve is constructed and shown in Fig. 2.A.1 and Fig. 2.A.2 for two cases, one with the polymer design viscosity of 60 cp and the other with reduced polymer viscosity of 12 cp. Polymer injection reduces the mobility ratio, causing the fw(Sw) curves to shift to the right. The greater the polymer viscosity the more the polymer-flood curve shifts to the right. The recovery of the 1D polymer flood at polymer breakthrough, mobility ratio at shock front and recovery at 2 PV injection can be extracted from the fractional-flow diagram, as shown in Table 2.A.1. Although the case shown in Fig. 2.A.1 and Fig. 2.A.2 is a secondary polymer flood, the mobility ratio at the shock front and recovery after 2 PV injection would be identical for polymer floods in secondary and tertiary modes.

Table 2.A.1: Recoveries after polymer breakthrough for the design viscosity case versus reduced viscosity.

	Waterflood	**Design viscosity, 60 cp**	**Reduced viscosity, 12 cp**
Oil recovery at breakthrough, %	28%	0.55	0.46
Mobility ratio at shock front[a]	1.47	0.12	0.76
Fraction of movable oil recovered at 2 PV injection[b]		0.97	0.92

[a] Mobility behind the front divided by mobility ahead of the front

[b] $(S_{wavg} - S_{wc}) / (1 - S_{wc} - S_{or})$

Table 2.A.1 shows that even in a homogenous 1D reservoir without gravity segregation there is less oil recovered at polymer breakthrough and after 2 PV injection with the lower viscosity. The mobility ratio at the shock front is smaller for the design viscosity than the reduced viscosity, which suggests a better mobility control and more uniform sweep in a 2D heterogeneous reservoir for the design viscosity case.

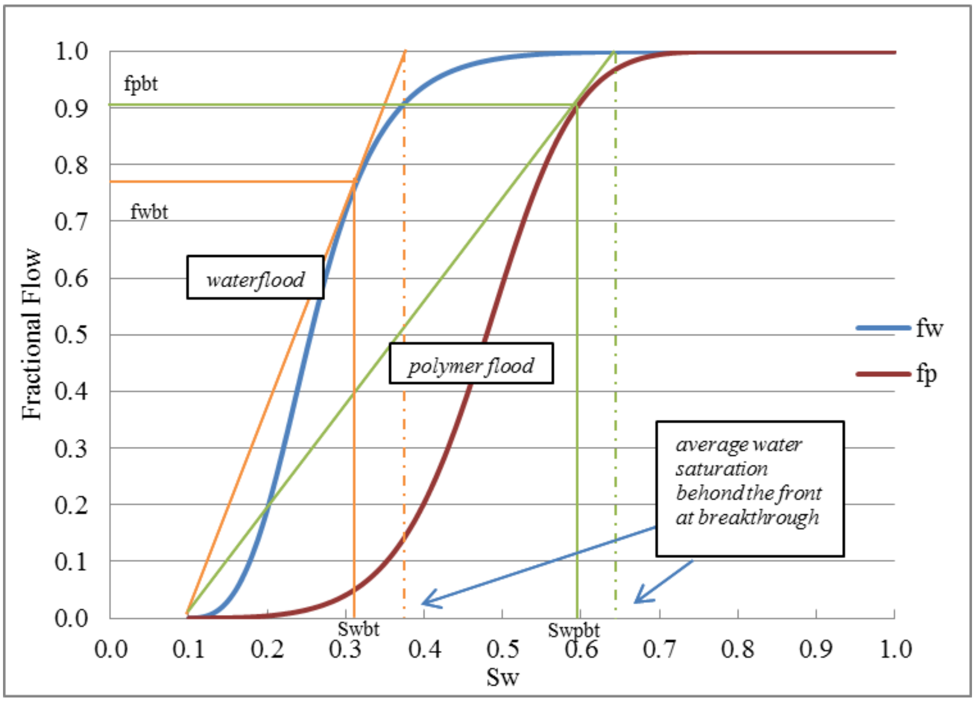

Figure 2.A.1: Graphical construction of water and polymer fractional flow in secondary mode for the design polymer in-situ viscosity of 60 cp.

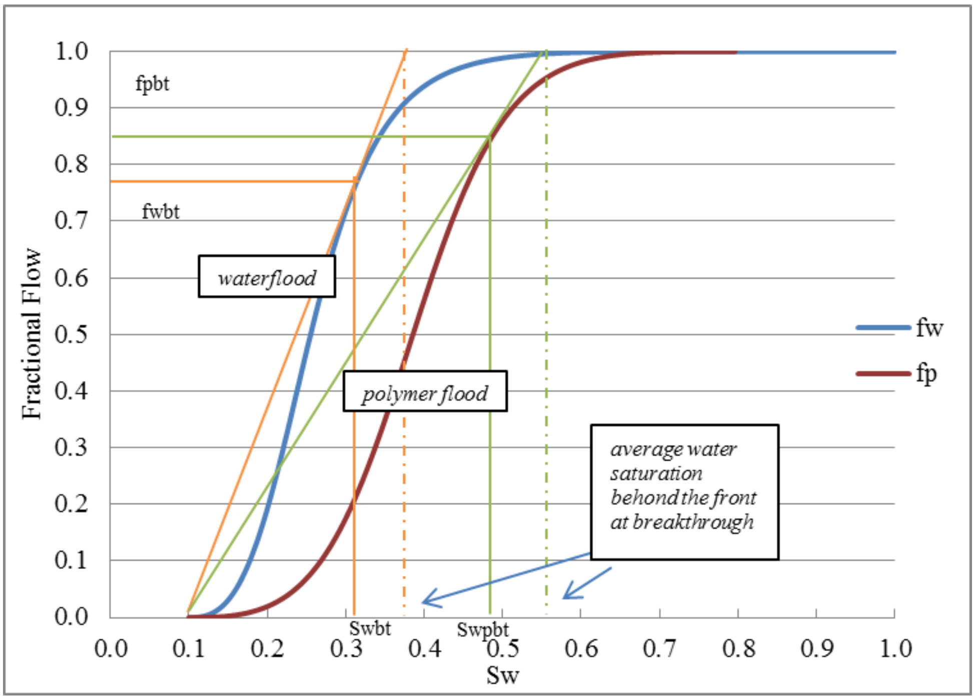

Figure 2.A.2: Graphical construction of water and polymer fractional flow in secondary mode for the reduced polymer in-situ viscosity of 12 cp.

APPENDIX 2.B: EFFECT OF GRAVITY

Gravitational force affects crossflow in communicating layers. These forces tend to increase the water saturation on the bottom layers (Craig, 1993). Fig. 2.4 shows the oil recovery during the waterflood phase of our case study for different levels of heterogeneity and layer ordering. As this figure shows, arrangement of the layers plays a less-important role than the effect of heterogeneity. This suggests gravity is not dominant on our case-study results. With the high-permeable layer on the top and the permeability decreasing with depth (schematic A in Fig. 2.3), gravity tends to increase oil recovery. Gravity reduces oil recovery for the permeability arrangement in which permeability increases with depth (schematic C in Fig. 2.3). If gravity was not relevant at all, permeability arrangements in schematics A and C would behave identically, but, as Fig. 2.4 shows, oil recovery is not the same for the two permeability arrangements; hence the arrangement of layers matters in this case study.

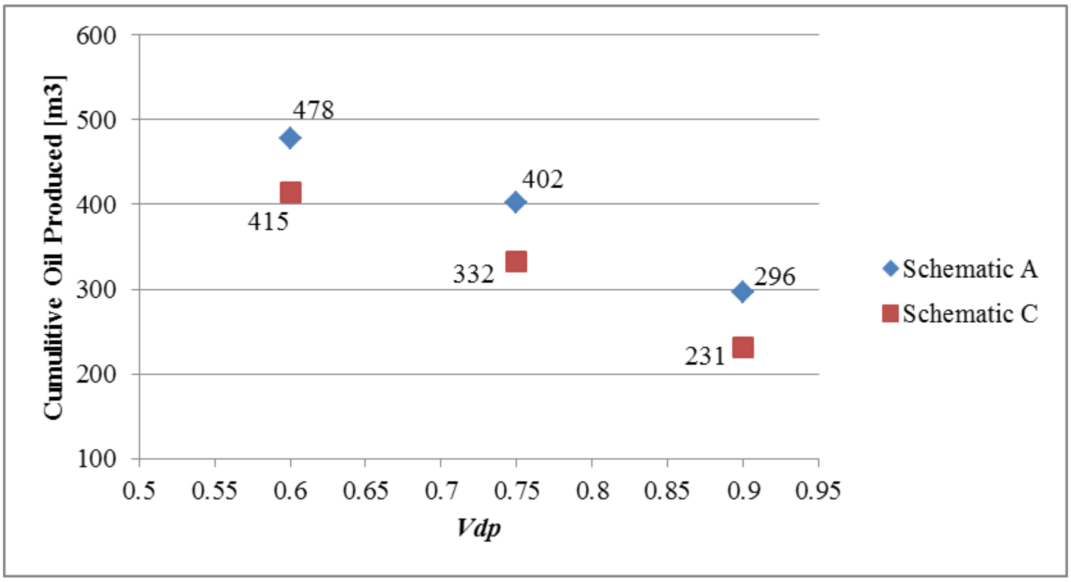

Figure 2.B.1: Effect of gravity on Cumulative Oil Production (after 10 years of waterflood) in different permeability arrangements.

APPENDIX 2.C: CONFIDENCE INTERVALS BASED ON THE t-DISTRIBUTION

The confidence interval is an estimate of the range in which a given percentage of a statistical population lies. If a datum lies outside the 95% confidence interval, there is less than 5% chance that a randomly selected member of that population would be so far from the population mean. Though imperfect, this is a standard test for the likelihood that a new case is derived from the same statistical population as the original sample Hawkins (1980).

The confidence interval (CI) is inferred from the mean, X_{avg}, and standard deviation, σ, of a sample from the population using the t statistic:

$$CI = X_{avg} \pm t^{*} \sigma \qquad (2.C.1)$$

The value of t* for the 95% confidence interval for a set of 9 data samples (8 degrees of freedom) is 2.306.

APPENDIX 2.D: DIFFERENT SCENARIOS OF POLYMER IN-SITU VISCOSITY LOSS

Here we present different scenarios of polymer in-situ viscosity loss (10%, 20%, 50%, 60%, 70% and 90%) and the associated effect on different well signals.

Table 2.D.1: Discerning the process with 54 cp polymer viscosity from the case with 60 cp polymer viscosity.

Perm. Distribution	*Vdp*	Rise in P_{inj}		Polymer BT [Yr]		Oil Bank Arrival Time [Yr]		Min. Oil Cut		Max P_{inj} [Bar]		End Cumoil [m^3]	
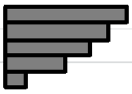	**0.9**	0.101	-	10.23	Outlier	10.73	-	0.047	-	146.94	Outlier	658.56	-
	0.75	0.068	-	10.36	-	11.27	-	0.061	-	148.48	Outlier	839.93	-
	0.6	0.053	-	10.55	-	11.84	-	0.063	-	152.68	-	886.15	-
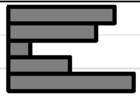	**0.9**	0.144	-	10.24	Outlier	10.03	-	0.049	-	143.32	Outlier	706.09	-
	0.75	0.084	-	10.31	-	10.03	-	0.057	-	149.67	Outlier	841.44	-
	0.6	0.056	-	10.39	-	10.05	-	0.069	-	153.67	-	885.46	-
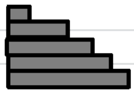	**0.9**	0.106	-	10.24	Outlier	10.60	-	0.034	-	145.89	Outlier	655.93	-
	0.75	0.068	-	10.32	-	10.80	-	0.051	-	147.55	Outlier	838.32	-
	0.6	0.054	-	10.43	-	11.10	-	0.058	-	151.72	-	885.27	-

Table 2.D.2: Discerning the process with 48 cp polymer viscosity from the case with 60 cp polymer viscosity.

Perm. Distribution	*Vdp*	Rise in P_{inj}		Polymer BT [Yr]		Oil Bank Arrival Time [Yr]		Min. Oil Cut		Max P_{inj} [Bar]		End Cumoil [m^3]	
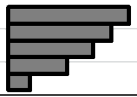	**0.9**	0.089	-	10.21	Outlier	10.79	-	0.047	-	137.92	Outlier	642.71	-
	0.75	0.060	-	10.34	-	11.21	-	0.061	-	138.70	Outlier	826.72	-
	0.6	0.046	-	10.53	-	11.79	-	0.063	-	142.27	Outlier	876.04	-
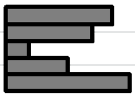	**0.9**	0.129	-	10.22	Outlier	10.03	-	0.049	-	134.69	Outlier	689.96	-
	0.75	0.075	-	10.29	-	10.03	-	0.057	-	139.56	Outlier	828.94	-
	0.6	0.049	-	10.38	-	10.05	-	0.069	-	143.27	Outlier	875.18	-
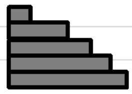	**0.9**	0.093	-	10.22	Outlier	10.60	-	0.034	-	136.70	Outlier	639.32	-
	0.75	0.059	-	10.30	-	10.79	-	0.051	-	137.66	Outlier	824.62	-
	0.6	0.047	-	10.41	-	11.05	-	0.058	-	141.24	Outlier	874.79	-

Table 2.D.3: Discerning the process with 30 cp polymer viscosity from the case with 60 cp polymer viscosity.

Perm. Distribution	***Vdp***	**Rise in P_{inj}**		**Polymer BT [Yr]**		**Oil Bank Arrival Time [Yr]**		**Min. Oil Cut**		**Max P_{inj} [Bar]**		**End Cumoil [m^3]**	
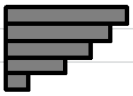	**0.9**	0.05	-	10.17	Outlier	10.84	-	0.047	-	122.34	Outlier	610.89	-
	0.75	0.033	-	10.30	-	11.29	-	0.060	-	122.25	Outlier	796.56	-
	0.6	0.025	-	10.48	-	11.83	-	0.062	-	124.65	Outlier	852.97	-
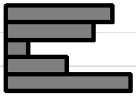	**0.9**	0.074	-	10.17	Outlier	10.03	-	0.049	-	120.71	Outlier	655.19	-
	0.75	0.043	-	10.24	Outlier	10.03	-	0.057	-	122.14	Outlier	801.46	-
	0.6	0.027	-	10.33	-	10.05	-	0.069	-	125.32	Outlier	851.74	-
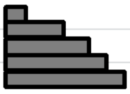	**0.9**	0.052	-	10.17	Outlier	10.72	-	0.034	-	121.10	Outlier	605.55	-
	0.75	0.033	-	10.26	-	10.87	-	0.051	-	121.02	Outlier	792.84	-
	0.6	0.026	-	10.36	-	11.10	-	0.058	-	123.48	Outlier	851.02	-

Table 2.D.4: Discerning the process with 24 cp polymer viscosity from the case with 60 cp polymer viscosity.

Perm. Distribution	***Vdp***	**Rise in P_{inj}**		**Polymer BT [Yr]**		**Oil Bank Arrival Time [Yr]**		**Min. Oil Cut**		**Max P_{inj} [Bar]**		**End Cumoil [m^3]**	
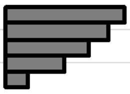	**0.9**	0.028	-	10.14	Outlier	10.79	-	0.047	-	115.43	Outlier	593.7	-
	0.75	0.018	-	10.27	-	11.23	-	0.060	-	115.04	Outlier	778.74	-
	0.6	0.014	Outlier	10.46	-	11.88	-	0.062	-	116.86	Outlier	839.14	-
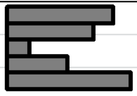	**0.9**	0.042	-	10.14	Outlier	10.03	-	0.049	-	114.10	Outlier	634.75	-
	0.75	0.025	-	10.21	Outlier	10.03	-	0.057	-	114.29	Outlier	785.28	-
	0.6	0.015	-	10.30	-	10.06	-	0.069	-	117.21	Outlier	837.75	-
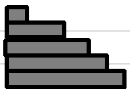	**0.9**	0.029	-	10.15	Outlier	10.69	-	0.034	-	114.18	Outlier	585.61	Outlier
	0.75	0.018	-	10.23	Outlier	10.72	-	0.051	-	113.72	Outlier	773.88	-
	0.6	0.014	Outlier	10.34	-	11.09	-	0.058	-	115.59	Outlier	836.73	-

Table 2.D.5: Discerning the process with 18 cp polymer viscosity from the case with 60 cp polymer viscosity.

Perm. Distribution	***Vdp***	**Rise in P_{inj}**		**Polymer BT [Yr]**		**Oil Bank Arrival Time [Yr]**		**Min. Oil Cut**		**Max P_{inj} [Bar]**		**End Cumoil [m^3]**	
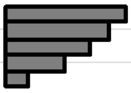	**0.9**	0.016	-	10.12	Outlier	10.90	-	0.047	-	102.96	Outlier	552.59	Outlier
	0.75	0.011	Outlier	10.25	-	11.27	-	0.060	-	102.26	Outlier	737.26	-
	0.6	0.008	Outlier	10.46	-	12.02	-	0.062	-	103.01	Outlier	803.76	-
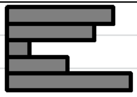	**0.9**	0.025	-	10.12	Outlier	10.03	-	0.049	-	101.69	Outlier	583.49	Outlier
	0.75	0.015	-	10.18	Outlier	10.03	-	0.057	-	100.62	Outlier	745.85	-
	0.6	0.009	Outlier	10.28	-	10.06	-	0.068	-	102.65	Outlier	801.84	-
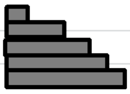	**0.9**	0.016	-	10.13	Outlier	10.71	-	0.034	-	101.74	Outlier	535.88	Outlier
	0.75	0.010	Outlier	10.21	Outlier	10.88	-	0.050	-	100.82	Outlier	728.46	-
	0.6	0.008	Outlier	10.32	-	11.14	-	0.058	-	101.74	Outlier	799.54	-

Table 2.D.6: Discerning the process with 9 cp polymer viscosity from the case with 60 cp polymer viscosity.

Perm. Distribution	***Vdp***	**Rise in P_{inj}**		**Polymer BT [Yr]**		**Oil Bank Arrival Time [Yr]**		**Min. Oil Cut**		**Max P_{inj} [Bar]**		**End Cumoil [m^3]**	
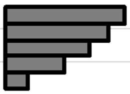	**0.9**	0.007	Outlier	9.93	Outlier	10.88	-	0.046	-	90.93	Outlier	500.74	Outlier
	0.75	0.004	Outlier	10.07	Outlier	11.34	-	0.060	-	90.85	Outlier	682.68	-
	0.6	0.003	Outlier	10.26	-	12.05	-	0.062	-	91.02	Outlier	752.26	-
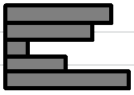	**0.9**	0.010	Outlier	9.93	Outlier	10.03	-	0.049	-	90.92	Outlier	513.71	Outlier
	0.75	0.007	Outlier	9.99	Outlier	10.03	-	0.057	-	89.96	Outlier	691.27	-
	0.6	0.004	Outlier	10.08	Outlier	10.60	-	0.068	-	90.17	Outlier	749.36	-
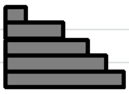	**0.9**	0.006	Outlier	9.94	Outlier	10.77	-	0.034	-	90.02	Outlier	470.93	Outlier
	0.75	0.004	Outlier	10.02	Outlier	10.92	-	0.050	-	89.32	Outlier	654.64	-
	0.6	0.003	Outlier	10.12	Outlier	11.31	-	0.057	-	89.79	Outlier	740.29	-

Table 2.D.7: Discerning the process with 6 cp polymer viscosity from the case with 60 cp polymer viscosity.

Perm. Distribution	***Vdp***	**Rise in P_{inj}**		**Polymer BT [Yr]**		**Oil Bank Arrival Time [Yr]**		**Min. Oil Cut**		**Max P_{inj} [Bar]**		**End Cumoil [m^3]**	
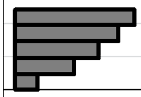	**0.9**	0.005	Outlier	9.88	Outlier	11.01	-	0.046	-	87.56	Outlier	442.36	Outlier
	0.75	0.003	Outlier	10.01	Outlier	11.53	-	0.059	-	87.49	Outlier	585.12	Outlier
	0.6	0.002	Outlier	10.21	Outlier	12.27	Outlier	0.061	-	87.42	Outlier	675.11	-
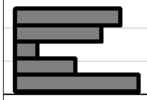	**0.9**	0.006	Outlier	9.87	Outlier	10.03	-	0.049	-	87.38	Outlier	413.58	Outlier
	0.75	0.005	Outlier	9.94	Outlier	10.03	-	0.057	-	87.46	Outlier	589.29	Outlier
	0.6	0.003	Outlier	10.03	Outlier	10.91	-	0.066	-	87.34	Outlier	662.27	-
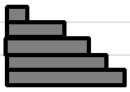	**0.9**	0.005	Outlier	9.88	Outlier	10.98	-	0.033	-	87.36	Outlier	370.96	Outlier
	0.75	0.003	Outlier	9.97	Outlier	11.13	-	0.050	-	87.28	Outlier	531.38	Outlier
	0.6	0.002	Outlier	10.08	Outlier	11.55	-	0.056	-	88.51	Outlier	632.29	-

3

DISCERNING IN-SITU PERFORMANCE OF AN EOR AGENT IN THE MIDST OF GEOLOGICAL UNCERTAINTY: II. FLUVIAL-DEPOSIT RESERVOIR

An enhanced-oil-recovery (EOR) pilot test has multiple goals, among them to make money (if possible), demonstrate oil recovery, verify the properties of the EOR agent in-situ, and provide the information needed for scale-up to an economic process. Given the complexity of EOR processes and the inherent uncertainty in the reservoir description, it is a challenge to discern the properties of the EOR agent in-situ in the midst of geological uncertainty. We propose a numerical case study to illustrate this challenge: a polymer EOR process designed for a 3D fluvial-deposit water-oil reservoir. The polymer is designed to have a viscosity of 20 cp in-situ. We start with 100 realizations of the 3D reservoir to reflect the range of possible geological structures honoring the statistics of the initial geological uncertainties. For a population of reservoirs representing reduced geological uncertainty after five years of waterflooding, we select three groups of 10 realizations out of the initial 100 with similar

---

This chapter is from the published article: S. A. Fatemi; J. D. Jansen; W. R. Rossen, 2019. Discerning In-Situ Performance of an Enhanced-Oil-Recovery Agent in the Midst of Geological Uncertainty: II. Fluvial-Deposit Reservoir. *SPE J.* 24 (03): 1076–1091.

water breakthrough dates at the four production wells. We then simulate five years of polymer injection. We allow that the polymer process might fail in-situ and viscosity could be 30% that intended. We test whether the signals of this difference at injection and production wells would be statistically significant in the midst of the geological uncertainty. Specifically, we compare the deviation caused by loss of polymer viscosity to the scatter caused by the geological uncertainty using a 95% confidence interval. Among the signals considered, polymer breakthrough time, minimum oil cut and rate of rise in injection pressure with polymer injection give the most reliable indications of whether a polymer viscosity was maintained in-situ. Unfortunately, given the likelihood of an unknown extent of fracturing of the injection well, injection pressure may be an unreliable indicator of in situ polymer viscosity.

3.1 INTRODUCTION

Chemical EOR processes represent a small fraction of commercially successful EOR projects. This is mainly due to uncertainty in predictions of processes (Sheng, 2011; Lake et al., 2014). For polymer flooding, the integrity of polymer viscosity is essential for the effectiveness of the process and its behavior can be uncertain (Weiss and Baldwin, 1985). Evaluation of the impact of uncertainties in the performance of an EOR process to increase the possibility of success and predict possible failure is of prime importance because a process that did not achieve the desired objectives in one formation might be successful in another field if it demonstrates that it achieves its technical objectives.

Researchers have studied uncertainty in EOR process performance and uncertainty in the geological description, but not the two together. Previous research has examined uncertainty in performance parameters of surfactant-flooding (interfacial tension) and CO_2-EOR (asphaltene deposition or minimum miscibility pressure) performance parameters including Brown and Smith (1984), Denney (2011) and Stanley (2014). There have also been studies on the effect of geological heterogeneities and their uncertainty on how an EOR process performs. Heterogeneity and geological factors have different impacts on the various EOR processes, including polymer and alkaline-surfactant-polymer, thermal and gas-injection (miscible and immiscible) EOR. Studies of the effects of geological heterogeneity and uncertainty on EOR performance include Kumar et al. (2008), Chen et al. (2008), Soleimani et al. (2011) and Popov et al. (2010).

In this paper we investigate the impact of both sources of uncertainty together in a statistical approach based on the workflow described in Fatemi et al. (2017). The workflow displays the key steps in discerning in-situ performance of an EOR process in the midst of geological uncertainty in an organized structure where two sources of uncertainty are defined, uncertainty in the performance of the EOR process itself and uncertainty in our knowledge of the subsurface. In the earlier work we used for illustration a layer-cake model with an extreme level of geological uncertainty; here we apply the workflow to a case with a more sophisticated geological model and a level of uncertainty more representative of a field after a period of waterflood. In the earlier work we used for illustration a layer-cake model with an extreme level of geological uncertainty; here we apply the workflow to a case with a more realistic geological model and a level of uncertainty more representative of a field after a period of waterflood. We present a case study based on the “modified Egg Model” (Jansen et al., 2014) to illustrate this challenge: a polymer EOR process designed for a 3D fluvial-deposit water-oil reservoir. The polymer is designed to have a viscosity of 20 cp in situ. We start with 100 realizations of this 3D reservoir to reflect the range of possible geological structures honoring the statistics of the initial geological uncertainties. Next we group the realizations on the basis of a measure of similarity that reflects the interaction between heterogeneity and the reservoir flow mechanisms (Mantilla and Srinivasan, 2011). After five years of waterflooding, we rank the reservoir models in different groups of 10 realizations, out of the initial 100 equiprobable realizations, with similar water breakthrough dates at the four production wells. We form three sets of 10-member realizations and apply the methodology accordingly.

For a polymer flood to meet its technical success, we want the polymer in situ viscosity (as one of the more important properties of the polymer process design) to meet its technical design value. Then, to represent EOR process failure, we allow that the polymer process might fail in situ and viscosity could be 30% of that intended. This failure could be the result of mechanical degradation in surface facilities or on entering the perforations, faulty translation from laboratory-measured properties to properties in situ, faulty characterization of resident reservoir brine, or chemical or biological degradation of polymer. We then simulate five years of polymer injection. We assume that throughout the reservoir polymer viscosity is less than that the design value. We test whether the signals of this difference at injection and production wells would be statistically significant in the midst of the geological uncertainty. Specifically, we compare the deviation caused by loss of polymer viscosity to the scatter caused by the geological uncertainty using a 95% confidence interval. Various signals are monitored to see which are the most reliable indications of whether a polymer viscosity was maintained in situ. We further investigate the statistical significance of each signal.

Any EOR field trial can produce unexpected results arising from a misunderstanding of either the geology of the reservoir or of the EOR process. The workflow presented here could be applied to other EOR processes by defining possible mechanism of failure for those processes. Interpolation of field pilot results requires the ability to distinguish the effects of geological and process-performance uncertainty.

3.2 CASE STUDY DESCRIPTION

We consider a modified version of the standard “Egg Model”, which is a fluvial-deposit water-oil reservoir model containing eight injection wells and four production wells (Jansen et al., 2014 based on earlier work by Van Essen et al., 2009). The model has seven layers and contains 18,553 grid blocks, 8×8×4 m in size. Production from the reservoir is simulated over a time horizon of five years of waterflood followed by five years of polymer flood. The average reservoir pressure is set at 400 bar, and the initial water saturation is taken to be uniform over the reservoir at a value of 0.1. The remaining geological and fluid properties used in this case study are presented in Table 3.1. The reservoir is located in a fluvial depositional environment with known main flow direction. A set of 100 geological realizations of the reservoir was generated by van Essen based on geological insight rather than a geostatistical method. The number of 100 realizations is assumed to be large enough to be a good representation of this range (Van Essen et al., 2009). We have modified the oil viscosity in this model to make the reservoir a candidate to undergo polymer flood (Dickson et al., 2010). The well locations and absolute-permeability field of the first realization of the set are depicted in Fig. 3.1. Fig. 3.2 displays the absolute-permeability field of six realizations randomly selected from the set, without the wells.

Table 3.1: Reservoir and fluid properties of the modified Egg Model.

Property	**Value**	**SI Units**
Water density	1000	kg/m^3
Oil density	900	kg/m^3
Water viscosity	10^{-3}	Pa.s
Oil viscosity	20×10^{-3}	Pa.s
Water compressibility	10^{-10}	1/bar
Oil compressibility	10^{-10}	1/bar
Initial Reservoir Pressure	400	bar
Porosity	0.2	-

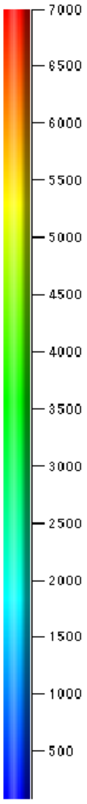

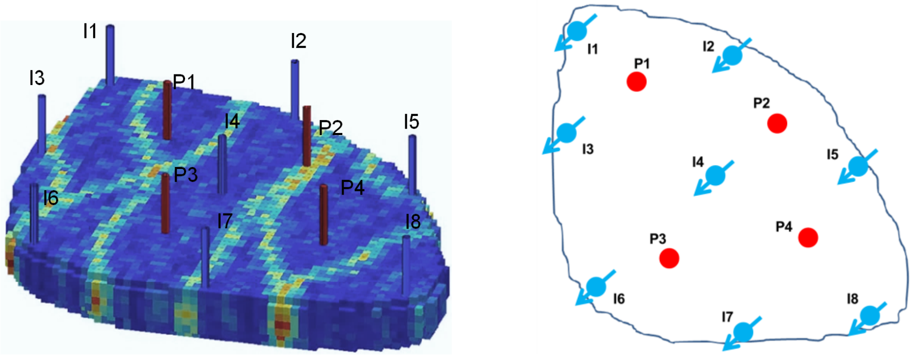

Figure 3.1: Permeability field and well locations (Jansen et al., 2014; after Van Essen et al., 2009).

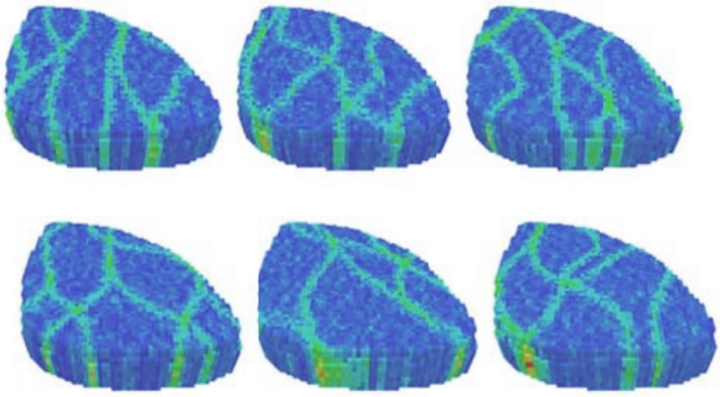

Figure 3.2: Permeability field of six randomly chosen realizations out of a set of 100, showing alternative fluvial structures (Jansen et al., 2014; after Van Essen et al., 2009).

Our case study fits the criteria for a polymer EOR candidate based on the screening benchmarks suggested by Saleh et al. (2014), as shown in Table 3.2.

Table 3. 2: Suggested values for a reservoir candidate to go through a polymer flood process Saleh et al., 2014.

Property	Suggested in Literature	Case Study
In situ oil viscosity (cp)	10–1000	20
Initial oil saturation (%)	> 30%	90%

3.2.1 REPRESENTATION OF UNCERTAINTY IN POLYMER PERFORMANCE

We represent uncertainty in process performance using two different values of polymer viscosity in situ: 6 cp and 20 cp. For simplicity in this study, various detailed influential mechanisms of potential polymer viscosity loss in situ are excluded. In our simulations, we represent the failure to attain the design viscosity in situ by injecting polymer with a concentration corresponding to a viscosity of 6 cp (250 ppm) instead of 20 cp (600 ppm) based on the input polymer rheology table. Since we exclude adsorption from our study, this change in polymer concentration in the simulation does not retard the advance of the polymer bank. For a different EOR process, the possible mode of failure might be loss of miscibility (miscible flooding), failure to achieve ultra-low interfacial tension (surfactant flooding), etc.

3.2.1.1 FRACTIONAL-FLOW THEORY IN POLYMER FLOODING

It is useful to perform a 1D fractional-flow analysis of any reservoir system to identify whether it is suitable for a particular recovery process before undertaking a detailed reservoir simulation study. One of the simplest and most widely used methods of estimating the displacement efficiency in an immiscible displacement process is the Buckley-Leverett method (Fanchi, 2005; Craft et al., 1991; Dake, 2001; Lake et al., 2014). Our purpose here is to compare the displacement efficiency in 1D for the design polymer flood versus the reduced-viscosity polymer flood. The recovery of the 1D polymer flood at polymer breakthrough, mobility ratio at shock front and recovery at 2 PV injection can be extracted from the fractional flow diagram, as shown in Table 3.3.

Table 3.3: Recoveries after polymer breakthrough for the design viscosity case versus reduced viscosity in 1D secondary polymer flood.

	Design viscosity, 20 cp	Reduced viscosity, 6 cp
Oil recovery at polymer breakthrough, %	47%	40%
Mobility ratio at shock front*	0.26	0.38
Fraction of movable oil recovered at 2 PV injection**	0.97	0.9

** Mobility behind the front divided by mobility ahead of the front*

** ($S_{wavg} - S_{wc}$) / ($1 - S_{wc} - S_{or}$), where S_{wavg} is average water saturation behind the shock front, S_{wc} is connate water saturation, and S_{or} is residual oil saturation.

Table 3.3 shows that even in a homogenous 1D reservoir without gravity segregation the viscosity reduction results in a lower recovery at polymer breakthrough and after 2 PV injection. The mobility ratio at the shock front is smaller for the design viscosity than for the reduced viscosity, which suggests a better mobility control and a more uniform sweep in a 3D heterogeneous reservoir for the design viscosity case.

3.2.2 REPRESENTATION OF GEOLOGICAL UNCERTAINTY

As described above, we start with 100 realizations of this reservoir model to reflect the range of possible geological structures reflecting the initial geological uncertainty. Before production begins, all reservoir models are equally probable because they all honor the static conditioning data and the prior geologic interpretations. After 5 years of waterflood data are collected, however, many of these geological realizations are no longer plausible. To represent the reduced range of possibilities consistent with waterflood data, we choose from the original set groups of reservoirs with relatively similar waterflood performance; specifically, similar waterflood breakthrough times in the four production wells. Arpat and Caers, 2004) introduced the term *distance* between reservoir models, referring to a measure of similarity between different geological model realizations. We define a parameter to represent the relative difference in water breakthrough times of the realizations at the four production wells and call it the root-mean-square break-through time difference (RMSBTD) D_{ij} between realizations *i* and *j*. It is calculated as:

$$D_{ij} = \frac{1}{4}\sqrt{\sum_{k=1}^{4}\left(t_{i,k} - t_{j,k}\right)^{2}} \tag{3.1}$$

where *t* is the water break-through time and *k* is a counter over the production wells.

We rank and group realizations according to this parameter. For example, Fig. 3.3 shows water production in one of the realizations where water breakthrough happens early in the simulation, and Table 3.4 shows water breakthrough time of four production wells for two of the realizations and the RMSBTD of the two.

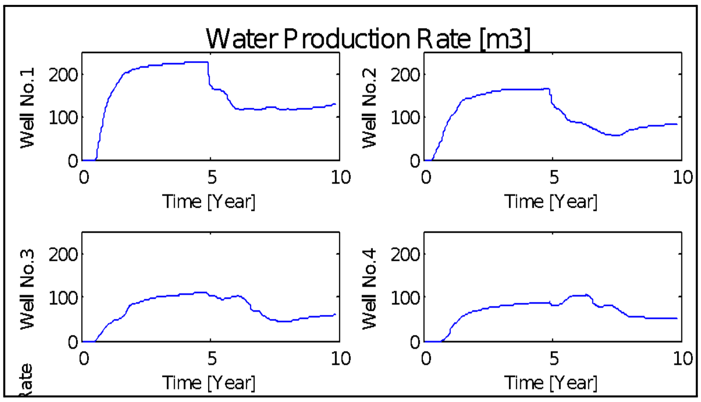

Figure 3.3: Water production in four producers in one realization. Water breakthrough happens early in the simulation.

Table 3.4: Water breakthrough time of four producers in two different realizations (1, 2) and their typical distance value.

Realization Number	Prod 1 (days)	Prod 2 (days)	Prod 3 (days)	Prod 4 (days)	Root-mean- square break-through time difference (days)
1	285	123	356	341	
2	510	122	185	442	75

Then we build a symmetrical 100×100 matrix of RMSBTD for each realization against all other realizations. From this we form 10-member cases with similar behavior, i.e., sets with the smallest RMSBTD among all other sets in the matrix. We then rank these 10-member sets in an ascending order according to the RMSBTD value and further characterize them according to their average water breakthrough time in each producer. We pick three sets of realizations to represent the reduced geological uncertainty at the start of the polymer flood, i.e. after 5 years of waterflood. The first set has the smallest RMSBTD value (least variability in water arrival times at all wells) among the three sets, 22 days. The earliest waterflood breakthrough in this set occurs in producer P2 in almost all of its members, with an average of 175 days. There is a high-permeability channel directly to injectors I2 and I4 in all cases. The members of the second set, with a larger RMSBTD (more-variable water breakthrough times) of 28 days, do not overlap with members of the first set. The earliest waterflood breakthrough time also occurs mainly in producer P2 (average time 177 days). There is a high-permeability channel to injectors I2, I4 and I5 in most members of this set. An exceptionally slow breakthrough to producer P1 (474 days) also characterizes this set. The third set, with a somewhat larger RMSBTD, 29 days, has no members in common with the second set and eight out of ten of its members are distinct from the first set. For most members, waterflood breakthrough time is earliest in producer P3 (average 185 days). In this case there is a high-permeability channel to injectors I4, I6 and I7 in all cases. Refer to appendix 3.A for details of waterflood breakthrough time of the three sets.

On these three 10-member groups of realizations representing reduced geological uncertainty, we run our polymer flood simulations and implement our uncertainty analysis approach.

3.3 DEVELOPMENT SCENARIO AND PROCEDURE

We run the polymer-flood simulations using a proprietary fully-implicit reservoir simulator (Van Doren et al., 2011). In each simulation run, five years of water injection is followed by five years of polymer-slug injection. Figs. 3.4 to 3.6 show results of the simulation for four producers and eight injectors for one of the realizations.

Polymer-injection wells are liable to an unknown extent of fracturing during polymer injection (Seright et al., 2009). Rather than represent this fracturing and the increase in injectivity explicitly, we represent the resulting increased ability to inject polymer indirectly by allowing a very large maximum value of injection-well pressure (545 bar) during polymer injection. This is not the actual injection pressure of these wells, but allows indirectly for increased polymer injection in these wells without representing the fracturing process explicitly.

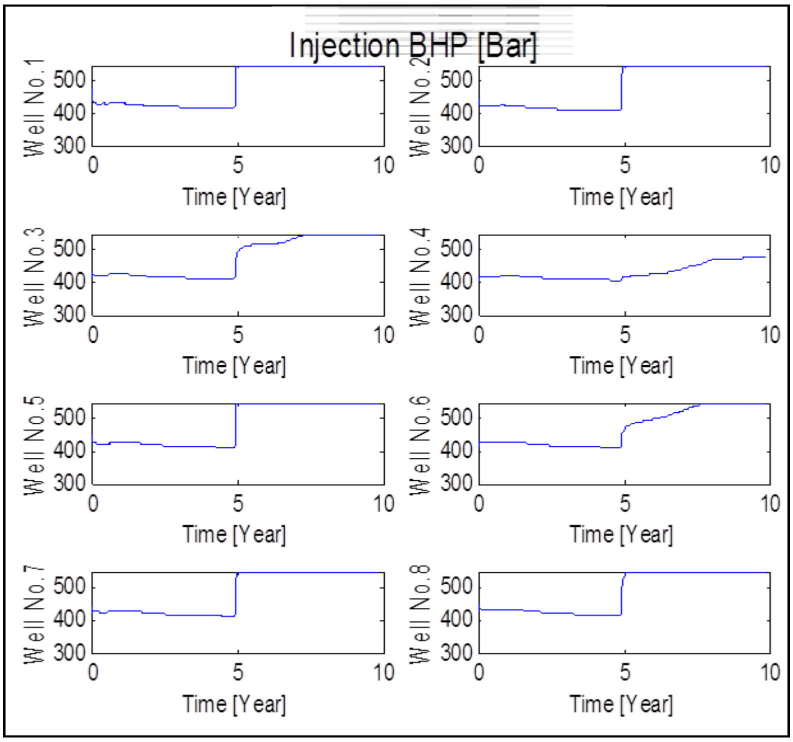

Figure 3.4: Injection BHP of eight injectors.

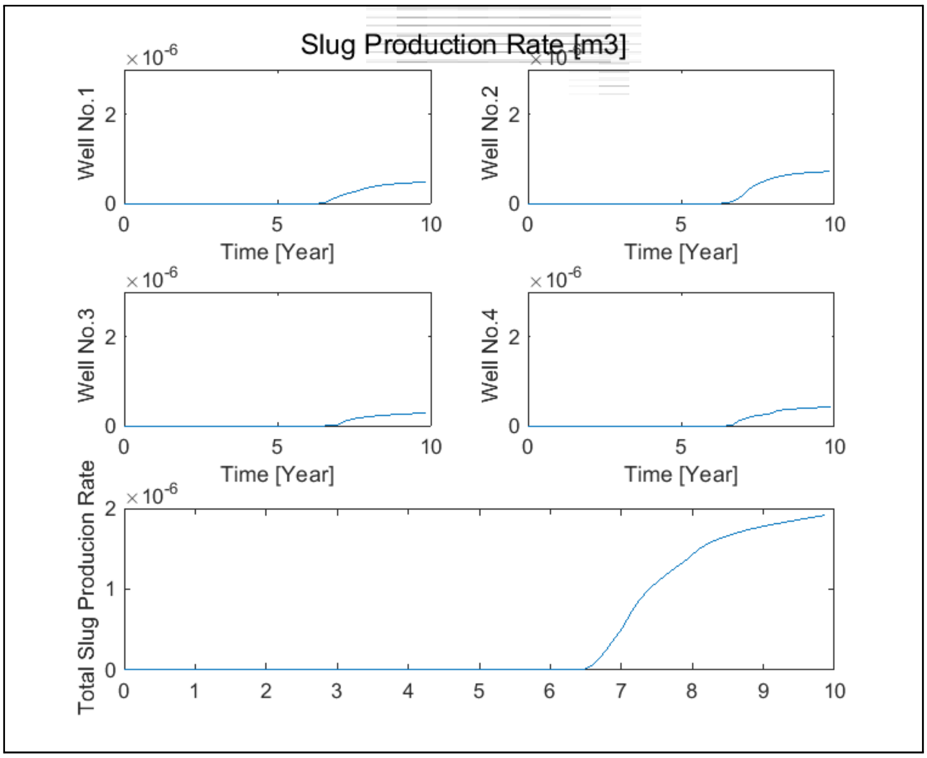

Figure 3.5: Polymer slug production rate in four producers and total polymer production rate.

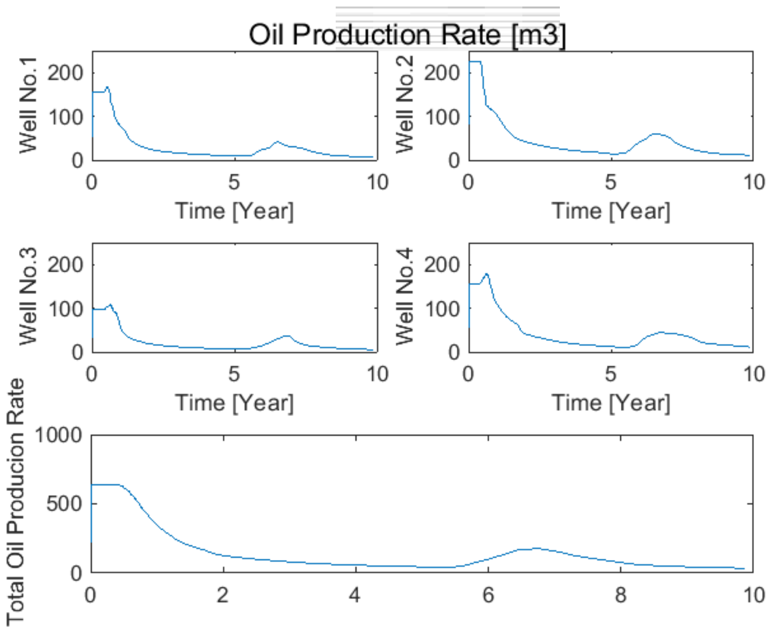

Figure 3.6: Oil production rate in the four producers and total oil production rate.

As shown in Fig. 3.3, water is injected for 5 years, and it breaks through early in the waterflood phase in four production wells. A polymer slug is then injected and causes a rise in injection pressure as shown in Fig. 3.4. Breakthrough of polymer happens sometime after injection as shown in Fig. 3.5. Fig. 3.6 shows the oil production profile in four producers; there is an incremental amount of oil produced due to the polymer flood. We identify five polymer-flood signals to study Fatemi et al. (2015):

Polymer breakthrough time, years (Polymer BT)

Change in injection pressure upon polymer injection in one year, bars (Rise in P_{inj})

Minimum oil cut (Min. Oil Cut)

Time of initial increase in oil production rate, years (Oil Bank Arrival Time)

Cumulative oil production at end of process, m^3 (End Cumoil)

3.4 VERTICAL SWEEP

Fig. 3.7 shows the permeability map of the first realization in the Egg Model where we can visually see the high permeability streaks. In order to analyse the effectiveness of the polymer injection to sweep the non-channel pay, we can compare the snapshots of three different times during the simulation run.

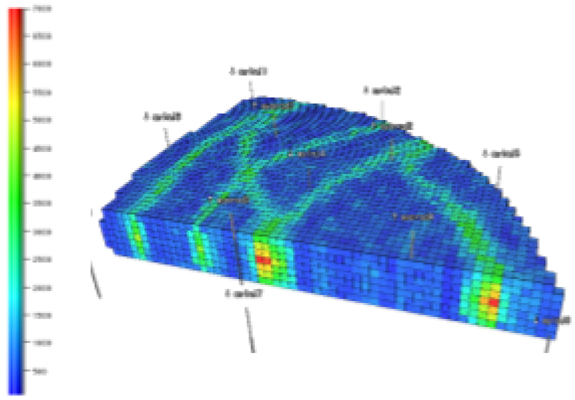

Figure 3.7: Slice of the permeability map of layer 4 of realization no.1.

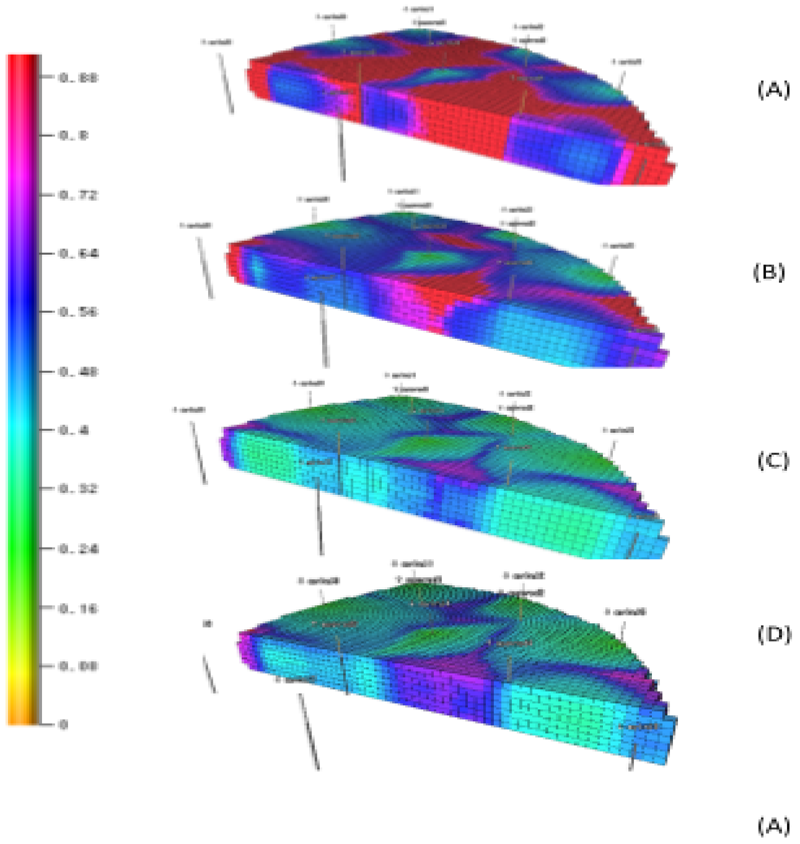
0. 88
0. 8
0. 72
0. 64
0. 56
0. 48
0. 4
0. 32
0. 24
0. 16
0. 08
0
(A)
(B)
(C)
(D)
(A)

Figure 3.8: Oil saturation in realization no. 1 at (A): water breakthrough time, (B): end of waterflood period, (C): end of polymer flood for 20 cp case and (D): end of polymer flood for 6 cp case.

Fig. 3.8 shows the oil saturation map of the reservoir in three different times: Around the water breakthrough time, end of waterflood period and end of the polymer flood period for both the 20cp and 6cp in-situ viscosities.

As Fig. 3.8 shows, the polymer flood causes better sweep in the channel pay as well as the non-channel pay. The less viscous polymer slug gives worse sweep, especially of non-channel pay, as shown in Fig. 3.8 C and D.

We allow that the polymer process might fail in situ and viscosity could be 30% that intended. Comparing the signals listed above for a polymer viscosity in situ of 20 cp to those for a viscosity of 6 cp, we test whether the signals of this difference at injection and production wells would be statistically significant at a 95% confidence interval in the midst of the geological uncertainty, represented by the 10-member cluster of reservoir descriptions. More specifically, 'Polymer BT' and 'Oil Bank Arrival' for the first (earliest) producer of the four for the 6 cp simulation run are compared against the population of values for the first producer of the 20 cp viscosity case. For the rest of the signals, average values of the four producers (as in 'Min. Oil Cut', and 'End Cumoil') or eight injectors (as in Rise in P_{inj}) are compared against the average signal values of the 20 cp viscosity representation. As mentioned before, we consider three different sets of realizations. For each reservoir description we then ask if the given signal with 6 cp polymer viscosity lies in the rejection zone of the confidence interval. If the answer is yes, it is labelled as an "outlier" in the adjacent column (meaning the signal can be distinguished in the midst of geological uncertainty) and otherwise labelled as "not outlier" and left as blank in the adjacent column (meaning the signal cannot be distinguished from geological uncertainty). Table 3.5 shows the summary of signal analysis of the case with 20cp in situ viscosity for all the production and injections wells of the first set (representing the least RMSBTD) against the 6cp case for the first set of realizations. Readers can refer to Appendix 3.B for detailed statistical calculations of signals for each case.

Table 3. 5: Summary of the results of discerning the process with 6 cp polymer viscosity from the case with 20 cp polymer viscosity for the first 10-member set of geological realizations.

Global viscosity 20cp Vs. Global viscosity 6cp for the first set					
Confidence Interval	**Rise in P_{inj}, 1 Year**	**1st Polymer BTTime, (Year)**	**1st Oil Bank Arrival Time (Year)**	**Average Min Oil Cut**	**End CumOil, m^3**
Upper Limit	0.3312	6.47	5.30	0.083	564
Lower Limit	0.2232	5.25	4.84	0.053	514
Outliers Detected (out of 10)	10	8	9	5	6

Of the signals considered, there is one column with only outliers. For this set of realizations, one could discern the effect of viscosity with confidence based on the 'rise in P_{inj} upon polymer injection in one year'. This signal could discern the failure of the polymer in situ in the midst of geological uncertainty. If unintended and uncontrolled fracturing of the injection well is considered likely during polymer injection, however, injection pressure may be a reliable indicator of in situ polymer viscosity if determined from a diagnostic fracture-injection / falloff test (Craig and Jackson, 2017). The signals 'polymer breakthrough time' and 'time of initial increase in oil production rate' also discern the effect of viscosity with confidence in almost all of the cases. A combination of 'minimum oil cut' and 'cumulative oil production at end of simulation' could enable one to tell the difference in all the cases.

Tables 3.6 and 3.7 show the summarized results for the second and third 10-member sets of geological realizations, we perform the same statistical analysis as described for the first set.

Table 3. 6: Summary of the results of discerning the process with 6 cp polymer viscosity from the case with 20 cp polymer viscosity for the second 10-member set of geological realizations.

Global viscosity 20cp Vs. Global viscosity 6cp for the second set					
Confidence Interval	**Rise in P_{inj}, 1 Year**	**1st Polymer BTTime, (Year)**	**1st Oil Bank Arrival Time (Year)**	**Average Min Oil Cut**	**End CumOil, m^3**
Upper Limit	0.352	6.39	5.48	0.089	552
Lower Limit	0.195	5.26	4.69	0.050	518
Outliers Detected (out of 10)	10	8	7	3	8

Table 3.7: Summary of the results of discerning the process with 6 cp polymer viscosity from the case with 20 cp polymer viscosity for the third 10-member set of geological realizations.

Global viscosity 20cp Vs. Global viscosity 6cp for the third set					
Confidence Interval	**Rise in P_{inj}, 1 Year**	**1st Polymer BTTime, (Year)**	**1st Oil Bank Arrival Time (Year)**	**Average Min Oil Cut**	**End CumOil, m^3**
Upper Limit	0.331	6.47	5.3	0.083	564
Lower Limit	0.223	5.25	4.84	0.053	514
Outliers Detected (out of 10)	9	10	6	6	8

In these sets, as in the first set, ‘rate of rise in P_{inj}’ and ‘polymer breakthrough time’ could discern the failure of the polymer in situ in the midst of geological uncertainty at almost all of the cases. Also combining the signals of ‘time of initial increase in oil production rate’, ‘minimum oil cut’ and ‘cumulative oil production at end of simulation’ could enable one to tell the difference in all of the cases. In all cases, outlier status was indicated in at least three of the five signals. Specifically, a combination of ‘minimum oil cut’ and ‘cumulative oil production at end of simulation’ identified outliers in all cases.

3.5 SUMMARY AND DISCUSSION

We present the modified ‘Egg Model’ as a case study illustrating the challenges in discerning the properties of an EOR agent in situ from well data in the midst of geological uncertainty. This study extends earlier work Fatemi et al. (2017) by including a more realistic geological description and more injection and production wells. In this case study, signals are more responsive than in the first case study, mainly due to a more realistic geological description. Results of this study verify the conclusions of the previous work. Changes in polymer breakthrough time are a reliable indicator of failure of polymer viscosity in situ in this case study. Rate of rise of injection-well pressure during polymer injection is also a reliable indicator, though a diagnostic fracture-injection / falloff test may be necessary to verify reliability of the injection pressure data (Craig and Jackson, 2017). Moreover, in this case study, other signals such as a combination of ‘time of initial increase in oil production rate’, ‘minimum oil cut before the oil bank’ and ‘final cumulative oil recovery’ give a statistically significant indication of loss of polymer viscosity in situ in majority of the cases.

APPENDIX 3.A

Table 3.A.1: Water breakthrough time of the four producers in members of the three sets.

No.	Realization	Prod 1	Prod 2	Prod 3	Prod 4
1	3	252	151	318	344
2	81	224	139	315	377
3	1	285	123	356	341
4	52	258	184	354	376
5	42	279	185	368	368
6	60	226	142	263	281
7	64	237	213	248	350
8	97	258	159	240	416
9	48	196	247	260	303
10	25	308	202	286	233
	Avg	252.3	174.5	300.8	338.9
No.	**Realization**	**Prod 1**	**Prod 2**	**Prod 3**	**Prod 4**
1	51	480	134	209	259
2	86	475	140	156	236
3	40	474	155	155	217
4	47	527	210	187	237
5	63	399	104	246	278
6	20	432	175	251	357
7	31	504	221	286	308
8	67	541	215	144	334
9	39	487	165	363	252
10	18	419	251	294	217
	Avg	473.8	177	229.1	269.5
No.	**Realization**	**Prod 1**	**Prod 2**	**Prod 3**	**Prod 4**
1	80	290	292	170	304
2	77	281	253	194	235
3	24	290	359	103	313
4	54	285	313	217	220
5	82	385	321	135	311
6	90	311	193	110	270
7	30	288	408	145	252
8	64	237	213	248	350
9	26	327	379	263	316
10	48	196	247	260	303
	Avg	289	297.8	184.5	287.4

APPENDIX 3.B

Table 3.B.1: Signal values of the first 10-member set of geological cases calculated for the case with 20 cp polymer viscosity, with upper and lower bounds of the 95% confidence interval (CI+, CI-) for each signal.

Realization		**Rise in P_{inj} 5Y to 6Y**									**Polymer BT [Year]**				
		inj1	**inj2**	**inj3**	**inj4**	**inj5**	**inj6**	**inj7**	**inj8**	**avg**	**prod1**	**prod2**	**prod3**	**prod4**	**1st**
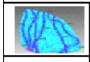	**3**	0.159	0.105	0.298	0.380	0.380	0.374	0.373	0.373	0.305	6.13	5.65	6.42	6.89	5.65
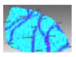	**81**	0.362	0.375	0.282	0.273	0.122	0.363	0.364	0.180	0.290	6.26	5.85	6.38	6.61	5.85
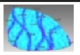	**1**	0.166	0.214	0.322	0.388	0.384	0.381	0.242	0.377	0.309	6.23	5.43	6.37	6.87	5.43
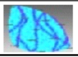	**52**	0.369	0.368	0.364	0.057	0.126	0.141	0.301	0.363	0.261	6.13	5.87	6.26	6.49	5.87
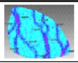	**42**	0.159	0.367	0.304	0.260	0.122	0.194	0.259	0.258	0.240	6.11	6.19	6.36	6.39	6.11
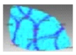	**60**	0.354	0.371	0.296	0.049	0.363	0.235	0.362	0.355	0.298	6.14	5.93	6.09	6.75	5.93
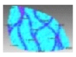	**64**	0.350	0.349	0.178	0.359	0.154	0.346	0.121	0.355	0.277	6.33	6.45	6.39	6.58	6.33
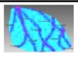	**97**	0.364	0.109	0.263	0.209	0.354	0.278	0.114	0.284	0.247	6.18	5.52	5.86	6.58	5.52
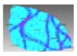	**48**	0.348	0.121	0.320	0.348	0.164	0.368	0.296	0.148	0.264	6.04	5.96	5.95	6.44	5.95
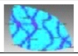	**25**	0.361	0.369	0.294	0.062	0.365	0.293	0.158	0.336	0.280	6.19	6.27	5.96	6.23	5.96
CI +										0.3312					6.47
CI -										0.2232					5.25

Oil Bank Arrival Time [Year]					**Min. Oil Cut**					**End Cumoil ×10^3 [m^3]**
prod1	**prod2**	**prod3**	**prod4**	**1st**	**prod1**	**prod2**	**prod3**	**prod4**	**avg**	
5.56	5.70	5.04	5.50	5.04	0.058	0.058	0.061	0.058	0.059	548
5.37	5.14	5.09	5.19	5.09	0.071	0.066	0.066	0.066	0.068	542
5.25	5.56	5.36	5.68	5.25	0.056	0.056	0.056	0.058	0.057	558
5.38	5.08	5.04	5.41	5.04	0.075	0.071	0.072	0.075	0.073	542
5.30	5.22	4.96	5.27	4.96	0.076	0.075	0.075	0.075	0.075	536
5.16	5.13	5.02	5.03	5.02	0.078	0.077	0.075	0.075	0.076	532
5.38	5.08	5.04	5.26	5.04	0.072	0.070	0.070	0.071	0.071	519
5.41	5.75	5.48	5.07	5.07	0.064	0.068	0.064	0.065	0.065	540
5.33	5.50	5.66	5.23	5.23	0.064	0.064	0.066	0.064	0.065	547
5.19	5.30	4.96	5.48	4.96	0.066	0.067	0.068	0.075	0.069	528
				5.30					0.083	564
				4.84					0.053	514

Table 3.B.2: Discerning the process with 6 cp polymer viscosity from the case with 20 cp polymer viscosity for the first 10-member set of geological realizations.

Realization		**Rise in P_{inj} 5Y to 6Y**										**Polymer BT [Year]**					
		inj1	**inj2**	**inj3**	**inj4**	**inj5**	**inj6**	**inj7**	**inj8**	**avg**		**prod1**	**prod2**	**prod3**	**prod4**	**1st**	
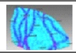	**3**	0.091	0.052	0.176	0.237	0.231	0.170	0.191	0.214	0.160	**Outlier**	5.52	5.20	5.84	5.85	5.20	**Outlier**
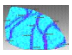	**81**	0.331	0.306	0.136	0.121	0.075	0.186	0.218	0.110	0.186	**Outlier**	5.48	5.23	5.59	6.18	5.23	**Outlier**
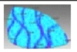	**1**	0.109	0.237	0.195	0.198	0.260	0.252	0.152	0.287	0.214	**Outlier**	5.68	5.19	5.64	5.91	5.19	**Outlier**
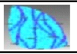	**52**	0.238	0.316	0.312	0.037	0.070	0.090	0.177	0.179	0.170	**Outlier**	5.60	5.21	5.67	5.82	5.21	**Outlier**
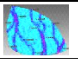	**42**	0.071	0.329	0.126	0.105	0.070	0.081	0.105	0.104	0.101	**Outlier**	5.63	5.21	5.69	5.74	5.21	**Outlier**
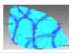	**60**	0.362	0.255	0.162	0.036	0.204	0.134	0.219	0.254	0.210	**Outlier**	5.48	5.22	5.55	5.90	5.22	**Outlier**
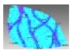	**64**	0.307	0.309	0.104	0.212	0.092	0.301	0.075	0.304	0.205	**Outlier**	5.50	5.41	5.79	5.67	5.41	-
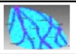	**97**	0.205	0.015	0.108	0.081	0.313	0.100	0.062	0.117	0.100	**Outlier**	5.56	5.20	5.52	5.96	5.20	**Outlier**
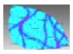	**48**	0.346	0.364	0.364	0.361	0.288	0.385	0.242	0.128	0.367	**Outlier**	5.50	5.52	5.40	5.90	5.40	-
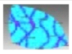	**25**	0.319	0.331	0.269	0.241	0.354	0.377	0.294	0.389	0.384	**Outlier**	5.59	5.13	5.58	5.65	5.13	**Outlier**

Realization	**Oil Bank Arrival Time [Year]**						**Min. Oil Cut**						**End Cumoil ×10^3 [m^3]**	
	prod1	**prod2**	**prod3**	**prod4**	**1st**		**prod1**	**prod2**	**prod3**	**prod4**	**avg**			
3	5.12	5.14	4.39	5.20	4.39	**Outlier**	0.047	0.047	0.050	0.047	0.047	**Outlier**	521	-
81	5.02	4.75	4.67	4.81	4.67	**Outlier**	0.056	0.051	0.052	0.051	0.053	**Outlier**	518	-
1	4.83	5.08	5.19	5.21	4.83	**Outlier**	0.045	0.044	0.045	0.046	0.045	**Outlier**	523	-
52	5.02	4.67	4.38	5.02	4.38	**Outlier**	0.058	0.056	0.057	0.058	0.057	-	509	**Outlier**
42	4.56	4.74	4.28	4.66	4.28	**Outlier**	0.060	0.060	0.060	0.060	0.060	-	506	**Outlier**
60	4.77	4.73	4.45	4.58	4.45	**Outlier**	0.059	0.059	0.059	0.059	0.059	-	507	**Outlier**
64	4.72	4.68	4.64	5.01	4.64	**Outlier**	0.056	0.056	0.056	0.059	0.057	-	503	**Outlier**
97	5.04	5.23	5.06	5.12	5.04	-	0.049	0.050	0.049	0.049	0.050	**Outlier**	513	**Outlier**
48	5.06	5.15	5.24	4.81	4.81	**Outlier**	0.049	0.049	0.050	0.050	0.050	**Outlier**	521	-
25	4.70	4.82	4.45	4.92	4.45	**Outlier**	0.053	0.054	0.054	0.056	0.054	-	508	**Outlier**

Table 3.B.3: Summary of signal values of the second set of geological realizations with 20 cp polymer viscosity, with upper and lower bounds of the 95% confidence interval (CI+, CI-) for each signal.

Realization Realization		Slope Pinj 5Y to 6Y	Polymer BT [year]	Oil Bank Arrival Time [year]	Min. Oil Cut	End ([
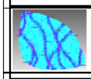	51 51	0.233 0.16 Outlier	5.74 5.44 Outlier	5.00 4.99 -	0.054 0.06 Outlier	524 527057
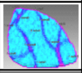	86 86	0.263 0.17 Outlier	5.55 5.31 Outlier	5.03 5.02 -	0.076 0.08 Outlier	534 519947
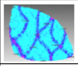	40 40	0.243 0.18 Outlier	5.66 5.30 Outlier	5.14 4.83 Outlier	0.074 0.07 -	537 520955
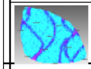	47 47	0.285 0.20 Outlier	6.26 5.45 Outlier	4.99 4.91 Outlier	0.071 0.06 Outlier	542 528153
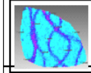	63 63	0.279 0.19 Outlier	5.60 5.23 Outlier	4.96 4.93 Outlier	0.069 0.07 -	534 523858
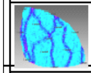	20 20	0.228 0.16 Outlier	5.74 5.43 Outlier	5.08 5.06 -	0.082 0.08 Outlier	551 533343
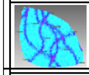	31 31	0.315 0.20 Outlier	6.04 5.36 Outlier	4.95 4.94 Outlier	0.070 0.07 -	534 525566
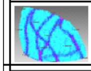	67 67	0.259 0.19 Outlier	5.58 5.24 Outlier	5.02 4.98 -	0.070 0.07 -	533 520722
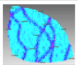	39 39	0.328 0.21 Outlier	5.97 5.48 Outlier	5.08 4.93 Outlier	0.073 0.07 -	532 525908
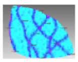	18 18	0.306 0.21 Outlier	6.10 5.62 Outlier	5.55 5.53 Outlier	0.055 0.05 Outlier	528 523865
CI +		0.352	6.39	5.48	0.089	552
CI -		0.195	5.26	4.69	0.050	518

Table 3.B.4: Discerning the process with 6 cp polymer viscosity from the case with 20 cp polymer viscosity for the second set of geological realizations.

Realization		F	Slope Pinj 5Y to 6Y		Polymer BT [year]		Oil Bank Arrival Time [year]		Min. Oil Cut		End Cu [m³	
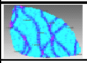	51		0.109 0.16	Outlier Outlier	5.166 5.44	Outlier Outlier	4.640 4.99	Outlier -	0.048 0.06	Outlier Outlier	522 527057	-
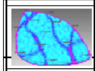	86		0.117 0.17	Outlier Outlier	5.047 5.31	Outlier Outlier	4.673 5.02	Outlier -	0.057 0.08	- Outlier	510 519947	Outlier
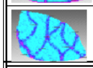	40		0.123 0.18	Outlier Outlier	5.031 5.30	Outlier Outlier	4.719 4.83	- Outlier	0.056 0.07	- -	511 520955	Outlier
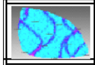	47		0.138 0.20	Outlier Outlier	5.182 5.45	Outlier Outlier	4.678 4.91	Outlier Outlier	0.053 0.06	- Outlier	518 528153	Outlier
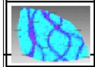	63		0.132 0.19	Outlier Outlier	4.969 5.23	Outlier Outlier	4.589 4.93	Outlier Outlier	0.051 0.07	- -	513 523858	Outlier
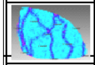	20		0.109 0.16	Outlier Outlier	5.161 5.43	Outlier Outlier	4.709 5.06	- -	0.059 0.08	Outlier Outlier	523 533343	-
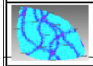	31		0.143 0.20	Outlier Outlier	5.286 5.56	- Outlier	4.609 4.94	Outlier Outlier	0.051 0.07	- -	515 525566	Outlier
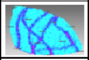	67		0.136 0.19	Outlier Outlier	4.979 5.24	Outlier Outlier	4.635 4.98	Outlier -	0.052 0.07	- -	510 520722	Outlier
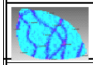	39		0.145 0.21	Outlier Outlier	5.203 5.48	Outlier Outlier	4.589 4.93	Outlier Outlier	0.052 0.07	- -	515 525908	Outlier
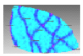	18		0.144 0.21	Outlier Outlier	5.336 5.62	- Outlier	5.142 5.53	- Outlier	0.041 0.05	Outlier Outlier	513 [illegible]	Outlier

Table 3.B.5: Summary of signal values of the third set of geological realizations with 20 cp polymer viscosity, with upper and lower bounds of the 95% confidence interval (CI+, CI-) for each signal.

Realization Realization		Rise in P_{inj} 5Y to 6Y Slope P_{inj} 5Y to 6Y	Polymer BT [Year] Polymer BT	Oil Bank Arrival Time [Year] Oil Bank Arrival Time	Min. Oil Cut Min. Oil	End Cumoil ×10³ [m³] End CumOil
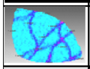	80	0.305 0.23	5.65 5.76	5.04 5.22	0.059 0.07	548 540305
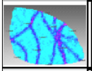	77	0.290 0.30	5.85 6.12	5.09 5.39	0.068 0.06	543 529730
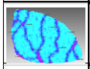	24	0.309 0.18	5.43 5.47	5.25 4.95	0.057 0.07	558 554955
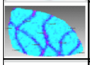	54	0.261 0.35	5.87 6.26	5.04 5.15	0.073 0.06	542 537584
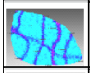	82	0.240 0.25	6.11 5.64	4.96 5.24	0.075 0.06	536 541160
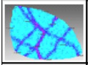	90	0.298 0.27	5.93 5.62	5.02 4.95	0.076 0.08	532 541192
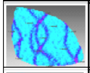	30	0.277 0.26	6.33 5.98	5.04 5.40	0.071 0.07	519 541250
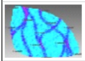	64	0.247 0.28	5.52 6.33	5.07 5.04	0.065 0.07	540 519091
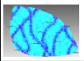	26	0.264 0.25	5.95 6.38	5.23 5.37	0.065 0.06	547 542890
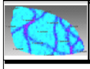	48	0.280 0.26	5.96 5.95	4.96 5.23	0.069 0.06	528 546895
CI + CI +		0.331 0.30	6.47 6.20	5.30 5.33	0.083 0.07	564 547265
CI -		0.223	5.25	4.84	0.053	514

Table 3.B.6: Discerning the process with 6 cp polymer viscosity from the case with 20 cp polymer viscosity for the third set of geological realizations.

Realization		Rise in P_{inj} 5Y to 6Y		Polymer BT [Year]		Oil Bank Arrival Time [Year]		Min. Oil Cut		End Cumoil ×10^3 [m^3]	
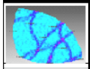	80	0.122	Outlier	4.95	Outlier	4.97	-	0.0561	-	512	Outlier
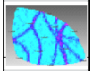	77	0.151	Outlier	5.14	Outlier	4.78	Outlier	0.0504	Outlier	512	Outlier
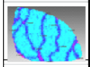	24	0.075	Outlier	4.66	Outlier	4.69	Outlier	0.0527	Outlier	523	-
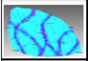	54	0.169	-	5.09	Outlier	4.82	-	0.0483	Outlier	517	Outlier
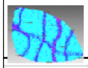	82	0.102	Outlier	4.74	Outlier	4.96	-	0.0507	Outlier	517	Outlier
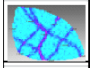	90	0.112	Outlier	4.68	Outlier	4.70	Outlier	0.0635	-	514	Outlier
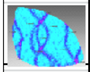	30	0.121	Outlier	4.80	Outlier	4.80	Outlier	0.0509	Outlier	518	Outlier
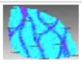	64	0.165	Outlier	5.06	Outlier	4.80	Outlier	0.0571	-	502	Outlier
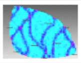	26	0.165	Outlier	5.06	Outlier	4.80	Outlier	0.0571	-	502	Outlier
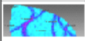	48	0.125	Outlier	5.0[illegible]	Outlier	4.97	-	0.0506	Outlier	522	-

Realization	Slope P_{inj} 5Y to 6Y	Polymer BT	Oil Bank Arrival Time	Min. Oil Cut	End CumOil
80	0.28	5.76	5.22	0.07	540305
77	0.30	6.12	5.39	0.06	529730
24	0.18	5.47	4.95	0.07	554955
54	0.35	6.26	5.15	0.06	537584
82	0.25	5.64	5.24	0.06	541160
90	0.27	5.62	4.95	0.08	544192
30	0.26	5.98	5.40	0.07	541230
64	0.28	6.35	5.04	0.07	519091
26	0.25	6.38	5.37	0.06	542890
48	0.16	[illegible]	[illegible]	0.06	546895

4

DISCERNING IN-SITU PERFORMANCE OF AN EOR AGENT IN THE MIDST OF GEOLOGICAL UNCERTAINTY III: NORNE FIELD

Considering the complexity of EOR processes and the inherent uncertainty in the reservoir description, it is a challenge to discern the properties of the EOR agent in situ in the midst of geological uncertainty. We propose a case study to illustrate this challenge: a polymer EOR process designed for a synthetic complex reservoir model, the modified “Norne Field”. Specifically, we statistically analyze a number of injection and production-well signals for their ability to detect a failure of the EOR process in the midst of an uncertain geological description of the reservoir. Our study includes both uncertainty in the EOR process itself and in the reservoir description.

We consider two possible modes of failure of the EOR process. First, a mistake in the screening and design phase of the polymer flood process causes a global reduction in

---

This chapter is from the submitted article: S. A. Fatemi, W. R. Rossen, 2021. Discerning In-Situ Performance of an Enhanced-Oil-Recovery Agent in the Midst of Geological Uncertainty: III. Norne Field. *SPE Reservoir Evaluation & Engineering*.

polymer-slug viscosity throughout the reservoir. Second, subsurface thermal or chemical instabilities cause polymer to progressively lose its in situ viscosity near the injectors. We study different scenarios in which a polymer fails and by one or two modes try to discern this failure by analyzing several signals at injection and production wells. We start with an ensemble of reservoir models to reflect the range of possible geological structures honoring the statistics of the initial geological uncertainties. We then use the Ensemble Kalman Filter (EnKF) to update the initial reservoir ensemble by integrating the waterflood production data over a period of 30 years. The updated reservoir models are used to simulate 30 years of polymer injection. We allow that the polymer process might fail in situ (through the two failure scenarios) and test whether the signals of this difference at injection and production wells would be statistically significant in the midst of the geological uncertainty. Specifically, we compare the deviation caused by loss of polymer viscosity to the scatter caused by the geological uncertainty at the 95% confidence interval. In addition, we also try to distinguish between the failure scenarios. Among the signals considered, rate of rise in the injection pressure and incremental oil arrival time give reliable indications of whether the polymer viscosity was maintained in situ, and if not, which mechanism caused the failure.

4.1 INTRODUCTION

Chemical EOR processes represent a relatively small fraction of commercially successful EOR projects. This is in part due to uncertainty in predictions of processes (Sheng, 2011; Lake et al., 2014). For polymer flooding, the long-term chemical performance and the integrity of polymer viscosity is essential for the effectiveness of the process. The actual performance of polymer in the reservoir can be uncertain in spite of thorough laboratory tests (Weiss and Baldwin, 1985). Separate evaluation of the impacts of geological and process uncertainties on the performance of an EOR process is important, because a process that did not achieve the desired objectives in one formation might be successful in another field if it demonstrates that it achieved its technical objectives.

Researchers have studied uncertainty in EOR process performance, and uncertainty in the geological description, but not the two together. Previous research has examined uncertainty in chemical flooding and CO_2-EOR process performance parameters (Brown and Smith, 1984; Denney ,2011; Stanley, 2014; Adepoju et al., 2017). Reservoir heterogeneity also plays an important role on the success of chemical enhanced oil recovery. Experimental data from Craig (1993) and field data from Sorbie and Clifford (1988) are examples of studies that have demonstrated the detrimental effects of reservoir heterogeneity on the performance of oil-displacement processes. In this paper we investigate the impact of both sources of uncertainty together in a statistical approach based on the workflow described in chapter 3 (Fatemi et al., 2017). In earlier studies, we used for illustration a layer-cake model with an extreme level of geological uncertainty and then a fluvial-reservoir model. In that case study, we started with an initial ensemble of 100 realizations and used a measure of similarity to make groups of 10-member clusters with similar waterflood performance, to reflect reservoir uncertainty at the start of the EOR process (Fatemi et al., 2019). Here we apply the workflow to a case with a more-realistic geological model and a level of uncertainty more representative of a field after a period of waterflood. We present the “Norne Field” case study for this challenge (Lie et al., 2012). We start with 50 realizations of this reservoir model to reflect the range of possible geological structures honoring the statistics of the initial geological uncertainties. We then use the Ensemble Kalman Filter (EnKF) to update the initial reservoir ensemble, integrating 30 years of waterflood production data. We use the updated reservoir models to simulate polymer EOR process with an in situ viscosity of 18 cp.

For a polymer flood to meet its technical objectives, the polymer viscosity in situ (as one of the more important properties of the polymer process design) must meet its technical design value. To represent EOR process failure, we allow that the polymer process might fail in situ through either or both of two different mechanisms. The first is a global viscosity loss, where we stipulate that viscosity could be half of that intended, everywhere in the reservoir. The second is a progressive viscosity loss upon injection, where polymer decays and loses its viscosifying power over residence time in the reservoir. We allow that throughout the reservoir polymer viscosity could be lost by either mechanism or a combination of both. We test whether the signals of these differences at injection and production wells would be statistically significant in the midst of the updated geological uncertainty, and whether the signals can tell which mechanism of failure has occurred. Specifically, for a population of reservoirs representing geological uncertainty, we compare the deviation caused by loss of polymer viscosity to the scatter caused by the geological uncertainty using the statistical confidence-interval approach. Various signals are monitored to see which are the most reliable indications of polymer viscosity loss and which can differentiate between different polymer-viscosity-loss mechanisms.

4.2 NORNE FIELD

The Norne Field is located 200 km from the Norwegian coast in the Norwegian Sea. The structure is approximately 3×9 km and sea depth in the area is 380 m; reservoir depth is 2500 - 2700 m. It was discovered in 1991 and is operated by Equinor. The Norne pilot project is a benchmark case established for different studies supported by the IO Center at Norwegian University of Science and Technology (NTNU) in the area of Integrated Operations, i.e. Smart Fields, Fields of the Future, Digital Oil Fields, and e-Fields (Luo et al., 2017). The relative location to the neighboring fields and the structure of Norne are shown in Fig. 4.1.

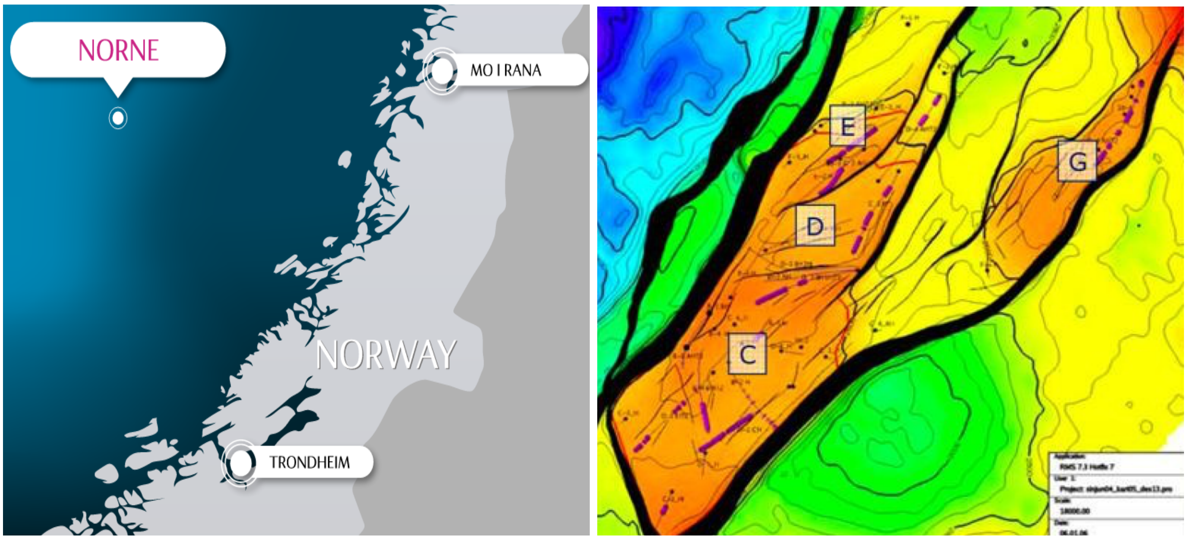

Figure 4.1: The location and structure of the Norne Field (Adlam, 1995).

4.3 CASE-STUDY DESCRIPTION

We consider a modified version of the Norne Field benchmark case which is a two-phase water and oil reservoir. It contains 46 grid blocks in the X-direction, 112 grid blocks in the Y-direction and 22 layers with variable grid block-sizes of 80-100 m in X and Y-directions. There are 9 vertical injectors and 5 vertical producers perforated in all layers of the model. The horizontal log-permeability and porosity fields are generated for each layer based on a Gaussian distribution. The porosity field has a mean of 0.25 and a standard deviation of 0.05.

The mean value of the horizontal log-permeability field increases monotonically with depth in each layer and has a Dykstra-Parson's coefficient of 0.78. Vertical permeability is calculated using a fixed ratio, $k_v / k_h = 0.1$. Fig. 4.2 shows the permeability field of the first realization of the set and the well locations and Fig. 4.3 shows the permeability map of different layers of the first realization. All producers operate at a bottom-hole pressure of 335 bar and the injectors operate at a maximum injection rate of 6000 m^3/day as the primary constraint and a maximum bottom-hole pressure of 900 bar as a secondary constraint. We allow such a large bottomhole pressure to account indirectly for increased injectivity resulting from fracturing during polymer injection, which we do not represent explicitly in the simulations. Production from the reservoir is simulated over a time horizon of thirty years of waterflood followed by thirty years of polymer flood. The average reservoir pressure is initially set at 350 bar, and the initial water saturation is taken to be uniform over the reservoir at a value of 0.2. We modified the oil viscosity in this case study to represent a candidate reservoir for a polymer flood process (Dickson et al., 2010). The geological and fluid properties used in this case study are presented in Table 4.1. The PVT properties and relative-permeability curves are kept fixed while generating the data as well as running the Ensemble Kalman Filter.

Table 4. 1: Reservoir and fluid properties of the modified Norne Field

Property	Value	SI Units
Water density	1000	kg/m^3
Oil density	900	kg/m^3
Water viscosity	10^{-3}	Pa.s
Oil viscosity	20×10^{-3}	Pa.s
Water compressibility	10^{-5}	1/bar
Oil compressibility	10^{-5}	1/bar
Corey parameters		
k_{rwo}	0.3	
n_w	2	
k_{ro}	1	
n_o	3	
S_{wr}	0.2	
S_{or}	0.2	

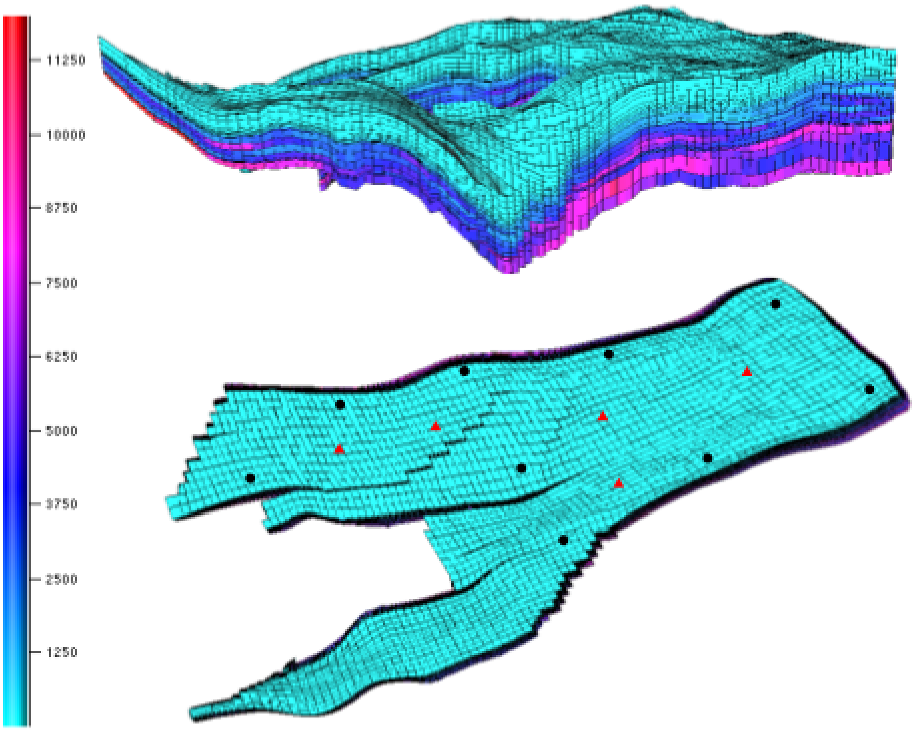
11250
10000
8750
7500
6250
5000
3750
2500
1250

Figure 4.2: Horizontal permeability field (in md) of realization number 1 and the top view of the well locations. Black circles show the injectors and red triangles show the producers.

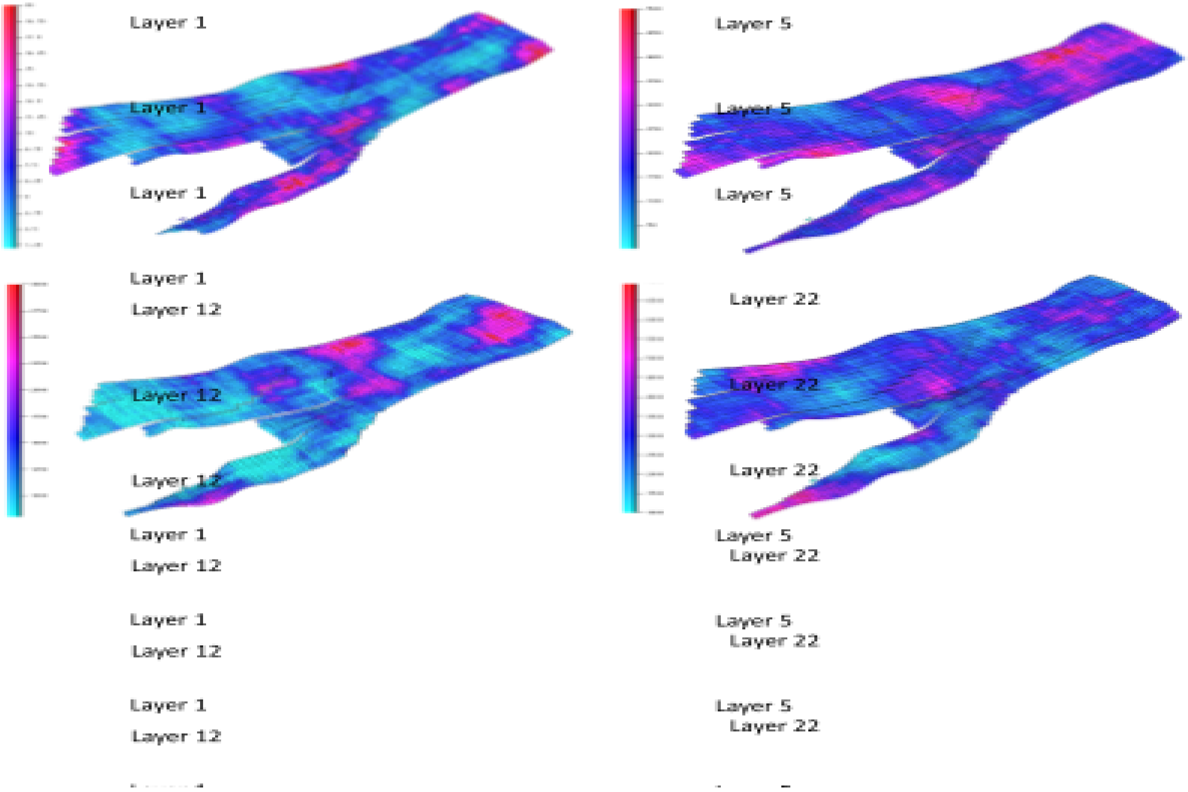
Layer 1
Layer 1
Layer 1
Layer 1
Layer 12
Layer 12
Layer 12
Layer 1
Layer 12
Layer 1
Layer 12
Layer 1
Layer 12
Layer 5
Layer 5
Layer 5
Layer 22
Layer 22
Layer 22
Layer 5
Layer 22
Layer 5
Layer 22
Layer 5
Layer 22

Figure 4.3: Horizontal permeability field (in md) for layers 1, 5, 12 and 22 of realization 1.

4.3.1 REPRESENTATION OF UNCERTAINTY IN POLYMER-FLOOD PERFORMANCE

In this study, among the various mechanisms of polymer mobility in-situ we focus on two of the more-important mechanisms that cause polymer failure in field applications and represent this uncertainty in process performance as follows:

- A global viscosity loss, where polymer in-situ viscosity is a fraction of that intended everywhere in the reservoir. This failure could be the result of mechanical degradation in surface facilities or upon entering the perforations or a faulty translation from laboratory-measured properties to properties in situ. In our simulations, we represent this type of failure by injecting the polymer concentration corresponding to 9 cp (50% viscosity loss) instead of that corresponding to 18 cp (based on the polymer-rheology algorithm in the simulator). Since we exclude adsorption from our study, this change in polymer concentration in the simulation does not retard the advance of the polymer bank.
- A progressive viscosity loss, where polymer viscosity in situ declines over time due to decay of polymer molecules. Upon polymer injection, certain types of polymers will change their molecular structure over time, e.g. increased degree of hydrolysis or chemical or thermal degradation. This causes a change in polymer-slug viscosity over time (Sorbie and Clifford, 1988). The viscosity loss is quantified as a function of time of polymer exposure to the reservoir. The rate of viscosity decay is expressed using Eq. 4.1. At zero exposure time the viscosity is the initial design polymer viscosity, while at very large exposure time the viscosity tends to the water viscosity:

$$\frac{\mu_p}{\mu_p^{\circ}} = e^{-\frac{t}{\tau}} + \frac{\mu_w}{\mu_p^{\circ}}\left(1 - e^{-\frac{t}{\tau}}\right) \tag{4.1}$$

The left hand side of this equation is the ratio of polymer viscosity over time to the initial injected polymer viscosity. The decay constant τ can be derived from experimental data. The exposure time *t* can be tracked by introduction of a passive tracer in the injected fluid, with a specific injection time. As the injected fluid moves through the reservoir the tracer carries the value of its injection time. Specifically, the simulator calculates the average injection time of polymer in each grid block from a material balance on polymer, accounting for injection times of polymer flowing in from adjacent grid blocks and that resident in the grid block. The difference between the actual time and the average injected time is the exposure time for polymer in the given grid block. Fig. 4.4 shows the map of the decay factor (for decay constants of 10 years and 2 years) at the end of the polymer-flood simulation for one of the realizations. In Fig. 4.4b, the greater exposure time of the injected polymer in the reservoir (i.e., further from the injectors) causes more polymer decay and loss of viscosity. In selecting this second mechanism of polymer viscosity loss, we distinguish between processes that reduce polymer viscosity everywhere and those that effect in situ viscosity differently near and far from the injection well. The latter group would include polymer adsorption. Our goal is to determine whether the two types of process failure can be distinguished from their effects on process performance.

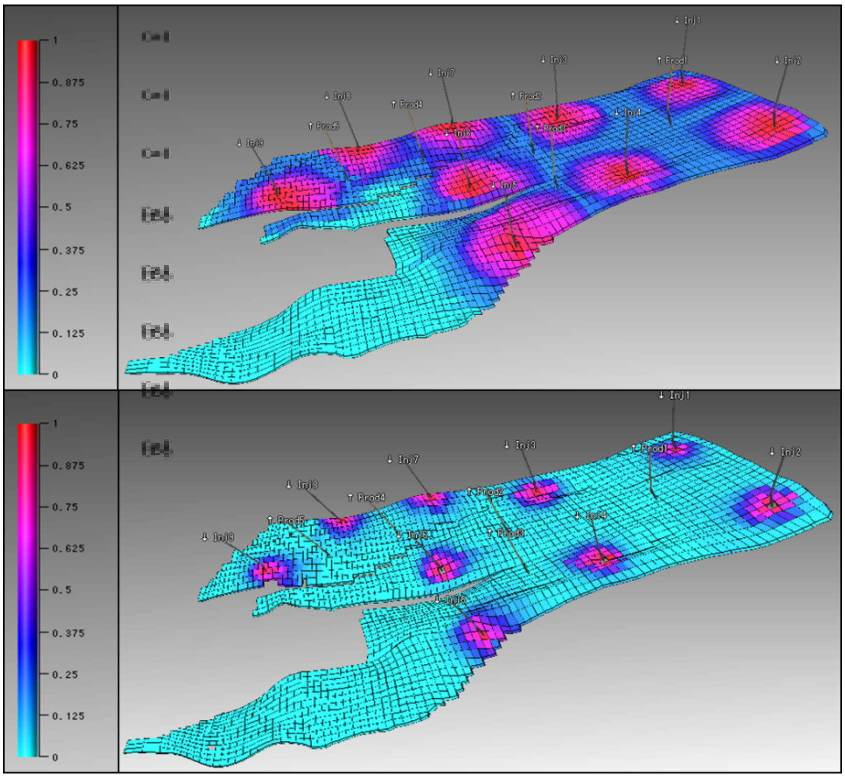

Figure 4.4: Decay factor map in layer 22 of realization number 50: (a) τ = 10 year, (b) τ = 2 year. Deep red corresponds to initial viscosity, and light blue to complete loss of viscosity.

4.4 REPRESENTING GEOLOGICAL UNCERTAINTY USING ENSEMBLE KALMAN FILTER (ENKF)

After a period of waterflooding, the geological uncertainty is reduced. We carried out a computer-assisted history match (Emerick and Reynolds, 2011) by means of the widely used

Ensemble Kalman Filter (EnKF) to estimate the uncertainty in future performance. The method has become a popular approach in the reservoir-simulation community for history-matching, and many applications to field cases have been published (Lorentzen et al., 2003; Evensen, 2009; Aanonsen et al., 2009; Chen and Oliver, 2010; Emerick and Reynolds, 2013; Zhang et al., 2017).

There are two main steps in the EnKF algorithm: the forecast step and the assimilation step. We start with 50 realizations of this reservoir model to reflect the initial geological uncertainty. There is no guarantee that an ensemble size of 50 is adequate to avoid problems with spurious correlations (Emerick and Reynolds, 2011). Therefore we chose to implement the EnKF with a distance-based covariance localization using the methodologies suggested by Cohn (1999). EnKF with covariance localization yields better data matches and predictions and avoids propagation of spurious correlations than with EnKF without localization (Pointe and Ma, 2011).

The state vector includes a static-model parameter, horizontal log-permeability, along with dynamic parameters, i.e. pressure and water saturation in every grid block. The simulated data are generated synthetically by running the simulator with the reference model from a stochastic realization of the field and adding noise to the values obtained to generate measurements. The measurement errors are assumed Gaussian with zero mean, and standard deviation was set as 15%. The measurements considered are:

-Producers: pressures, oil and water rates, water cut.

-Injectors: pressures, water-injection rates.

The EnKF was used to match the well data (5 producers and 9 injectors) every 2.5 years during the waterflood period.

4.4.1 HISTORY-MATCH RESULTS

The final history-match results are reported in Figs. 4.5 and 4.6. The grey lines represent the simulation results of the prior ensemble (before the assimilation). The blue line indicates the posterior ensemble mean and the red line is the synthetic truth. Fig. 4.7 compares the permeability maps of the prior and posterior realizations for several layers of one of the randomly selected realizations of the ensemble.

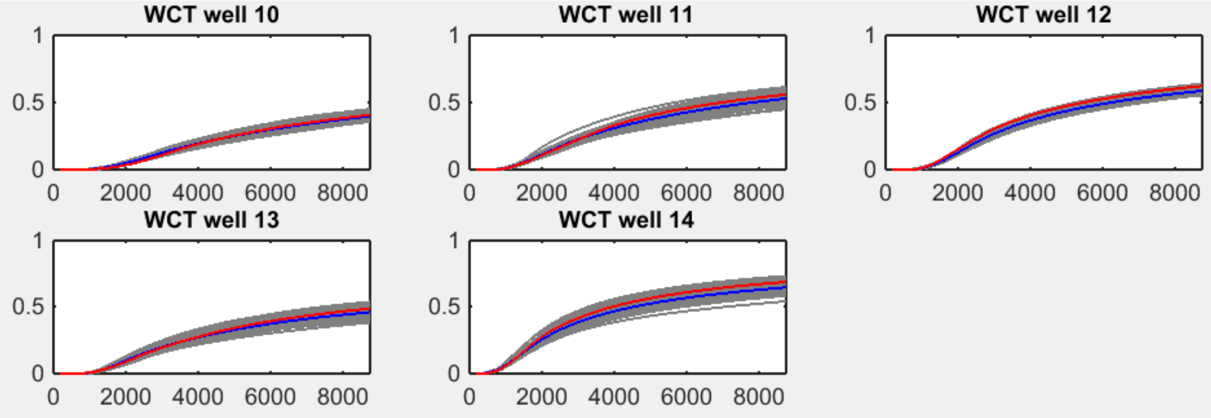

Figure 4.5: Water cut for the producers; grey is the prior ensemble waterflood, blue is the posterior ensemble mean and red is the synthetic truth.

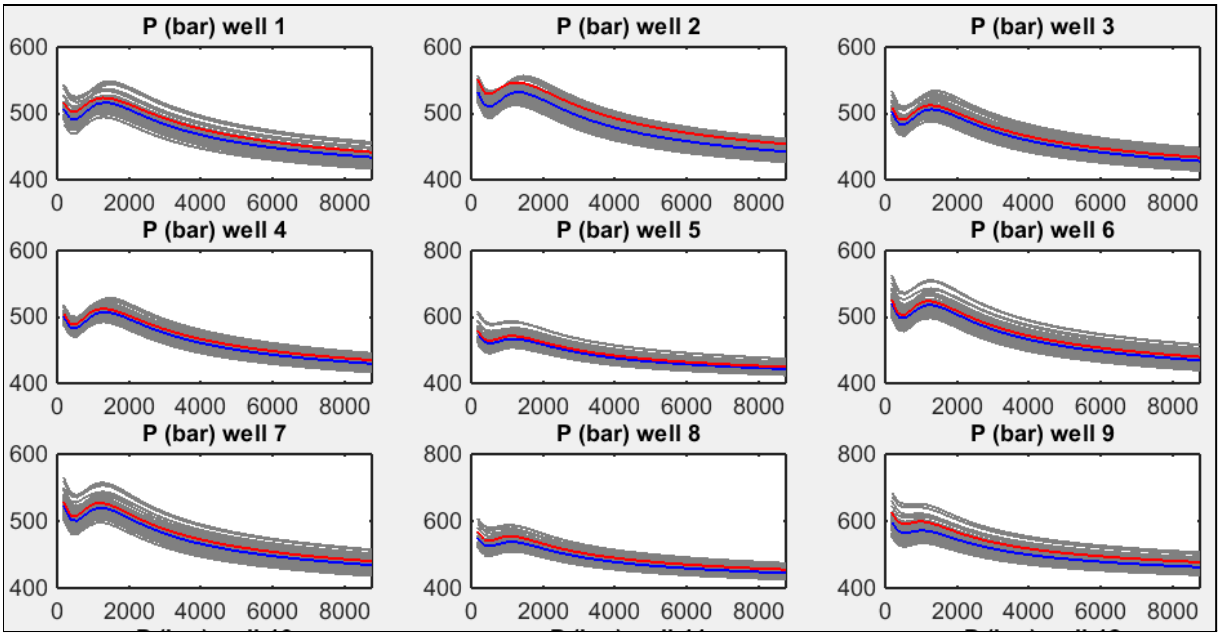

Figure 4. 6: Injection bottom-hole pressure for the injectors; grey is the prior ensemble waterflood, blue is the posterior ensemble mean and red is the synthetic truth.

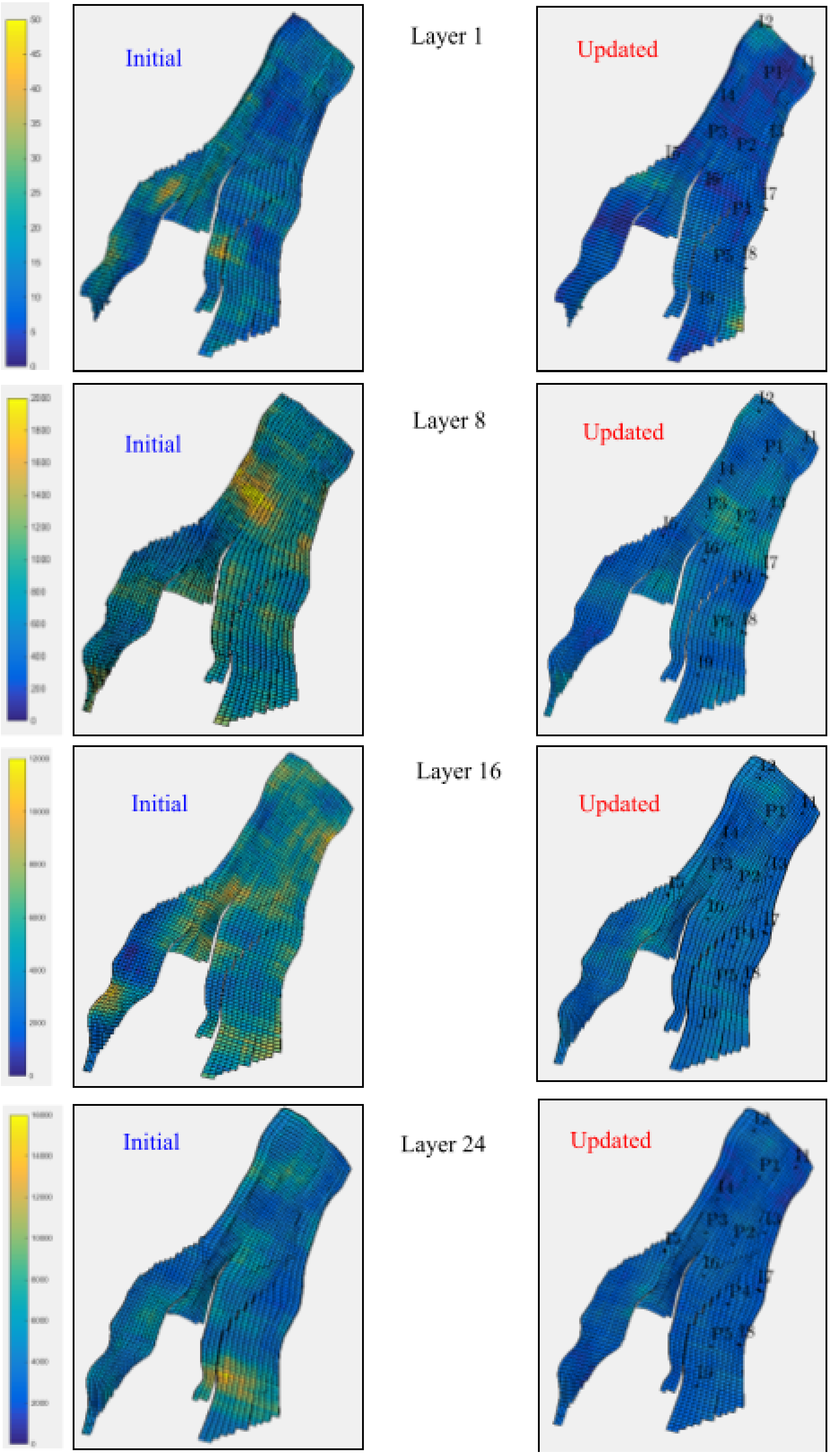

Figure 4.7: Permeability maps of the prior and posterior estimates for several layers of realization 10.

4.5 DEVELOPMENT SCENARIO AND PROCEDURE

We run the polymer-flood simulations using a proprietary fully implicit reservoir simulator (Van Doren et al., 2011). In each simulation run, 30 years of water injection is followed by 30 years of polymer-slug injection. We identify five polymer-flood signals to study:

- Earliest polymer breakthrough time at any well, days (Polymer BT)
- Earliest oil-bank arrival time at any well after polymer injection, days (1st Oil Bank Arrival)
- Average rise in injection pressure six months after polymer flood starts, bar (Rise in P_{inj})
- Average minimum oil cut (Min. Oil Cut)
- Cumulative oil production at the end of the polymer flood, m^3 (Cum. Oil Prod.)

We allow that the polymer process might fail in-situ by either of the two mechanisms described previously and study different scenarios of polymer process failure including cases where either or both of the failure mechanisms are involved:

1. Polymer in situ viscosity 18 cp: decay constant either 10 Year or 2 Year
2. Decay constant 10 Year: polymer in situ viscosity either 18 cp or 9 cp
3. Polymer in situ viscosity 9 cp: decay constant either 10 Year or 2 Year
4. Polymer in situ viscosity 18 cp and decay constant 10 Year, vs. polymer in situ viscosity 9 cp and decay constant 2 Year

Scenarios 1 and 3 consider only a progressive viscosity loss while scenario 2 considers only a global polymer viscosity loss. Scenario 4 is a combination of both polymer failure mechanisms. We test whether the signals of the difference for each scenario at injection and production wells would be statistically significant (using the 95% confidence interval) in the midst of the geological uncertainty represented by the updated ensemble (after EnKF). Specifically, 'Polymer BT' and 'Oil Bank Arrival' for the first of the five producers when it occurs for the failure simulation run is compared against the population of signal values of the first producer where it occurs for the design-viscosity case. For 'Min. Oil Cut', an average value of the five producers is compared against the average signal values of the design-viscosity representation. For 'Cum. Oil Prod.', the value is compared against the signal value of the design-viscosity representation. During a field trial, best practice is to run 50 simulations for 60 years of waterflood and utilize a decline-curve analysis to calculate an expected value of cumulative oil. Here, we assume the variance is the same for the cumulative oil production and the incremental oil during the polymer flood and consider a cumulative oil production at the end of the polymer flood.

4.6 RESULTS

Figs. 4.8 through 4.11 show the plot of the signal analysis of the four scenarios, and Tables 4.2 through 4.5 show the upper and lower limits of each signal for that scenario and the number of outliers detected in comparing the design and failure simulation runs.

Figure 4.8: Signal analysis of scenario #1: values of five signals for the design and failure cases. Blue squares are the design signal values and red triangles are the failure signal values.

Table 4. 2: Results of signal analysis of scenario #1.

Scenario#1: Global viscosity 18cp decay constant either 10 Year or 2 Year					
Confidence Interval	**1st Polymer BTTime (Year)**	**1st Oil Bank Arrival Time (Year)**	**Average Min Oil Cut**	**Rise in P_{inj}, 6 Months**	**Cum. Oil Prod. (m^3)**
Upper Limit	32.2462	31.2363	0.11066	0.817110686	81818165.07
Lower Limit	31.7617	30.2382	0.1009	0.676999931	72061754.93
Outliers Detected (out of 50)	12	50	49	50	50

Figure 4.9: Signal analysis of scenario #2: values of five signals for the design and failure cases. Blue squares are the design signal values and red triangles are the failure signal values.

Table 4. 3: Result of signal analysis of scenario #2.

Scenario#2: Decay constant: 10 Year, global viscosity either 18 cp or 9 cp					
Confidence Interval	**1st Polymer BTTime (year)**	**1st Oil Bank Arrival Time (year)**	**Average Min Oil Cut**	**Rise in P_{inj}, 6 Months**	**Cum. Oil Prod. (m^3)**
Upper Limit	32.2462	31.2363	0.11066	0.817110686	81818165.07
Lower Limit	31.7617	30.2382	0.1009	0.676999931	72061754.93
Outliers Detected (out of 50)	20	44	5	50	26

Figure 4.10: Signal analysis of scenario #3: values of five signals for the design and failure cases. Blue squares are the design signal values and red triangles are the failure signal values.

Table 4. 4: Result of signal analysis of scenario #3.

Scenario#3: Global viscosity 9cp, decay constant either 10 Year or 2 Year					
Confidence Interval	**1st Polymer BTTime (year)**	**1st Oil Bank Arrival Time (year)**	**Average Min Oil Cut**	**Rise in P_{inj}, 6 Months**	**Cum. Oil Prod. (m^3)**
Upper Limit	32.454	31.7384	0.10902	0.393582562	76187748.48
Lower Limit	31.943	31.038	0.09943	0.325993487	67515211.52
Outliers Detected (out of 50)	13	50	49	50	50

Figure 4.11: Signal analysis of scenario #4: values of five signals for the design and failure cases. Blue squares are the design signal values and red triangles are the failure signal values.

Table 4. 5: Result of signal analysis of scenario #4.

Scenario #4: Global viscosity: 18 cp and decay constant: 10 Year vs. Global viscosity: 9 cp and decay constant: 2 Year					
Confidence Interval	**1st Polymer BTTime (year)**	**1st Oil Bank Arrival Time (year)**	**Average Min Oil Cut**	**Rise in P_{inj}, 6 Months**	**Cum. Oil Prod. (m^3)**
Upper Limit	32.2462	31.2363	0.11066	0.817110686	81818165.07
Lower Limit	31.7617	30.2382	0.1009	0.676999931	72061754.93
Outliers Detected (out of 50)	7	50	50	50	50

In all scenarios, '1st Oil Bank Arrival Time' and 'Rise in P_{inj}' are reliable indicators of a failed polymer flood process (irrespective of the mechanism involved) in almost all of the cases. In scenarios 1 and 3 where only one decay mechanism is involved, loss of viscosity can be discerned by the two mechanism mentioned above as well as the 'Min. Oil Cut' signal and 'Cum. Oil Prod'. This suggests we can tell what mechanism caused the in situ viscosity loss between the two. '1st polymer breakthrough time' was not a reliable indicator of in situ polymer loss in this case study.

4.7 SUMMARY AND CONCLUSIONS

In this case study, we consider a realistic reservoir geological description and start with an initial ensemble of realizations that could be a candidate to undergo polymer-flood process. We then perform a history-match using EnKF to assimilate the 30 years of waterflood data to update the prior ensemble. We then simulate 30 years of polymer flood on the updated ensemble for different scenarios with two mechanisms of polymer in situ viscosity loss. We study five signals to discern in situ polymer viscosity loss in the midst of geological uncertainty. In the event of a progressive decay of polymer viscosity we can discern a polymer flood failure in the midst of geological uncertainties using the 'min. oil cut' signal. '1st oil bank arrival time' and 'rise in P_{inj}' are reliable signals of viscosity loss analysis for both mechanisms. 'Cum. oil prod.' is a reliable signal for scenarios 1, 3 and 4 but not scenario 2 where there is only a global polymer viscosity loss.

5

CONCLUSIONS AND RECOMMENDATIONS

In this chapter we first provide general conclusions and observations from this research and follow with specific conclusions of each chapter of the thesis. Finally, we present a few recommendations to continue this research.

5.1 CONCLUSIONS

An enhanced-oil-recovery (EOR) pilot test has multiple goals, among them to demonstrate oil recovery, verify the properties of the EOR agent in-situ, and provide the information needed for scale-up to an economic process. Uncertainty remains a matter of concern regarding the actual performance of an EOR agent in the reservoir despite extensive laboratory and field scale tests for the compatibility and the efficiency of the injected chemical, such as in-situ viscosity of a polymer agent. It is necessary to evaluate the impacts of geological as well as EOR process uncertainties on the performance of an EOR process to better examine if the process achieved its technical objectives. Given the complexity of EOR processes and the inherent uncertainty in the reservoir description, it is a challenge to discern the properties of the EOR agent in-situ in the midst of geological uncertainty. This project aims to determine whether one can discern the technical success of a polymer EOR process from available reservoir pressure and rate signals, given the inherent uncertainty in the reservoir geological description. We analyze three case studies of increasing complexity to illustrate this challenge and identify the responsive signals to discern in-situ performance of a polymer agent amid the geological uncertainty.

5.1.1 LAYER-CAKE MODEL

Chapter 2 presents a workflow and a simple initial study of a polymer flood to illustrate the issues involved in attempting to distinguish EOR process performance from well data in the midst of geological uncertainty. This initial test case involves an especially simple reservoir description: a two-dimensional layer-cake reservoir with injection from one side and production from the other. Different spatial arrangements of high- and low-permeability layers are assumed. EOR process failure is represented by a fivefold reduction in polymer-solution viscosity from the expected value.

Among the signals considered here, the rate of rise in injection pressure upon polymer injection and maximum pressure in the injection well give the most reliable indications of whether polymer viscosity was maintained in-situ. Given the chances of fracturing of the injection well (Seright et al., 2009), injection pressure could be an unreliable indicator of in-situ polymer viscosity injection, especially if the extent of this fracturing is unknown. In that case a diagnostic fracture-injection/falloff test might substitute for the well pressure data (Craig and Jackson, 2017).

Among the other signals considered, it was hardest to distinguish failure of the EOR process in reservoirs that, among the ensemble of equi-probable reservoirs, were relatively homogeneous. For these cases the waterflood by itself performed relatively well; the failure of the EOR process was hard to distinguish from the possibility of greater reservoir heterogeneity. Failure was easiest to identify if the actual reservoir was among the more heterogeneous cases considered possible. In those cases, the additional loss in performance from failure of the EOR process produced a result outside the confidence interval.

Previous studies that considered the effect of geological uncertainty alone on EOR process performance, but not the possibility of technical failure of the process itself, establish the range of outcomes for a process that performs in-situ as designed. In effect, they establish the confidence interval beyond which a failed EOR process could be identified.

The range of geological uncertainty in this initial case study could be viewed as extreme. We assume that injectivity is known but that very little is known about the extent of reservoir heterogeneity, even at the wells. On the other hand, the extent of failure of the polymer in-situ, i.e. a loss of viscosity by a factor of 5, could be considered extreme as well. Moreover, we consider a two-well situation, whereas in a multi-well setting the effect of viscosity changes may result in different signals in the different wells.

5.1.2 FLUVIAL RESERVOIR (EGG MODEL)

Chapter 3 extends the work of Chapter 2 by including a more-realistic geological description and more injection and production wells. In addition, the initial range of geological uncertainty is conditioned to 10 years of waterflood, in that only reservoirs with roughly similar breakthrough times in the production wells are carried forward in the analysis. We assume that polymer viscosity in situ could be 30% of that expected.

In this case study, signals are more responsive than in the first case study, mainly due to a more realistic (less extreme) geological variability. Results of this study verify the conclusions of the previous chapter. Changes in polymer breakthrough time are a reliable indicator of failure of polymer viscosity in situ in this case. The rate of rise of injection-well pressure during polymer injection is also a reliable indicator, though a diagnostic fracture-injection/falloff test may be necessary to verify the reliability of the injection-pressure data (Craig and Jackson 2017). Moreover, in this case study, other signals, such as a combination of ‘time of initial increase in oil production rate’, ‘minimum oil cut before the oil bank’ and ‘final cumulative oil recovery,’ give a statistically significant indication of loss of polymer viscosity in situ in the majority of the cases.

5.1.3 NORNE FIELD MODEL

Chapter 4 extends the work of the previous chapters by including a realistic reservoir geological description and two distinct mechanisms of EOR process failure. Specifically, the first mechanism results in a global loss of viscosity, and the second in a progressive loss of viscosity with increasing distance from the injection well. The second class of failure could reflect chemical degradation of polymer, the process we modeled explicitly, or, roughly, an unexpectedly high level of adsorption slowing or preventing propagation of polymer far from the injection well. The Ensemble Kalman Filter is applied to 30 years of waterflood history to update the initial ensemble of geological realizations. We then allow that the polymer process might fail in-situ by either of the two failure mechanisms and examine scenarios where either or both of the failure mechanisms are involved. Specifically, polymer viscosity everywhere could be 50% of that intended, and/or polymer viscosity could degrade faster than expected, with a time constant of 2 years instead of the expected time constant of 10 years.

In all scenarios, ‘1st oil bank arrival time’ and ‘rise in P_{inj}’ are reliable indicators of a failed polymer flood process (by either mechanism) in almost all of the cases. Faster decay of polymer viscosity, without the global loss of viscosity, results in statistically significant deviation from the expected values of the two signals mentioned above as well as in ‘min. oil cut’ and ‘cum. oil prod.’ A case of global viscosity loss but not accelerated decay shows deviation in the first two signals but not in ‘min. oil cut’ and ‘cum. oil prod.’ This suggests one can tell which failure mechanism failed in situ by comparing these four signals. ‘1st polymer breakthrough time’ was not a reliable indicator of in situ polymer loss by either mechanism in this case study.

5.2 RECOMMENDATIONS

We recommend extension of our analysis to different EOR methods, such as surfactant flooding, foam processes or CO_2-EOR, and ways these processes might fail. The challenge would be to distinguish a successful EOR process from the various types of failure for that process by analyzing the well-pressure and rate data to test whether the measurements send a signal that is statistically significant as an indication of failure. Ultralow interfacial tension (IFT) or low residual oil saturation for the surfactant process, a given mobility or injectivity for a foam process and minimum miscibility pressure, degree of swelling, or absence of asphaltene deposition for a CO_2-EOR process could be technical criteria for success of the EOR agent in-situ. EOR process description often involves a large number of parameters, so we would recommend an approach to other EOR processes like that used here for polymer flooding: a limited number of parameters representing process performance as simply as possible.

The approach should also be extended to additional methods of reservoir monitoring, which are under continual development and improvement, such as cross-well electromagnetic readings, cross-well seismic, well temperature readings, etc.

Reservoir description is optimized using techniques such as ensemble Kalman filter as in Chapter 4 (Aanonsen et al., 2009). A more-direct, but much more complicated, approach to determining EOR process parameters simultaneously with reservoir description would involve optimizing both EOR process parameters and reservoir description simultaneously, to obtain the best fit to EOR field-trial results. Production data from before the field trial should be included as well, since they also reflect reservoir description. A somewhat simpler approach would find optimal EOR process parameters from a fit to field-trial data using a population of reservoirs representing the range of descriptions based on production data before the field trial. This would exclude insights from the trial itself, which might modify the reservoir description.

REFERENCES

Aanonsen, S. I., G. Nævdal, D. S. Oliver, A. C. Reynolds and B. Vallès (2009). The Ensemble Kalman Filter in Reservoir Engineering-a Review. *SPE Journal* 14(3), https://doi.org/10.2118/117274-PA.

Adepoju, O., H. Hussein and A. Chawathe (2017). Assessment of Chemical Performance Uncertainty in Chemical EOR Simulations. Paper. Alternate Assessment of Chemical Performance Uncertainty in Chemical EOR Simulations. presented at SPE Reservoir Simulation Conference, Conference, https://doi.org/10.2118/182596-ms.

Adlam, J. (1995). The Norne Field Development Overview. USA, *Offshore Technology Conference*.

Aguiar, J. I. and C. Mansur (2016). The Influence of Polymer Flooding on Produced Oily Water: A Review. *Brazilian Journal of Petroleum and Gas* 10: 49-61, https://doi.org/10.5419/bjpg2016-0005.

Akkutlu, I. Y. and Y. C. Yorisos (2005). The effect of heterogeneity on in-situ combustion: Propagation of combustion fronts in layered porous media. *SPE Journal* 10(4): 394-404, https://doi.org/10.2118/75128-PA.

Al-Honi, M., M. Greaves and A. Y. Zekri (2002). Enhanced recovery of medium crude oil in heterogeneous reservoirs using air injection/in situ combustion-horizontal well technology. *Petroleum Science and Technology* 20(5-6): 655-669, https://doi.org/10.1081/LFT-120003587.

Al-Mudhafar, W. and D. Rao, (2016). Quantifying the Effects of Reservoir Heterogeneity and Anisotropy on Field Scale-CO2 EOR Flooding Performance through the Cyclic GAGD Process.

Alkhatib, A. M. and P. R. King (2015). The Use of the Least-Squares Probabilistic-Collocation Method in Decision Making in the Presence of Uncertainty for Chemical-Enhanced-Oil-Recovery Processes. *SPE Journal* 20(4), https://doi.org/10.2118/170587-PA.

Alvarado, V. and E. Manrique, (2010). Enhanced Oil Recovery Field Planning and Development Strategies. UK, *Elsevier*.

Arpat, G. B. and J. Caers (2004). A Multiple-scale, Pattern-based Approach to Sequential Simulation. Geostatistics Banff 2004. Netherlands, *Springer Netherlands*. **1:** 255-264.

Ballin, P. R., A. G. Journel and K. Aziz (1992). Prediction Of Uncertainty In Reservoir Performance Forecast. *Journal of Canadian Petroleum Technology* 31(04): 12, https://doi.org/10.2118/92-04-05.

Brown, C. E. and P. J. Smith (1984). The Evaluation of Uncertainty in Surfactant EOR Performance Prediction. Paper. Alternate The Evaluation of Uncertainty in Surfactant EOR Performance Prediction. presented at SPE Annual Technical Conference and Exhibition, Conference, https://doi.org/10.2118/13237-ms.

Chen, Q., M. G. Gerritsen and A. R. Kovscek (2008). Effects of Reservoir Heterogeneities on the Steam-Assisted Gravity-Drainage Process. *SPE Reservoir Evaluation & Engineering* 11(5), https://doi.org/10.2118/109873-PA.

Chen, Y. and D. S. Oliver (2010). Cross-covariances and localization for EnKF in multiphase flow data assimilation. *Computational Geosciences* 14(4): 579–601, https://doi.org/10.1007/s10596-009-9174-6.

Chiotoroiu, M.-M., J. Peisker, T. Clemens and M. Thiele (2017). Forecasting Incremental Oil Production of a Polymer-Pilot Extension in the Matzen Field Including Quantitative Uncertainty Assessment. *SPE Reservoir Evaluation & Engineering* Preprint(Preprint), https://doi.org/10.2118/179546-PA.

Cohn, G. G. a. S. E. (1999). Construction of correlation functions in two and three dimensions. *Q. J. Royal Meteorological Soc.* 125: 723–757.

Craft, B. C., M. Hawkins and R. E. Terry, (1991). Applied Petroleum Reservoir Engineering. New Jersy, USA, *Prentice Hall*.

Craig, D. P. and R. A. Jackson (2017). Calculating the Volume of Reservoir Investigated During a Fracture-Injection/Falloff Test DFIT. Paper. Alternate Calculating the Volume of Reservoir Investigated During a Fracture-Injection/Falloff Test DFIT. presented at SPE Hydraulic Fracturing Technology Conference and Exhibition, Conference, https://doi.org/10.2118/184820-ms.

Craig, F. F., (1993). The Reservoir Engineering Aspects of Waterflooding, Second Edition. USA, *Society of Petroleum Engineers*.

Dake, L. P., (2001). Practice of Reservoir Engineering Developments in Petroleum Science. USA, *Elsevier Science*.

Damsleth, E. and H. Omre (1997). Geostatistical Approaches in Reservoir Evaluation. *Journal of Petroleum Technology* 49(05): 498-501, https://doi.org/10.2118/37681-JPT.

Denney, D. (2011). Alkaline/Surfactant/Polymer Flood: Single-Well Chemical-Tracer Tests - Design, Implementation, and Performance. *Journal of Petroleum Technology* 63(06): 86-88, https://doi.org/10.2118/0611-0086-JPT.

Denney, D. (2011). Uncertainty Management in a Major CO2 EOR Project. *Journal of Petroleum Technology* 63(7), https://doi.org/10.2118/0711-0112-JPT.

Dickson, J. L., A. L. Dios and P. L. Wylie (2010). Development Of Improved Hydrocarbon Recovery Screening Methodologies. SPE Improved Oil Recovery Symposium. Tulsa, Oklahoma, USA, *Society of Petroleum Engineers*.

Dykstra, H. and R. L. Parsons (1956). The Prediction of oil Recovery by Water Flood. https://doi.org/10.2118/733-G.

Elraies, K. A. (2012). An experimental study on ASP process using a new polymeric surfactant. *Journal of Petroleum Exploration and Production Technology* 2(4): 223-227, https://doi.org/10.1007/s13202-012-0039-5.

Emerick, A. A. and A. C. Reynolds (2011). History Matching a Field Case Using the Ensemble Kalman Filter With Covariance Localization. *SPE Reservoir Evaluation & Engineering* 14(4), https://doi.org/10.2118/141216-PA.

Emerick, A. A. and A. C. Reynolds (2013). Ensemble smoother with multiple data assimilation. *Computers & Geosciences* 55: 3-15, https://doi.org/10.1016/j.cageo.2012.03.011.

Esposito, A., A. Perrone, R. Sabatino and E. Della Rossa (2017). Maximizing Project Value While Minimizing Risk: Innovative Application of Robust Optimization With Use of Proxy Models. Offshore Mediterranean Conference and Exhibition. Ravenna, Italy, *Offshore Mediterranean Conference*: 13.

Evensen, G., (2009). Data Assimilation The Ensemble Kalman Filter, *Springer-Verlag Berlin Heidelberg*.

Fanchi, J. R., (2005). Principles of Applied Reservoir Simulation. USA, *Elsevier*.

Fatemi, S. A., J. D. Jansen and W. R. Rossen (2015). Discerning In-Situ Performance of an EOR Agent In the Midst of Geological Uncertainty. 18th European Symposium on Improved Oil Recovery. Dresden, Germany.

Fatemi, S. A., J. D. Jansen and W. R. Rossen (2017). Discerning in-situ performance of an EOR agent in the midst of geological uncertainty I: Layer cake reservoir model. *Journal of Petroleum Science and Engineering* 158: 56-65, https://doi.org/10.1016/j.petrol.2017.08.021.

Fatemi, S. A., J. D. Jansen and W. R. Rossen (2019). Discerning In-Situ Performance of an Enhanced-Oil-Recovery Agent in the Midst of Geological Uncertainty: II. Fluvial-Deposit Reservoir. *SPE Journal* 24(03): 1076-1091, https://doi.org/10.2118/174613-PA %J SPE Journal.

Fedutenko, E., C. Yang, C. Card and L. X. Nghiem (2012). Forecasting SAGD Process Under Geological Uncertainties Using Data-Driven Proxy Model. SPE Heavy Oil Conference Canada. Calgary, Alberta, Canada, *Society of Petroleum Engineers*: 12.

Flaaten, A., Q. Nguyen, G. Pope and J. Zhang (2009). A Systematic Laboratory Approach to Low-Cost, High-Performance Chemical Flooding. *SPE Reservoir Evaluation & Engineering - SPE RESERV EVAL ENG* 12: 713-723, https://doi.org/10.2118/113469-PA.

Gharbi, R., E. Peters and A. Garrouch (1997). Effect of heterogeneity on the performance of immiscible displacement with horizontal wells. *Journal of Petroleum Science and Engineering - J PET SCI ENGINEERING* 18: 35-47, https://doi.org/10.1016/S0920-4105(97)00016-8.

Green, D. W. and G. P. Willhite, (2018). Enhanced Oil Recovery, *Society of Petroleum Engineers*.

Hawkins, D. M., (1980). Identification of Outliers, *Springer Netherlands*.

Hazarika, K. and S. B. Gogoi (2019). Effect of alkali on alkali–surfactant flooding in an Upper Assam oil field. *Journal of Petroleum Exploration and Production Technology*, https://doi.org/10.1007/s13202-019-00794-3.

Hirasaki, G. J. (1984). Properties Of Log-Normal Permeability Distribution For Stratified Reservoirs, *Society of Petroleum Engineers*.

Hocine, S., B. Pousset, T. Courtaud and G. Degré (2018). Long Term Thermal Stability of Chemical EOR Surfactants. SPE EOR Conference at Oil and Gas West Asia. Muscat, Oman, *Society of Petroleum Engineers*: 14.

Jansen, J. D., R. M. Fonseca, S. Kahrobaei, M. M. Siraj, G. Van Essen and P. Van den Hof (2014). The egg model – a geological ensemble for reservoir simulation. *Geosci. Data J.* 1: 192-195, https://doi.org/10.1002/gdj3.21.

Jensen, J., L. W. Lake, P. Corbett and D. Goggin, (2000). Statistics for Petroleum Engineers and Geoscientists. USA, *Elsevier*.

Jia, H. (2018). Effect of reservoir heterogeneity on air injection performance in a light oil reservoir. *Petroleum* 4(1): 15-24, https://doi.org/10.1016/j.petlm.2017.10.006.

Khan, M. B. and M. S. Khan (2018). Experimental investigation on effect of alkali, salts on the rheological properties of polyacrylamide and mixed assembly of polymer-surfactant. *Chemical Data Collections* 13-14: 60-72, https://doi.org/10.1016/j.cdc.2018.01.004.

Khataniar, S. and E. J. Peters (1992). The effect of reservoir heterogeneity on the performance of unstable displacements. *Journal of Petroleum Science and Engineering* 7(3): 263-281, https://doi.org/10.1016/0920-4105(92)90023-T.

Koneshloo, M., S. A. Aryana and X. Hu (2018). The impact of geological uncertainty on primary production from a fluvial reservoir. *Petroleum Science* 15(2): 270-288, https://doi.org/10.1007/s12182-018-0229-y.

Kumar, M., V. Hoang, C. Satik and D. Rojas (2006). High-Mobility-Ratio-Waterflood Performance Prediction: Challenges and New Insights.

Kumar, M., V. T. Hoang, C. Satik and D. H. Rojas (2008). High-Mobility-Ratio Waterflood Performance Prediction: Challenges and New Insights. *SPE Reservoir Evaluation & Engineering* 11(1), https://doi.org/10.2118/97671-PA.

Kumar, R., V. Shankar, S. K. Batra and A. Kumar (2017). Effect of Reservoir Heterogeneities and Model Uncertainties on Prediction Versus Actual Field Behavior- A Case Study. SPE Oil and Gas India Conference and Exhibition. Mumbai, India, *Society of Petroleum Engineers*.

Lake, L. W., R. Johns, W. R. Rossen and G. Pope, (2014). Fundamentals of Enhanced Oil Recovery. USA, *Society of Petroleum Engineers*.

Langtangen, H. P. (1991). Sensitivity analysis of an enhanced oil recovery process. *Applied Mathematical Modelling* 15(9): 467-474, https://doi.org/10.1016/0307-904X(91)90036-O.

Levitt, D. and M. Bourrel (2016). Adsorption of EOR Chemicals Under Laboratory and Reservoir Conditions, Part III: Chemical Treatment Methods. SPE Improved Oil Recovery Conference. Tulsa, Oklahoma, USA, *Society of Petroleum Engineers*: 23.

Lie, K. A., S. Krogstad, I. S. Ligaarden, J. R. Natvig, H. M. Nilsen and B. Skaflestad (2012). Open-source MATLAB implementation of consistent discretisations on complex grids. *Computational Geosciences* 16(2): 297-322, https://doi.org/10.1007/s10596-011-9244-4.

Lorentzen, R. J., G. Nævdal and A. C. V. M. Lage (2003). Tuning of parameters in a two-phase flow model using an ensemble Kalman filter. *International Journal of Multiphase Flow* 29: 1283-1309, https://doi.org/doi:10.1016/S0301-9322(03)00088-0.

Luo, X., T. Bhakta, M. Jakobsen and G. Naevdal (2017). An Ensemble 4D-Seismic History-Matching Framework With Sparse Representation Based On Wavelet Multiresolution Analysis. *SPE Journal* 22(3), https://doi.org/10.2118/180025-PA.

Lyon, B. K. and G. Popov (2017). Communicating and Managing Risk: The Key Result of Risk Assessment. *Professional Safety* 62(11): 35-44.

Ma, Y. Z., (2019). Quantitative Geosciences: Data Analytics, Geostatistics, Reservoir Characterization and Modeling, *Springer International Publishing*.

Mantilla, C. A. and S. Srinivasan (2011). Feedback control of polymer flooding process considering geologic uncertainty. SPE Reservoir Simulation Symposium. The Woodlands, Texas, USA, *Society of Petroleum Engineers*.

Møyner, O. and K.-A. Lie (2016). A Multiscale Restriction-Smoothed Basis Method for Compressible Black-Oil Models. *SPE Journal*, https://doi.org/10.2118/173265-PA.

Nasr-El-Din, H. A., B. F. Hawkins and K. A. Green (1992). Recovery of residual oil using the alkali/surfactant/polymer process: effect of alkali concentration. *Journal of Petroleum Science and Engineering* 6(4): 381-401, https://doi.org/10.1016/0920-4105(92)90064-8.

Nguyen, N., C. T. Q. Dang, Z. Chen and L. X. Nghiem (2016). Geological uncertainty and effects of depositional sequence on improved oil recovery processes. *Journal of Petroleum Exploration and Production Technology* 6(4): 801-813, https://doi.org/10.1007/s13202-016-0230-1.

Odell, P. M. and K. C. Lindsey (2010). Uncertainty Management in a Major CO2 EOR Project. Abu Dhabi International Petroleum Exhibition and Conference. Abu Dhabi, UAE, *Society of Petroleum Engineers*: 8.

Phukan, R., S. B. Gogoi and P. Tiwari (2019). Enhanced oil recovery by alkaline-surfactant-alternated-gas/CO2 flooding. *Journal of Petroleum Exploration and Production Technology* 9(1): 247-260, https://doi.org/10.1007/s13202-018-0465-0.

Pointe, P. L. and Y. Z. Ma, (2011). Uncertainty Analysis in Reservoir Characterization. United Kingdom, *AAPG*.

Pollack, A. and T. Mukerji (2019). Accounting for subsurface uncertainty in enhanced geothermal systems to make more robust techno-economic decisions. *Applied Energy* 254: 113666, https://doi.org/10.1016/j.apenergy.2019.113666.

Popov, Y., M. Spasennykh, D. Miklashevskiy, A. Parshin, V. Stenin, M. Chertenkov, S. Novikov and N. Tarelko (2010). Thermal Properties of Formations From Core Analysis: Evolution in Measurement Methods, Equipment, and Experimental Data in Relation to Thermal EOR. Canadian Unconventional Resources and International Petroleum Conference. Calgary, Alberta, Canada, *Society of Petroleum Engineers*.

Pyrcz, M. J. and C. V. Deutsch, (2014). Geostatistical Reservoir Modeling, *Oxford University Press*.

Rashid, B., A. Muggeridge, A. L. Bal and G. J. J. Williams (2010). Quantifying the Impact of Permeability Heterogeneity on Secondary-Recovery Performance. SPE Annual Technical Conference and Exhibition,. Florence, Italy, *Society of Petroleum Engineers*.

Sacconi, A. and H. Mahgerefteh (2020). Modelling start-up injection of CO2 into highly-depleted gas fields. *Energy* 191: 116530, https://doi.org/10.1016/j.energy.2019.116530.

Saleh, L. D., M. Wei and B. Bai (2014). Data Analysis and Updated Screening Criteria for Polymer Flooding Based on Oilfield Data. *SPE Reservoir Evaluation & Engineering* 17(1), https://doi.org/10.2118/168220-PA.

Scheidt, C., L. Li and J. Caers, (2018). Quantifying Uncertainty in Subsurface Systems, *Wiley*.

Seright, R. S., J. M. Seheult and T. Talashek (2009). Injectivity Characteristics of EOR Polymers. *SPE Reservoir Evaluation & Engineering* 12(05): 783-792, https://doi.org/10.2118/115142-PA %J SPE Reservoir Evaluation & Engineering.

Sheng, J., (2011). Modern Chemical Enhanced Oil Recovery Theory and Practice, *Elsevier*.

Soleimani, A., R. K. Penney, O. Hegazy, A. B. Ngah, A. E. Sulliman and R. D. Tewari (2011). Impact of Fluvial Geological Characteristics on EOR Screening of a Large Heavy Oil Field. SPE Enhanced Oil Recovery Conference. Kuala Lumpur, Malaysia, *Society of Petroleum Engineers*.

Sorbie, K. S. and P. J. Clifford, (1988). Water-Soluble Polymers for Petroleum Recovery. New York *Springer*.

Stanley, B. (2014). Effect of Uncertainty in PVT Properties on CO2 EOR. SPE Nigeria Annual International Conference and Exhibition. August, Lagos, Nigeria, *Society of Petroleum Engineers*.

Subbey, S., M. Christie and M. Sambridge (2004). Prediction under uncertainty in reservoir modeling. *Journal of Petroleum Science and Engineering* 44(1): 143-153, https://doi.org/10.1016/j.petrol.2004.02.011.

Torrealba, V. A., H. Hoteit and A. Chawathe (2019). Improving Chemical-Enhanced-Oil-Recovery Simulations and Reducing Subsurface Uncertainty Using Downscaling Conditioned to Tracer Data. *SPE Reservoir Evaluation & Engineering* 22(04): 1426-1435, https://doi.org/10.2118/187276-PA.

Van Doren, J., S. Douma, B. Wassing, H. Kraaijevanger and B.-R. de Zwart (2011). Adjoint-based Optimization of Polymer Flooding. Paper. Alternate Adjoint-based Optimization of Polymer Flooding. presented at SPE Enhanced Oil Recovery Conference, Conference, https://doi.org/10.2118/144024-ms.

Van Essen, G., M. Zandvliet, P. Van den Hof, O. Bosgra and J. D. Jansen (2009). Robust Waterflooding Optimization of Multiple Geological Scenarios. *SPE Journal* 14(1): 202-210, https://doi.org/10.2118/102913-PA.

Wang, D., L. Zhao, J. Cheng and J. Wu (2003). Actual Field Data Show that Production Costs of Polymer Flooding can be Lower than Water Flooding. Paper. Alternate Actual Field Data Show that Production Costs of Polymer Flooding can be Lower than Water Flooding. presented at SPE International Improved Oil Recovery Conference in Asia Pacific, Conference, https://doi.org/10.2118/84849-ms.

Wang, Y., H. Liu, Q. Zhang, Z. Chen, J. Wang, X. Dong and F. Chen (2020). Pore-scale experimental study on EOR mechanisms of combining thermal and chemical flooding in heavy oil reservoirs. *Journal of Petroleum Science and Engineering* 185: 106649, https://doi.org/10.1016/j.petrol.2019.106649.

Weiss, W. W. and R. W. Baldwin (1985). Planning and Implementing a Large-Scale Polymer Flood. *Journal of Petroleum Technology* 37(4), https://doi.org/10.2118/12637-PA.

Zhang, Y., Z. Fan, D. Yang, H. Li and S. Patil (2017). Simultaneous Estimation of Relative Permeability and Capillary Pressure for PUNQ-S3 Model With a Damped Iterative-Ensemble-Kalman-Filter Technique. *SPE Journal* 22(3), https://doi.org/10.2118/177846-PA.

LIST OF PUBLICATIONS

Journal Publications

Fatemi, S. A., Jansen, J. D., Rossen, W. R. (2017). Discerning in-situ performance of an EOR agent in the midst of geological uncertainty I: Layer cake reservoir model. *Journal of Petroleum Science and Engineering* 158 (8): 56-65.

Fatemi, S. A., Jansen, J. D., and W. R. Rossen (2019). Discerning In-Situ Performance of an Enhanced-Oil-Recovery Agent in the Midst of Geological Uncertainty: II. Fluvial-Deposit Reservoir. *SPE J. 24: 1076–1091.*

Journal Submission (Under Review)

Fatemi, S. A., Jansen, J. D., and W. R. Rossen (2021). Discerning In-Situ Performance of an Enhanced-Oil-Recovery Agent in the Midst of Geological Uncertainty: III. Norne Field. *SPE Reservoir Evaluation & Engineering.*

Conference Proceedings

Fatemi, S. A., Rossen, W. R. (2014) Discerning In Situ Performance of an EOR Agent in the Midst of Geological Uncertainty. IOR 2015 – 18th European Symposium on Improved Oil Recovery. Dresden, Germany.

Fatemi, S. A Rossen, W. R. (2015) Discerning In-Situ Performance of an EOR Agent In the Midst of Geological Uncertainty: II. Fluvial-Deposit Reservoir. SPE Asia Pacific Enhanced Oil Recovery Conference. Kuala Lumpur, Malaysia.

SUMMARY

Chemical floods such as polymer floods are enhanced oil recovery (EOR) techniques that have been proven at both laboratory and field scale to increase sweep and/or displacement efficiency. Even though the compatibility and the efficiency of the injected chemicals are thoroughly tested and validated in the laboratory, uncertainty still remains regarding their actual performance in the reservoir. These uncertainties can result from the differences in the scale of investigation (core scale to field scale), lack of adequate understanding of geological, mineralogical and petrophysical properties of the formation, and the long-term performance of the chemical slug in the reservoir. Therefore, any EOR field trial can produce unexpected results due to a misunderstanding of either the geological description of the reservoir or of the EOR process. Separate evaluation of the impacts of geological and process uncertainties on the performance of an EOR process is important to better demonstrate if the process achieved its technical objectives. Previous research has examined uncertainty in chemical flooding performance parameters as well as effects of geological heterogeneity and uncertainty on EOR process performance, but not the two together. In this thesis, to discern the performance of the EOR agent in-situ in the midst of geological uncertainty, we propose a general workflow and present three case studies for the challenge. The workflow could be extended to different EOR processes by including mechanisms of technical failure specific to that process, e.g. losing in-situ viscosifying power of the polymer agent during a polymer flood process.

In this dissertation, we first study a polymer EOR process in a 2D layer-cake reservoir where the polymer is designed to have a viscosity of 60 cp in-situ. In the first study, using a simplified representation of geological uncertainty, we allow that the polymer process might fail in-situ and viscosity could be only 20% of that intended. This failure could be the result of mechanical degradation in surface facilities or on entering the perforations, faulty translation from laboratory-measured properties to properties in-situ, or faulty characterization of resident reservoir brine. Several of these adverse events would give different polymer properties in different regions of the reservoir. In the initial study, we assume that throughout the reservoir polymer viscosity is everywhere a fixed fraction of that intended. We test whether the signals of this failure at the injection and production wells would be statistically significant in the midst of the geological uncertainty in the reservoir description. For a population of reservoirs representing a range of geological

uncertainty, we compare the deviation caused by loss of polymer viscosity to the scatter caused by the geological uncertainty using the confidence interval statistical approach. Various signals are then monitored to see which are the most reliable indications of whether a polymer viscosity was maintained in-situ. We further investigate the statistical significance of each signal. We also propose a workflow for such an evaluation that could be extended to any EOR process [chapter 2].

For a more realistic case study, we apply the workflow to a case with a more-sophisticated geological model (based on the "modified Egg Model") for a polymer EOR process designed for a 3D fluvial-deposit water-oil reservoir. The polymer is designed to have a viscosity of 20 cp in situ. We start with 100 realizations of this 3D reservoir to reflect the range of possible geological structures honoring the statistics of the initial geological uncertainties. Next we group the realizations on the basis of a measure of similarity that reflects the interaction between heterogeneity and the reservoir flow mechanisms. After five years of waterflooding, we rank the reservoir models into different groups of 10 realizations, out of the initial 100 equi-probable realizations, with similar water breakthrough dates at the four production wells. Each group of realizations thus represents reservoirs with roughly similar waterflood histories. As a group they represent the reduced geological uncertainty remaining after this period of waterflooding. To represent EOR process failure, we allow that the polymer process might fail in situ and viscosity could be 30% of that intended. We then simulate five years of polymer injection. We assume that throughout the reservoir polymer viscosity is less than the design value. We test whether the signals of this difference at injection and production wells would be statistically significant in the midst of the geological uncertainty: in other words, whether the process failure would be clearly visible in the midst of reservoir uncertainty [chapter 3].

Based on a real reservoir and a level of uncertainty more representative of a field after a period of waterflood, we apply the workflow to the the "Norne Field". We expand on previous studies by also testing the ability to distinguish between two different modes of process failure. We start with 50 realizations of this reservoir model to show the variety of possible fluvial-deposit scenarios for the geological description. We then use the Ensemble Kalman Filter (EnKF) to update the initial reservoir ensemble, integrating 30 years of waterflood production data. We use the updated reservoir models to simulate a polymer EOR process with an in-situ viscosity of 18 cp. To represent EOR process failure, we allow that the polymer process might fail in situ through either or both of two different mechanisms. The first is a global viscosity loss, where we stipulate that viscosity could be half of that intended, everywhere in the reservoir. The second is a progressive viscosity loss upon injection, where polymer decays and loses its viscosifying power over time (and therefore distance from the injection well). This second mechanism represents process where polymer viscosity is maintained near the injection well but not far away. These processes would reflect chemical degradation of polymer in situ or, more broadly, polymer absorption. We test whether the signals of these differences at injection and production wells would be statistically significant in the midst of the updated geological uncertainty, and whether the signals can distinguish which mechanism of failure has occurred [chapter 4].

SAMENVATTING

Chemische verdringingstechnieken zoals polymeer-verdringingstechnieken zijn methodes voor verbeterde oliewinning (“enhanced oil recovery”, EOR) die op laboratorium- en veldschaal zijn bewezen om de verdringing op veldschaal (“sweep”) en / of op porieschaal te verhogen. Hoewel de compatibiliteit en de efficiëntie van de geïnjecteerde chemicaliën grondig worden getest en gevalideerd in het laboratorium, blijft er nog steeds onzekerheid over hun werkelijke prestaties in het reservoir. Deze onzekerheden kunnen het gevolg zijn van de verschillen in de onderzoeksschaal (kernschaal tot veldschaal), gebrek aan voldoende kennis van de geologische, mineralogische en petrofysische eigenschappen van de formatie, en de langetermijnprestaties van de geïnjecteerde chemicaliën in het reservoir. Daarom kan elke EOR-veldproef onverwachte resultaten opleveren als gevolg van een verkeerd begrip van de geologische beschrijving van het reservoir of van het EOR-proces. Afzonderlijke evaluatie van de effecten van geologische en procesonzekerheden op de prestaties van een EOR-proces is belangrijk om beter aan te tonen of het proces zijn technische doelstellingen heeft bereikt. Eerder onderzoek heeft de onzekerheid in de prestatieparameters van chemische verdringingstechnieken onderzocht, evenals de effecten van geologische heterogeniteit en onzekerheid op de EOR-procesprestaties, maar niet de twee samen. In dit proefschrift stellen we een algemene werkwijze voor en presenteren we drie case studies om de prestatie van de EOR-agent in-situ te kwantificeren onder aanwezigheid van geologische onzekerheid. De workflow zou kunnen worden uitgebreid tot verschillende EOR-processen door mechanismen voor technische storingen op te nemen die specifiek zijn voor dat proces, bijv. verlies van in-situ viscosificerend vermogen van het polymeermiddel tijdens een polymeervloeistofproces.

In dit proefschrift bestuderen we eerst een polymeer EOR-proces in een 2D-l gelaagd reservoir waarbij het polymeer is ontworpen om een viscositeit te hebben van 60 cp in-situ. In de eerste studie, met behulp van een vereenvoudigde weergave van geologische onzekerheid, laten we toe dat het polymeerproces in-situ kan mislukken en dat de viscositeit slechts 20% van de beoogde viscositeit kan zijn. Dit falen kan het gevolg zijn van mechanische fouten in procesinstallaties aan het oppervlak of bij het binnendringen van de perforaties, foutieve vertaling van in het laboratorium gemeten eigenschappen naar eigenschappen in-situ, of foutieve karakterisering van het zoute water (pekel) in het reservoir. Deze nadelige effecten zullen mogelijkerwijs verschillende polymeereigenschappen geven in verschillende gebieden van het reservoir. In de eerste studie gaan we ervan uit dat de viscositeit van het polymeer overal in het reservoir een vaste fractie is van de beoogde fractie. We testen of de signalen van dit falen bij de injectie- en productieputten statistisch significant zouden zijn temidden van de geologische onzekerheid in de reservoirbeschrijving. Voor een populatie van reservoirs die een reeks geologische onzekerheden vertegenwoordigen, vergelijken we de afwijking veroorzaakt door verlies van polymeerviscositeit met de verstrooiing veroorzaakt door de geologische onzekerheid met behulp van de statistische benadering van het betrouwbaarheidsinterval. Verschillende signalen worden vervolgens gevolgd om te zien welke de meest betrouwbare indicaties zijn of een polymeerviscositeit in-situ werd gehandhaafd. We onderzoeken verder de statistische significantie van elk signaal. We stellen ook een werkwijze voor een dergelijke evaluatie voor die kan worden uitgebreid tot elk EOR-proces [hoofdstuk 2].

Voor een meer realistische casestudy passen we de workflow toe op een casus met een meer geavanceerd geologisch model (gebaseerd op het “gemodificeerde eiermodel”) voor een polymeer EOR-proces ontworpen voor een 3D-water-oliereservoir in een sterk heterogeen (fluviatiel) reservoir. Het polymeer is ontworpen om in-situ een viscositeit van 20 cp te hebben. We beginnen met 100 realisaties van dit 3D-reservoir om de reeks mogelijke geologische structuren weer te geven die voldoen aan de statistiek van de aanvankelijke geologische onzekerheden. Vervolgens groeperen we de realisaties op basis van een maatstaf van gelijkenis die de interactie tussen heterogeniteit en de reservoirstromingsmechanismen weerspiegelt. Na vijf jaar waterinjectie rangschikken we de reservoirmodellen in verschillende groepen van 10 realisaties, van de eerste 100 redelijk waarschijnlijke realisaties, met vergelijkbare waterdoorbraakdata bij de vier productieputten. Elke groep realisaties vertegenwoordigt dus reservoirs met ongeveer dezelfde waterinjectiegeschiedenis. Als groep vertegenwoordigen ze de verminderde geologische onzekerheid die overblijft na deze periode van waterinjectie. Om het mislukken van het EOR-proces weer te geven, staan we toe dat het polymeerproces in-situ kan mislukken en dat de viscositeit 30% van de beoogde viscositeit kan zijn. Vervolgens simuleren we vijf jaar polymeerinjectie. We nemen aan dat de viscositeit van het polymeer in het hele reservoir lager is dan de ontwerpwaarde. We testen of de signalen van dit verschil bij injectie- en productieputten statistisch significant zouden zijn temidden van de geologische onzekerheid: met andere woorden, of het procesfalen duidelijk zichtbaar zou zijn temidden van reservoironzekerheid [hoofdstuk 3].

Op basis van een echt reservoir en een niveau van onzekerheid dat representatiever is voor een veld na een periode van verdringing, passen we de workflow toe op het “Norne Field”. Bovendien testen we het vermogen om onderscheid te maken tussen twee verschillende vormen van procesfalen. We beginnen met 50 realisaties van dit reservoirmodel om de verscheidenheid aan mogelijke ’fluviatiele scenario's voor de geologische beschrijving te laten zien. Vervolgens gebruiken we het Ensemble Kalman-filter (EnKF) om het oorspronkelijke reservoirensemble bij te werken, waarbij we 30 jaar aan productiegegevens over waterinjectie integreren. We gebruiken de bijgewerkte reservoirmodellen om een polymeer EOR-proces te simuleren met een in-situ viscositeit van 18 cp. Om het mislukken van het EOR-proces weer te geven, staan we toe dat het polymeerproces in-situ kan mislukken via een of beide van twee verschillende mechanismen. De eerste is een globaal viscositeitsverlies, waarbij we bepalen dat de viscositeit de helft van de beoogde viscositeit kan zijn, overal in het reservoir. De tweede is een progressief viscositeitsverlies bij injectie, waarbij polymeer vervalt en zijn viscositeitsvermogen verliest na verloop van tijd (en dus afstand van de injectieput). Dit tweede mechanisme vertegenwoordigt een proces waarbij de viscositeit van het polymeer wordt gehandhaafd nabij de injectieput maar niet op grotere afstand van die put. Deze processen zouden chemische afbraak van polymeer in situ weerspiegelen of, breder, adsorptie van oppervlakteactieve stoffen. We testen of de signalen van deze verschillen bij injectie- en productieputten statistisch significant zouden zijn temidden van de geactualiseerde geologische onzekerheid, en of de signalen kunnen onderscheiden welk faalmechanisme is opgetreden [hoofdstuk 4].

ACKNOWLEDGEMENTS

Finishing this PhD thesis could have only been possible with the support, help, patience and contribution of many people.

First and foremost, I would like to sincerely thank Prof. Bill Rossen for his supervision of the thesis work. He was always there to help, guide and keep a close eye on every step of the way. Bill, I truly appreciate your patience and guidance during the past few years. Also Prof. Jan Dirk Jansen, I truly appreciate your guidance and insights during several meetings that we had.

Special thanks to Shell Global Solutions B.V for providing me with the scholarship to do my PhD in Delft University of Technology. Also thanks to employees of Shell some of whom I had occasional meetings with and learned a lot from. Bart Wassing and Cor van Kruijsdijk, many thanks for your generous support, I really appreciate your precious comments specially during the first two years of my PhD.

I also would like to thank and appreciate all the friends and staff at CiTG and in particular the petroleum engineering section who created a friendly and enjoyable working environment (in no special order): Jiakun, Tianqi, Chris, Jinyu, Elham, Leon, Ehsan, Rahul, Siavash, Saskia, Mojtaba, Bander, Ahmed, Durgesh, Matei, Nikita, Rodrigo, Elisa, Ania, Amin, Maryam, Daniel, Eduardo, Marc, Anke, Marlijn, Lydia, Margot and Ralf.

I would like to express my deepest gratitude to my mom and dad for their genuine love, help and sacrifice during my whole life, who have always had my back no matter what. Also thanks to my lovely sisters who have supported me since childhood, I love you and truly appreciate you.

Last but not least, my heartfelt appreciation goes to my lovely wife Matin for her support and encouragements along the way, I feel grateful and proud to have you by my side.

Amin
Delft
August, 2021

ABOUT THE AUTHOR

Amin Fatemi was born on 17 August 1984 in Kerman, Iran. He received his Bachelors degree in Petroleum Engineering from Petroleum University of Technology (PUT), Ahvaz, Iran. He continued his education towards a Masters degree in Chemical Engineering (Hydrocarbon Reservoirs) in Sharif University of Technology (SUT) in Tehran, Iran. Hereafter he moved to Muscat in Oman to work as a researcher in a collaboration program between Sultan Qaboos University (SQU) and Oman National Oil Company. Soon after, he decided to pursue his academic education in department of Geoscience & Engineering at Delft University of Technology as a PhD student. His PhD was sponsored by Shell Global Solutions International.